**Distribution Agreement**

In presenting this thesis or dissertation as a partial fulfillment of the requirements for an advanced degree from Emory University, I hereby grant to Emory University and its agents the non-exclusive license to archive, make accessible, and display my thesis or dissertation in whole or in part in all forms of media, now of hereafter known, including display on the worldwide web. I understand that I may select some access restrictions as part of the online submission of this thesis or dissertation. I retain all ownership rights to the copyright of the thesis or dissertation. I also retain the right to use in future works (such as articles or books) all or part of this thesis or dissertation.

Signature

_____ _____

Andrea Lynn Kasinski Date

Targeting Cell Survival Signaling for Therapeutic Discovery

By

Andrea Lynn Kasinski
Doctor of Philosophy

Graduate Division of Biological and Biomedical Sciences
Genetics and Molecular Biology

_____

Haian Fu, Ph.D.
Advisor

_____

Jeremy M. Boss, Ph.D.
Committee Member

_____

David Pallas, Ph.D
Committee Member

_____

Wei Zhou, Ph.D
Committee Member

Accepted:

_____

Lisa A. Tedesco, Ph.D.
Dean of the Graduate School

_____

Date

# Targeting Cell Survival Signaling for Therapeutic Discovery

By

Andrea Lynn Kasinski
B.A., Mathematics
State University of New York College at Buffalo, 1996

Advisor: Haian Fu, Ph.D.

An abstract of
a dissertation submitted to the Faculty of the Graduate
School of Emory University in partial fulfillment
of the requirements for the degree of
Doctor of Philosophy

Genetics and Molecular Biology
Graduate Division of Biological and Biomedical Sciences

2009

## Abstract

### Targeting Cell Survival Signaling for Therapeutic Discovery

**By: Andrea Lynn Kasinski**

The completion of the human genome sequence has greatly facilitated gene profiling to reveal tumor specific signatures and the identification of tumor-addicted oncogenes and pathways. These advances offer unprecedented opportunities for anticancer therapeutic discovery and development. The emerged cancer survival signaling pathways guide our characterization of promising therapeutic agents while lead us to novel strategies for targeting these tumor-addicted regulatory mechanisms. By taking advantage of these developments, my dissertation seeks (i) to understand the mechanism of action of a natural product analog, EF24, for anticancer therapeutic discovery and (ii) to unravel the transcriptional control machinery of a specific member of the 14-3-3 protein family, a master regulator of cell survival signaling, for future therapeutic interventions.

Curcumin, a natural product, has shown numerous therapeutic benefits but suffers from low potency and poor absorption. To overcome these limitations, a structural analog, EF24, was developed and exhibited a potent anticancer activity. However, its molecular target remains to be defined. My research describes a mechanism by which EF24 potently suppresses the NF-κB signaling pathway through direct action on the I-κB kinase (IKK): (i) EF24 rapidly blocks the nuclear translocation of NF-κB with a potency ten times better than that of curcumin, (ii) EF24 effectively inhibits TNFα-induced I-κB phosphorylation and degradation, and (iii) EF24 directly inhibits the catalytic activity of

IKKβ in an *in vitro* reconstituted system. This study identifies IKK as an effective target for EF24 and provides a molecular explanation for a superior activity of EF24 over curcumin. The effective inhibition of TNFα-induced NF-κB signaling by EF24 extends the therapeutic application of EF24 to other NF-κB-dependent diseases besides cancer, including various inflammatory diseases.

Dysregulated 14-3-3 proteins have been associated with poor survival of certain cancer populations. Targeting 14-3-3-mediated survival signaling has emerged as a promising anticancer strategy. However, the high level of sequence similarity among its seven isoforms and functional redundancy pose significant challenges. My research aims at defining the transcriptional mechanism that specifically controls the expression of a highly oncogenic isoform, 14-3-3ζ (*ywhaz*). Through a series of molecular and genetic approaches, my research identified five transcript variants of *ywhaz*, determined the importance of *ywhaz* variant 1c, revealed a functional CRE element within its promoter, and discovered two CREB family members as *ywhaz* transcription factors. Indeed, silencing of ATF-1, a CREB member, resulted in reductions in two of the five variants accompanied by significantly decreased 14-3-3ζ protein. This study defines the first transcriptional regulatory system that directs the expression of an oncogenic 14-3-3 isoform and reveals a mechanism by which ATF-1-mediated pathways control the expression and function of 14-3-3ζ and 14-3-3ζ-regulated signaling network.

# Targeting Cell Survival Signaling for Therapeutic Discovery

By

Andrea Lynn Kasinski
B.A., Mathematics
State University of New York College at Buffalo, 1996

Advisor: Haian Fu, Ph.D.

A dissertation submitted to the Faculty of the Graduate
School of Emory University in partial fulfillment
of the requirements for the degree of
Doctor of Philosophy

Genetics and Molecular Biology
Graduate Division of Biological and Biomedical Sciences

2009

## Acknowledgments

This thesis would not have been possible without the help, assistance, and patients of many individuals. This includes my thesis advisory committee members, my mentors (both past and present), my friends and most notably my family.

I have been fortunate while at Emory University to have had not one, but two incredible faculty to mentor me throughout my early scientific career. It is without hesitation that I owe a great deal of gratitude to my Ph.D advisor, Dr. Haian Fu. He taught me to strive in areas that I otherwise would not have, and persuaded me to reach for the top. Secondly, it is with a heavy heart that I acknowledge the former Dr. Dean Danner who believed in me more than I believed in myself. It was with Dr. Danners' direction that I choose to join the Ph.D. program at Emory University. He truly has made a footprint in my scientific career and my life as a whole.

It goes without saying that without my friends, both close and far, that this would not have been possible. I have been blessed with a great group of friends from middle school onward. They have been there for me throughout all of this. Specifically, I owe a special thank you to my best friend Susan Colosimo, who has been my rock. She has helped me through areas of my life outside of academia and gave me a little escape when I needed one.

I would like to thank my incredible family. My one and only sister, Darlene who I got to know so much better while living in Atlanta. I have been blessed to be so close to her, my brother-in-law, James, and their two beautiful children. I have had the opportunity to see my niece and nephew, Morgan and Matthew, grow before my eyes. They were my driving force. As were my Mother (and Father), whom without, none of this would have been possible.

Lastly and to who this thesis dissertation is dedicated to – my Father, Richard Kasinski. He believed in me like no one else. He told me that I could accomplish whatever I put my mind to. To him, I say "Thank you Dad, for listening to me when I needed to talk and for giving me answers when I felt like I ran out of options and most of all for being a father to me like no one else ever could". Your legacy lives on.

# Table of Contents

# List of Figures

## List of Tables

## List of Abbreviations

| | |
|---|---|
| AANAT | serotonin-N-acetyltransferase |
| ADP | adenosine diphosphate |
| AMP | adenosine monophosphate |
| ANK | ankyrin |
| ASK1 | apoptosis signal regulating kinase 1 |
| ATF-1 | activation transcription factor 1 |
| ATP | adenosine triphosphate |
| B | basic |
| BAD | Bcl-associated death promoter |
| BCL-3 | B-cell CLL/lymphomas 3 |
| BH3 | bcl-2 homology domain 3 |
| bZIP | basic leucin zipper |
| C/EBP | ccaat-enhancer-binding proteins |
| cAMP | cyclic AMP |
| CBP | CREB binding protein |
| ChIP | chromatin immunoprecipitation |
| CLL | chronic lymphocytic leukemia |
| CMI | cell mediated immune |
| COX | cyclooxygenase |
| CRE | cAMP response element |
| CREB | cAMP response element binding |
| CREM | cAMP response modulator |
| DD | death domain |
| DEAE | diethylaminoethyl |
| DNA | deoxyribonucleic acid |

| | |
|---|---|
| EMSA | electrophoretic mobility shift assay |
| ERK | extracellular signal-regulated kinases |
| EST | expressed sequence tag |
| EWS | ewing sarcoma |
| EXOS | exoenzyme S |
| FOXO | forkhead box O3 |
| GFP | green fluorescence protein |
| GRR | glycine-rich domain |
| GSK3β | glycogen synthase kinase 3 beta |
| GST | glutathionine S-transferase |
| GTP | guanosine triphosphate |
| HCA | high-content assay |
| HNOSCC | head-and-neck/oral squamous cell carcinomas |
| I-κB | inhibitor of kappa B |
| IAP | inhibitor of apoptosis |
| IFN | interferon |
| IKK | inhibitor of kappa B kinase |
| IL | interleukin |
| JNK | c-jun n-terminal kinase |
| κB | kappa B |
| KID | kinase inducible domain |
| LPS | lipopolysaccharide |
| LZ | leucin zipper |
| MAPK | mitogen activated protein kinase |
| MKK | mitogen activated protein kinase kinase |
| NCI | National Cancer Institute |
| NEMO | NF-κB essential modulator |

| | |
|---|---|
| NF-κB | nuclear factor kappa-B |
| NIK | NF-κB inducing kinase |
| PCR | polymerase chain reaction |
| PEST | proline-, glutamic acid-, threonine-rich domain |
| PGE2 | prostaglandin E2 |
| PKA | protein kinase A |
| PKC | protein kinase C |
| PTEN | phosphatase and tensin homology |
| Q2 | glutamine rich |
| RACE | rapid amplification of cDNA ends |
| RHD | rel homology domain |
| RLM | RNA ligase-mediated |
| RNA | ribonucleic acid |
| RT-PCR | reverse transcription polymerase chain reaction |
| SAPD | streptavidin pulldown |
| shRNA | short hairpin RNA |
| SRB | sulforhodamine B |
| STAT5a | signal transducer and activator of transcription 5a |
| TAD | transactivation domain |
| TERT | telomerase reverse transcriptase |
| TGFβ | transforming growth factor beta |
| Th-1 | T-helper cells class 1 |
| Th-2 | T-helper cells class 2 |
| TOR | target of rapamycin |
| TNFα | tumor necrosis factor alpha |
| UTR | untranslated region |
| YAP | yes-associated protein |

# Chapter 1:
# Introduction

Eukaryotic organisms have developed elaborate mechanisms to ensure that cell death and survival signals are tightly regulated. Aberrant survival or death signaling later in life can result in numerous pathological disorders in higher eukaryotes, including neurodegenerative diseases and cancers. Intracellular molecules involved in maintaining this life-to-death balance are often found to be dysregulated in these pathological disease states. Thus, understanding the intricate regulatory systems that control cell growth and survival may offer opportunities for therapeutic agent development. Additionally, such understandings can also guide the mechanism of action studies of promising therapeutic agents, which is vital for their clinical development.

My research seeks to understand the mechanism of action of a natural product-derived compound, which appears to target nuclear factor kappa B (NF-κB) mediated survival signaling. Further studies are aimed at identifying new therapeutic targets through unraveling a regulatory system dependent on the activating transcription factor 1 (ATF-1) that controls the expression of a major pro-survival protein, 14-3-3ζ. Background on curcumin, NF-κB, 14-3-3 proteins and the CREB/ATF-1 family of transcription factors are provided below.

## Curcumin

To circumvent the complications of toxicity when designing drugs, it is advantageous to identify small molecule inhibitors obtained from natural sources [1,2]. Typically, naturally derived compounds have well established toxicity profiles and a long history of consumption. Curcumin is one such compound.

Curcumin, a polyphenolic compound, was isolated and identified as the active ingredient from the rhizomes (tumeric) of the plant *Curcuma long linn*. Freely available in the human food supply, its major uses are as a natural coloring agent and as a spice to add the distinctive yellow color and flavor to curry powder. In many regions of the world, curcumin has been used for centuries in the diet and to treat a plethora of maladies from insect bites to heartburn and arthritis. More recently curcumin has been administered to suppress chronic inflammation and for the prevention and treatment of cancer [3]. Indeed curcumin's chemopreventive properties have led to Phase I and II clinical trials. The molecular events targeted by curcumin to suppress both inflammatory response and tumorigenesis are still being worked out; however curcumin has been shown to hold powerful natural antioxidant activates and can reduce the levels of cancer causing chemical carcinogens in the cell. Further, curcumin can inhibit the nuclear translocation of the transcription factor, NF-κB [4].

Despite having a small molecular weight and being a well-tolerated drug, curcumin presents with relative low bioavailability in both animal studies and in humans. To circumvent this problem, a group at Emory University developed a panel of curcumin analogues. These analogues were designed in an effort to retain the safety profile of curcumin while acting to enhance its absorption, which is important for improving the

bioavailability of the compound. One such analogue surfaced as a lead compound and was given the name, EF24. This particular analogue was more potent than the parent compound at inducing cell death and could reduce tumor size in nude mice [5,6]. Further the toxicity profile was similar to that of the parent compound, curcumin.

This section will give general background on curcumin including its current role in chemoprevention and chemotherapeutics. The challenges this molecule present will be addressed leading to the development of the more potent EF24. EF24 synthesis and preliminary tests will be reviewed as will its clinical potential.

## Curcumin's therapeutic potential

### *Curcumin's use as a chemopreventive agent*

Cancer chemoprevention entails the use of naturally or synthetically designed compounds to inhibit the three stages of carcinogenesis: initiation, promotion, and progression. Chemopreventive agents and chemotherapeutics are designed to stop cancer before it starts or to inhibit its further development and growth, respectively. As we live in a world that exposes us to multiple carcinogens, identifying safe chemopreventive agents is imperative to cancer-free survival. Indeed, curcumin is associated with numerous therapeutic benefits, including anti-inflammatory, antioxidant, antiviral, and anti-carcinogenic activities [7-11]. Furthermore, curcumin is capable of inhibiting all three stages of carcinogenesis. The first documented case of curcumin's chemopreventive activities were performed in a mouse model. Dalton's lymphoma cells were injected intraperitoneally and the chemopreventive effects of tumeric (of which curcumin is the active ingredient) were evaluated. While no control animal survived after 60 days, greater than 50% of the animals that were treated with 40 mg of tumeric survived and were

cancer free [12]. Further studies in rodents, determined that in addition to curcumin's suppression of tumor-formation, it can likewise reduce the multiplicity of tumors. One mechanism may be curcumin's ability to rid an organism of harmful carcinogens. Indeed, curcumin can induce activation of cellular antioxidants, and act as a reactive oxygen species scavenger that could explain this. Multiple pre-clinical animal studies have maintained these findings suggesting a role for curcumin in chemoprevention in the colon, duodenal, stomach, prostate, and breast [13-16]. Further, epidemiological data suggest that curcumin may be responsible for the lower rate of colorectal cancer in countries where tumeric consumption is high [17]. Individuals within these areas have a lower incidence of colorectal cancer relative to regions of the world where curcumin consumption is low. This data is supported by studies monitoring second-generation individuals whom migrate to the Western world. These individuals, whom now consume far less curcumin than their first-generation ancestors, develop increased risk for colorectal cancer, suggesting that the low levels of cancer in Eastern countries may be attributed to increased consumption of curcumin in the diet. As such, a positive correlation between curcumin consumption and cancer prevention has been proposed. These studies and others suggest that curcumin can be used for the prevention of cancer, but what about it's role as a therapeutic?

***Curcumin's use as a chemotherapeutic agent***

Although identifying novel chemopreventive agents is imperative, the elucidation of chemotherapeutics for the treatment and regression of existing tumors has exploded into a multi-billion dollar industry. This effort is aimed at identifying novel agents with limited toxicities, as chemotherapeutics currently in use cause multiple side effects that can be

attributed to their toxicity in tissues with actively dividing cells (ie. hair, skin, and lining of the gut). The absence of dose-limiting toxicity, even when curcumin is administered up to 12 g/day in human clinical trials, reveals the possibility of using curcumin to treat cancer with limited toxicity to adjacent healthy tissue [18]. Curcumin's well-established safety profile and its favorable and effective use as a chemopreventive agent, has enticed researchers to the potential use of curcumin as a chemotherapeutic. This suggests the possibility of using curcumin to treat pre-existing malignancies; albeit, much of this has been hindered by the pitfalls associated with curcumin, including its low potency and poor absorption [19].

**Curcumin's therapeutic challenges**

**Curcumin exhibits poor bioavailability**

The safety and efficacy of curcumin make it an attractive compound for the treatment of multiple human diseases. However, in spite of its safety profile, curcumin has not yet been approved for use as a therapeutic agent. Its poor bioavailability is a major contributing factor to this and can best be explained by curcumin's rapid metabolism and low absorption [19-21]. Meaning that most of what is consumed goes directly into the gastrointestinal tract and is expelled. Very little remains in the bloodstream. One of the first observations of curcumin was its low presence in serum. In an early study, Wahlstrom and Blennow analyzed plasma levels from rats that were orally given 1g/kg of curcumin [20]. Poor absorption from the gut was a main contributing factor to the low serum levels. Oral administration is one means by which to deliver a compound into the systemic system, however not all compounds can be absorbed this way. Evaluations of different mechanisms for administration are needed to determine if the reduced

bioavailability can be overcome. A more comprehensive study was set-up to determine if the mode of administration of curcumin changed the bioavailability. Although the time to peak plasma concentrations were different (2.25 μg/ml at 15 minutes post i.p., versus 0.22 μg/ml one hour post oral administration), both means of drug delivery resulted in quick clearance of the compound from the animal (i.p. declined in less than one hour, oral showed no curcumin after 6 hours) [22]. Even though decreased absorption of this compound is a factor contributing to its low serum levels, clearly there are other mechanisms involved in the clearance of curcumin.

Reduced bioavailability of a compound can also be attributed to increased metabolism of the compound. In fact, curcumin is subjected to conjugations after it is absorbed. The liver is the major organ responsible for curcumin's metabolism including conjugations to curcumin such as sulfation and glucuronidation [19]. One way by which the body rids itself of toxins, and drugs is glucuronidation. In this process, glucurnoic acid is linked to another substance via a glycosidic bond, leading to increased solubility in water. This process allows the body to excrete the metabolized product by the kidneys. Curcumin is removed from the body quickly, quite possibly due to its glucuronidation. In fact, 99% of curcumin in the plasma of rats is present as glucuronide conjugates [22]. This was also found to be a major metabolite in humans as well [21]. These studies suggest that although curcumin is an extremely safe compound, it may not be very effective owing to its poor absorption and quick metabolism. Therefore the next step entails developing additional strategies to heighten curcumin's efficacy.

## Techniques to improve upon the bioavailability of curcumin

### *Blocking glucuronidation*

To improve upon the bioavailability of curcumin, various approaches are being utilized. The first suggests the use of an adjuvant like piperine. Piperin, also a naturally occurring compound, is obtained from the extract of black pepper. Its main use is to inhibit enzymes important for drug metabolism such as those that interfere with glucuronidation. Combining curcumin with piperin in a rat model resulted in increased bioavailability to 154% over administration of curcumin alone [19]. More striking was a human study that produced a 20-fold increase in bioavailability when the combination was administered [19]. Although the bioavailability data are promising, tissue distribution in a mouse model suggests otherwise [23]. The only tissue with significant changes in uptake after co-administration was the brain, while uptake in other tissues was negligible. Further, due to piperin's inhibitory effects on drug metabolism, piperine needs to be utilized with caution by individuals on additional medications. These data suggest that alternative approaches to enhance curcumin's bioavailability need to be identified.

### *Generation of curcumin analogs to improve its pharmacological properties*

To circumvent the problems with curcumin and avoid the need for co-administration with a metabolic blocker, such as piperin, a second approach suggests the design of derivatives or analogs of curcumin.

Based on its safety profile, and low molecular weight, curcumin serves as an excellent lead compound for designing new drugs. As such, Dr. Dennis Liotta's group at Emory University devised a series of structurally altered curcumin analogs in an effort to retain the relatively safe toxicity profile of curcumin while increasing its potency [5]. A

computer-based topological search was conducted to identify lead analogs. Two such analogues incorporating a monoketone were identified and exhibited an improved cytotoxic effect over curcumin. These results stimulated a more thorough search for easily prepared and readily functionalized analogs with improved potency. The strategy adopted is captured by the following manipulation of curcumin: Two carbons and an oxygen were removed from the center of the molecule to produce a monoketone, terminal ring substituents were varied, and an extensible heterocyclic six-membered ring including the ketone was installed. Approximately 100 analogs were tested in various *in vitro* cell viability screens at Emory University. The top three were further evaluated at the National Cancer Institute (NCI) on the NCI's *in vitro* anti-cancer cell line screen. In this screen, compounds were assayed against the parent compound, curcumin and the currently used chemotherapeutic, cisplatin. With respect to inhibition of tumor cell growth by 50%, the lead compound, EF24, was 13.6 and 10.4 fold better than cisplatin and curcumin respectively [5]. Inhibition of tumor growth by 100% was also greater for EF24 over cisplatin (EF24 was 23.3 fold better) and curcumin (9.8 fold better) [6]. In the same study, in vivo tests of the lead compound were employed. A dose of EF24 at 20 mg/kg decreased tumor growth of solid breast tumors in the flanks of mice to 70% relative to control. Further, although a relatively high dose, 100 mg/kg reduced tumor size to 45% of control with no harmful side effects identified in the liver, kidney, or spleen [6]. An additional cell-based study from the same group found EF24 to induce G2/M cell cycle arrest followed by induction of apoptosis as evident by caspase-3 activation, phosphatidylserine externalization and increased number of cells with a sub-G1 DNA fraction [6]. This was found to coincide with EF24s rapid absorption and peak plasma half-

life.

Despite the fact that EF24 appears to act selectively against tumor cells in an *in vivo* model, the exact molecular events leading to tumor cell apoptosis and increased efficacy of this compound have not been defined. In an effort to determine the precise molecular mechanism of action of how this novel curcumin analogue exerts its enhanced anticancer activity, a thorough study of its target(s) was required. My research was intended to address this issue. A direct action of EF24 on NF-κB mediated signaling was discovered, which is described in Chapter 2. As such, an introduction of the NF-κB signaling pathway follows.

## NF-κB

### Introduction and identification of NF-κB

NF-κB is a transcription factor that was initially identified by Sen and Baltimore in 1986 as a B-cell specific protein [24]. Its activity was found to be pivotal for the initiation of immune system response [25,26]. However, further work identified that this factor is ubiquitously expressed with multiple roles outside of the immune system that were not initially appreciated. In fact, NF-κB is activated in response to stress, free radicals, and ultraviolet radiation, to name but a few. These stimuli, result in elevation of NF-κB target genes ranging from various chemokines and cytokines, to genes important for apoptotic avoidance and survival. Induction of NF-κB targets depends on κB sequences located within their promoters. This 11-nucleotide sequence (GGGGACTTTCC) is the binding site for NF-κB dimers [24]. Indeed NF-κB binds to this highly conserved sequence as both hetero- and homodimers. The REL-homology domain (RHD), which is a signature of all NF-κB family members, regulates NF-κB dimer formation [27-29].

The mammalian NF-κB family consists of five RHD members termed, p50, p52 (the cleaved N-terminal fragments of p105 and p100 respectively), p65 (also known as RELA), cREL, and RELB (Figure 1.1). The 300 amino-acid RHD is located near the amino-terminus of NF-κB family members and acts as the dimerization interface to allow formation of functional NF-κB hetero- and homo-dimers [27-29]. The formation of different dimers determines whether they will be activating or repressing NF-κB transcription factor units [30-32]. The ability of NF-κB dimers to activate or repress target genes is partly determined by the presence or absence of the transactivation domain (TAD), respectively [33]. Transcription induced by p65, RELB and cREL is positively regulated through the

TAD; however, neither p100 nor p105 contain a TAD domain [34]. Therefore, in order to induce transcription of target genes the two REL-homology members need to heterodimerize with a TAD-containing family member. Further, because p100 and p105 lack the TAD they can also function to repress transcription when bound to κB sites as homodimers or heterodimers of each other [34-36].

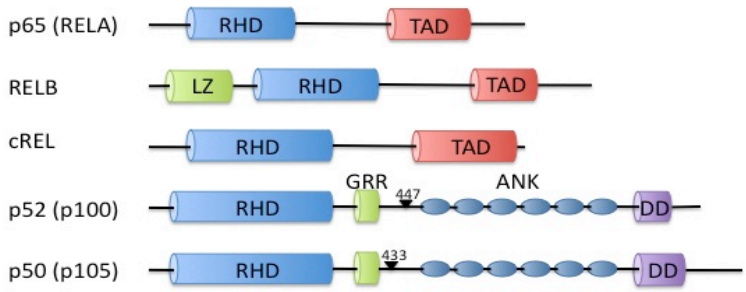


**Figure 1.1 Representation of NF-κB family members.** All members share the N-terminal REL homology domain. p52 and p50 lack the transactivation domain, which is imperative for inducing transcription from NF-κB target genes. The cleavage sites for p100 and p105 are shown as downward arrows (amino acids 447 and 433 respectively). RHD, rel homology domain; TAD, transactivation domain; LZ, leucine zipper; GRR, Glycine-rich region, DD, death domain.

**NF-κB in immune response and its tie to tumorigenesis**

It goes without saying that NF-κB is central to the immune system response [25,26]. However, NF-κB also induces genes involved in cell survival and anti-apoptosis, many of which are elevated in cancers [37-39]. As such, a remarkable discovery was made linking unchecked immune response, through sustained NF-κB signaling, to the development of cancer [40].

***Elevations in NF-κB activity lead to aberrant T-cell activation***

It is well established that rapidly proliferating T-cells require NF-κB for their further growth and proliferation [41-43]. For example, NF-κB induces activation of STAT5a (signal transducer and activator of transcription 5a), which is imperative for T-cell proliferation [44]. In dominant-negative-I-κB over-expressing cells, where NF-κB is in the inactive state, STAT5a is not activated and T-cells fail to grow. In fact inhibition of NF-κB in T-cells for prolonged periods of time results in their induced apoptosis [45]. Conversely, sustained NF-κB activation, leading to cytokine production, can alter T-cell mediated immune response [46,47]. This is evident for two classes of helper T-cells, Th-1 and Th-2. Both are involved in further cytokine production. However, the cytokines they produce are specific to each class and influence aspects of normal and disease physiology [48-50]. Th-1 cells induce production of interleukin (IL)-2, interferon (IFN)-γ and IL-12 [49]. A cell mediated immune (CMI) response is activated by Th-1 cells with Th-1 cytokines begin necessary for a strong CMI response that are decreased in many chronic infectious diseases. The CMI response can be suppressed by the second class of Th cells, Th-2 cells. This class releases, IL-4, IL-5, IL-6 and IL-10 and affects the humoral response [49]. The levels of each of these Th-cell populations and their released cytokines are found

altered in cancers [51]. Indeed, various malignancies have been associated with suppression of the CMI response and elevations in the humoral response (Figure 1.2) [52]. Further, the presence of a dominant Th-2-immune response in potentially curable tumors (such as lymphomas) is associated with a fatal outcome [52]. Suggesting an inverse correlation of active Th-2 cells with disease free progression. In fact, cancers use a wide variety of methods to evade an immune response, including the generation of immunosuppressive cytokines such as TGF-β, and IL-10 [53,54]. Activation of these cytokines accounts for much of the CMI inhibition. Additionally, IL-10, which can suppress the CMI response, is induced following NF-κB activation, further supporting a role for NF-κB in immune-response-induced carcinogenesis [55].

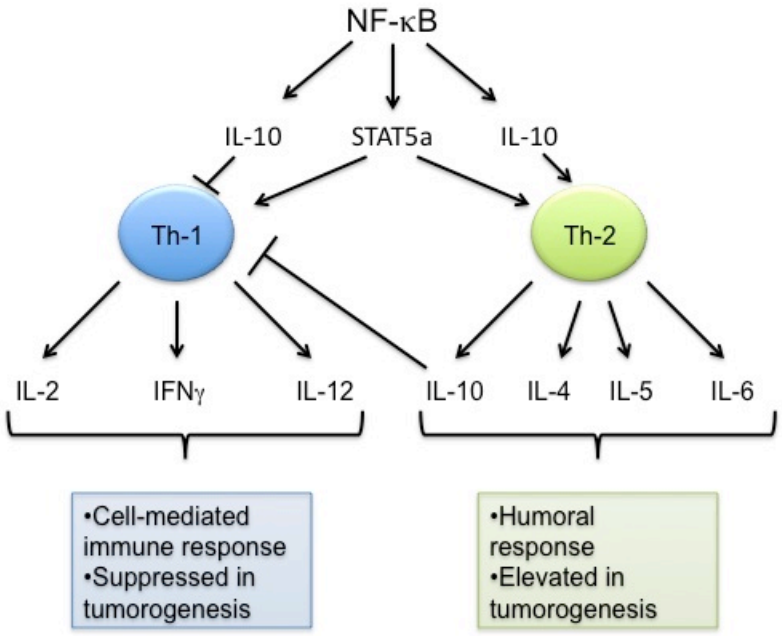


**Figure 1.2 NF-κB is central to helper T-cell activation and suppression.** NF-κB activation produces cytokines such as IL-10 that are responsible for activating the humoral response while causing suppression of the CMI response. CMI response is sustained as Th-2 cells continue to produce IL-10. The balance of these two responses is imperative for maintaining normal tissue homeostasis following an immune response. Alterations in their levels are attributed to immune response-induced carcinogenesis.

***Elevations in NF-κB activity lead to induction of Cox-2***

Many NF-κB targets have been implicated in tumorigenesis. One such gene, cyclooxygenase (Cox)-2, is elevated in both inflammatory disease and cancer. Cox enzymes are important in regulation of immune system response and play a key role in angiogenesis, inhibition of apoptosis, cell proliferation and motility, all of which are important for oncogenesis [56]. As such, Cox-2 expression is normally kept in check; however, in response to exposure to pro-inflammatory cytokines, its levels are elevated. Indeed, Cox-2 expression is correlated with local chronic inflammation and tumor blood-vessel formation in human prostate cancer [57]. In fact, in virtually all pre-malignant and malignant tumors, Cox-2 is constitutively expressed [58,59]. The mechanisms downstream of Cox-2 are what drive tumorigenesis. Cox is the rate-limiting enzyme in catalyzing the conversion of arachidonic acid to pro-inflammatory prostaglandins. One of the prostaglandin products induced by Cox-2, $PGE_2$, is believed to support tumor growth via induction of angiogenesis [60]. Further, upon its binding to receptors on T-cells, $PGE_2$ induces cyclic-AMP (cAMP) which further inhibits Th1 cells while stimulating the proliferation of Th-2 cells (Figure 1.3).

Cox-2 is also associated with cell proliferation and inhibition of apoptosis at least in part through the induction of the anti-apoptotic BH3 molecule, Bcl-2 (Figure 1.3) [61,62]. Bcl-2 proteins are involved in inhibiting mitochondria outer membrane permeabilization. The BH3 only protein, Bad forms heterodimers with Bcl-2 and a second anti-apoptotic molecule Bcl-$X_L$, leading to their inhibition [63]. However, elevations in Bcl-2 can suppress apoptosis by titrating out the pro-apoptotic signaling molecule, Bad. Further regulation of this signaling event will be elucidated in the section of 14-3-3 proteins.

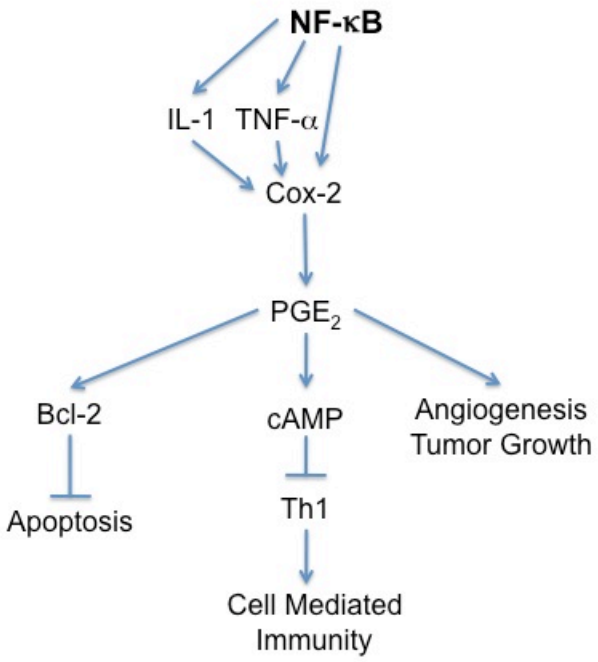


**Figure 1.3 Survival response elicited by the induction of Cox-2 through NF-κB and its downstream activators.** $PGE_2$ is a product of Cox-2 induced prostaglandin synthesis. Direct roles for $PGE_2$ in maintaining cell survival are indicated. See text for a more detailed description.

***Elevations in NF-κB activity lead to chemoresistance and radioresistance***

It is becoming increasingly clear that aberrant regulation of NF-κB accompanies both tumor formation and progression [64]. As such, many tumors present with elevated NF-κB. This sub-set of cancers is resistant to conventional chemotherapies. This is highlighted in tumors treated with radiation and chemotherapeutics such as cisplatin, doxorubicin, vincristine, and taxol [65]. These agents, intended to ablate these tumors, stimulate NF-κB activation. This is probably most likely a defense mechanism of the tumor, which causes it to be desensitized to these therapies resulting in chemoresistance and radoiresistance. In fact NF-κB activation induces expression of Bcl-2, an anti-apoptotic gene that can confer chemoresistance [66]. These hallmarks of NF-κB signaling make targeting this pro-survival pathway a potential means to control inflammatory diseases as well as cancers. Further, using NF-κB inhibitors in combination with traditional chemotherapies may act to sensitize tumor cells to these treatments.

As such, then next major question becomes how exactly is NF-κB signaling accomplished and by learning about its activation can drug targets be designed to suppress its activation?

**Signaling through NF-κB**

Activation of NF-κB target genes is achieved through one of two well-established pathways. Each of these is regulated by diverse stimuli with different players contained in each. This next section describes the activation of these two pathways.

***Alternative (non-canonical) NF-κB signaling***

The alternative pathway is important in the regulation of lymphoid organogenesis, development, selection, survival of B and T lymphocytes, and differentiation of antigen presenting cells [67]. As such, the immune system response depends on the alternative NF-κB pathway for its induction and maintenance. Activation of NF-κB by the alternative pathway is triggered by cytokines such as lymphotoxin B, B-cell activating factor, or CD40 ligand and by viruses such as human T-cell leukemia virus [68]. These cytokines and viruses bind to receptors on the cells surface and induce activation of NF-κB-inducing kinase (NIK). This kinase, not identified as an activator of classical NF-κB signaling, is specific to the alternative pathway. It is responsible for phosphorylating and activating the I-κB kinase (IKK)-α homodimer. The substrate for the homodimer is the ankyrin-containing and inhibitory molecule p100 [68]. IKK-α homodimers phosphorylate p100 on serine residues in both the N- and C-terminal regions followed by ubiquitination and cleavage of p100. The processed p100, now termed p52, combines with RelB and forms a heterodimer that then translocates to the nucleus to act on its target genes (Figure 1.4) [68].

***Classical NF-κB signaling***

Survival, proliferation, inflammation, and immune recognition are events regulated by the classical NF-κB pathway making it a highly desirable target for drug development [68]. In unstimulated cells, these actions are kept at bay, as NF-κB is in its inactive state, sequestered in the cytoplasm bound to one of the inhibitor of kappa B (I-κB) family members. Together the NF-κB dimers are regulated by a total of eight I-κBs (I-κBα, I-κBβ, I-κBε, I-κBζ, B-cell CLL/lymphoma 3 (BCL-3), I-κBNS (NF-κBd), p100 and

p105) (Figure 1.5). The I-κB proteins use a core domain composed of five to seven ankyrin repeats to bind to the RHD of NF-κB and thereby mask the nuclear localization signal found on NF-κB [69]. The prototypical NF-κB-I-κB complex expressed in the majority of the cells is a heterodimer of p50 and p65 retained in the cytoplasm when bound to I-κBα (Figure 1.4) [68]. Stimuli, such as cytokines, growth factors, and effector enzymes result in the phosphorylation of two critical serine residues on I-κB (Ser32/Ser36) by the inhibitor of kappa B kinase (IKK) [70]. This heterotrimeric complex is indispensable for NF-κB activation. The functional complex is made up of two catalytic subunits (IKKα and IKKβ) and a third regulatory factor (IKKγ, also referred to as NF-κB essential modulator (NEMO))[71,72]. Although all three subunits are required for activation via the classical pathway, IKKβ is found to be the main catalytic subunit responsible for the phosphorylation of I-κB (Figure 1.4) [70]. Upstream events leading to the initiation of this complex are not fully understood, however Akt seems to be one mediator of their activation [70]. Once phosphorylated by the IKK complex, I-κB then becomes a substrate for polyubiquitination by the E3 ubiquitin ligase complex at both Lys21 and Lys22 leading to rapid degradation by the 26s proteasome. This frees the NF-κB dimer, exposing its nuclear localization sequence allowing transloaction to the nucleus [73]. Inside the nuclear compartment NF-κB binds to κB sequences in the promoter or enhancer regions of target genes resulting in their expression or repression. This establishes that the activation of the IKK complex is crucial to the expression of NF-κB target genes via the classical pathway, and suppressing it's activation may be a promising approach for drug discovery.

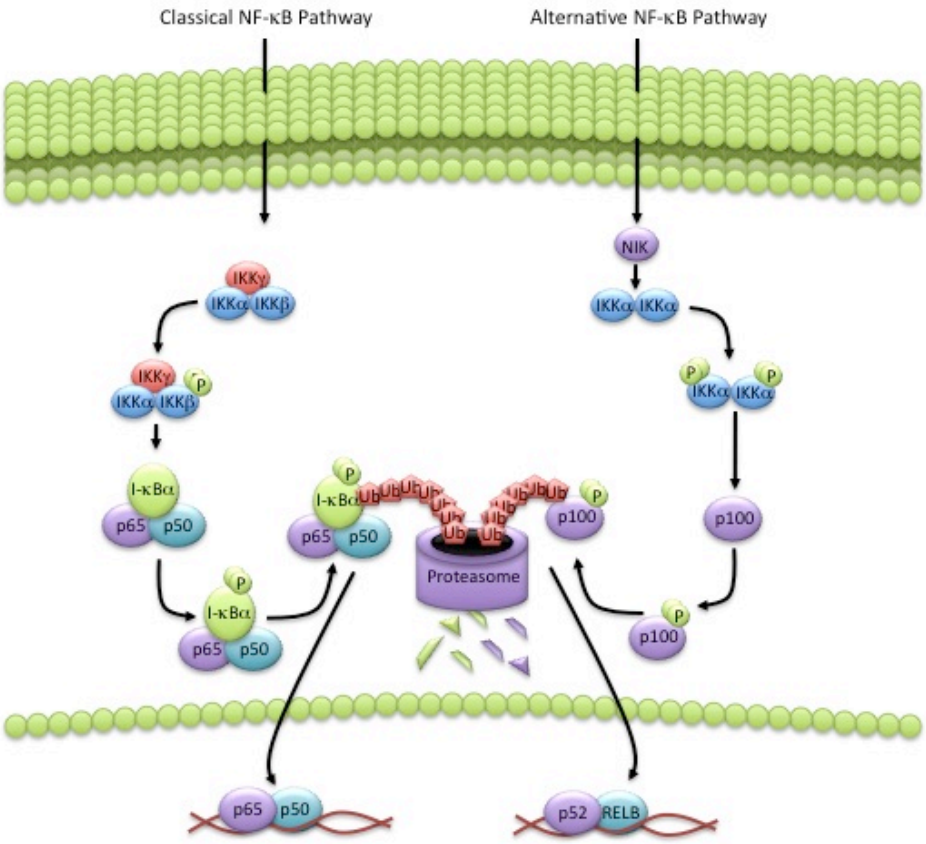


**<u>Figure 1.4</u> Signaling through the NF-κB Pathway.** The two major pathways governing NF-κB activation are shown. The classical pathway depends on phosphorylation of I-κB by the heterotrimeric IKK complex following proteasomal degradation of I-κB. The alternative pathway utilize the unprocessed p100 (also a member of the I-κB family of proteins) to retain itself in the cytoplasm until phosphorylated by IKK-α and subsequently processed to the mature p52. Binding of the mature form to RELB induces NF-κB target gene amplification.

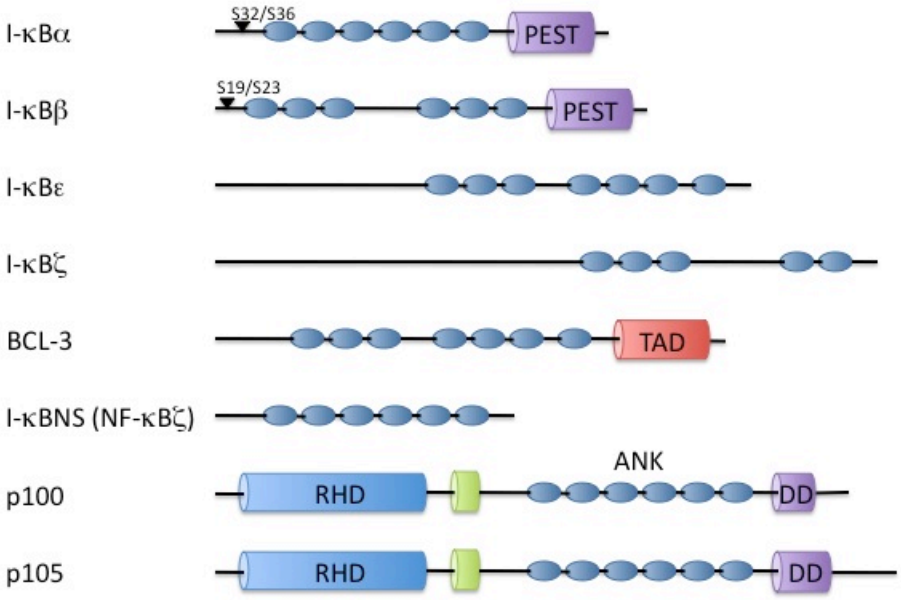


**Figure 1.5 Representation of the eight I-κB family members.** The canonical I-κB member is I-kB-α. Phosphoryaltion sites for I-κBα and I-κBβ are shown as a downward arrow. PEST, proline-, glutamic acid- and threonine-rich domain; TAD, transactivation domain; RHD, rel homology domain; ANK, ankyrin repeats; DD, death domain

**Targeting NF-κB pro-survival signaling for therapeutic development**

Experimental evidence reveals that compounds that can block NF-κB signaling can suppress cancer growth [74,75]. As such, more than 785 small molecule inhibitors aimed at impairing NF-κB signaling have been developed and/or identified [76]. These inhibitors can be subdivided into the various stages of the NF-κB signaling that they block. For instance there is a class of compounds that can weaken the interaction between NF-κB and its target promoter in the genome, to ones that halt nuclear translocation of the NF-κB heterodimer and others that completely block proteasomal degradation of I-κB [77,78].

***Targeting NF-κB through IKK inactivation***

An additional class of therapeutics is designed to impede on the kinase activity of the IKK complex, such that NF-κB is always found in the cytoplasm bound to its inhibitor (I-κB) [79]. This class offers the most selective and effective approach for inhibiting NF-κB. There is very little evidence that suggests that IKK proteins can phosphorylate proteins that are not involved in NF-κB signaling [79]. Additional support of the notion comes from studies showing that phenotypes due to the loss of IKKβ can be attributed to defective activation of the classical NF-κB pathway. Therefore, IKKβ is being pursued by many groups as an effective target for the development of therapeutic agents to be used for the treatment of cancer, inflammation, and metabolic diseases (see [79] for review).

Endeavors towards the development of safe and selective IKKβ inhibitors have been undertaken. Much of this effort entailed the screening large compound libraries, or the use of combinational chemistry to identify direct inhibitors. This has yielded the identification of a large, and rapidly growing, number of IKKβ inhibitors that act in the

low to mid nanomolar range [79]. Unfortunately, few of these are currently in the clinical trial stage, which could be attributed to the toxicity profile of these compounds. Therefore, identification of safe and novel inhibitors of NF-κB signaling is imperative to the treatment of both inflammation and cancer.

How the novel curcumin analog, EF24, acts on the NF-κB pathway is the focus of Chapter 2. Through molecular techniques, it has been determined that EF24 falls into the class of compounds that directly and effectively targets the IKK complex leading to impaired NF-kB signaling.

## 14-3-3 family of proteins

14-3-3 proteins are master-regulators of cell-survival signaling. For this reason, their elevated protein level in cancers comes as no surprise. It is hypothesized that there are both transcriptional and translational mechanism that govern this elevated protein load seen in tumors; however research at this end is lacking. Chapter 3 will discuss the identification of one mechanism that controls the expression of 14-3-3ζ at the transcriptional level. Accordingly, an introduction of the 14-3-3 family of proteins follows.

### Identification of 14-3-3 proteins

The 14-3-3 protein was initially identified as an abundant brain specific protein over four decades ago. Moore *et al.* fractionated 14-3-3 from soluble cow brain proteins using DEAE-cellulose chromatography followed by starch-gel electrophoresis and thus named it 14-3-3 based on its fraction number and gel-running pattern[80]. Later, several 14-3-3 proteins were discovered and grouped into a family containing multiple isoforms in various eukaryotic organisms (*see* [81,82] for review). For example, seven isoforms were found in mammalian cells, which were designated with Greek letters, β, ε, γ, η, σ, τ, and ζ [83].

### Genomic organization and species conservation of 14-3-3 isoforms

Genetically, different genes on separate chromosomes encode the seven mammalian isoforms. The diversity of the different genes is seen at both the level of transcription and at their genomic locus (Table 1.1). For example, *sfn*, the gene encoding the sigma isoform resides on chromosome 1. The entire gene is encoded by just one exon with a transcript size of 1315 nt that is translated into a protein primarily confined to cells of epithelial

origin [84]. Conversely, *ywhaz*, the ubiquitously expressed gene encoding 14-3-3ζ, spans over 34kb, encompasses 9 exons that encode for at lest 5 different 2.8kb transcript variants all with different 5'UTRs (see chapter 3). This complex organization suggests a greater mode of regulation at the genomic level for the zeta isoform. However, due to a lack of scientific studies focused in this area, this is purely speculative at this point.

| Isoform | Gene | RefSeq | Location | Genomic DNA (bp) | mRNA (bp) | Exons | Introns | CpG Island | % CpG |
|---|---|---|---|---|---|---|---|---|---|
| Beta1 | *ywhab* | NM_003404.3 | 20q13.12 | 22817 | 3104 | 7 | 5 | 214 bp | 24.8 |
| Beta2 | *ywhab* | NM_139323.2 | 20q13.12 | 22817 | 3009 | 6 | 4 | 214 bp | 24.8 |
| Sigma | *sfn* | NM_006142.3 | 1p36.11 | 1315 | 1315 | 1 | 0 | 216 bp | 15.7 |
| Gamma | *ywhag* | NM_012479.2 | 7q11.23 | 32200 | 3709 | 2 | 1 | 1371 bp | 18.5 |
| Zeta1 | *ywhaz* | NM_003406.2 | 8q22.3 | 34656 | 2829 | 6 | 4 | 2783 bp | 17.1 |
| Zeta2 | *ywhaz* | NM_145690.1 | 8q22.3 | 33358 | 2871 | 6 | 4 | 2783 bp | 17.1 |
| Tau | *ywhaq* | NM_006826.2 | 2p25.1 | 47000 | 2166 | 6 | 4 | 1373 bp | 18.4 |
| Epsilon | *ywhae* | NM_006761.3 | 17p13.3 | 55673 | 1777 | 6 | 4 | 1283 bp | 18.1 |
| Eta | *ywhah* | NM_003405.3 | 22q12.3 | 13111 | 1792 | 2 | 1 | 1259 bp | 22.7 |

**Table 1.1 Genetic information of seven 14-3-3 isoforms compiled from the UCSC Genome Database**

***Conservation of 14-3-3 between isoforms and species***

Although the various isoforms are quite divergent when comparing their genomic structure and transcripts, there is remarkable conservation at the amino acid level with more than 80% similarity between mammalian isoforms [85]. Further, the mammalian epsilon isoform shares 70% similarity with that of the *Saccharomyces cerevisiae* homologue, *bmh1*. Genetic complementation studies in yeast support this sequence conservation. Overexpression of the single *Dictyostelium discoideum* isoform or four of the six *Arabidopsis* isoforms was able to compensate for loss of both *bmh1* and *bmh2* in yeast [86,87]. Additionally, the 14-3-3 proteins also share some basic biochemical properties such as the ability to activate ADP-ribosyltransferase of exoenzyme S and activation of tryptophan hydroxylase [88-90]. These similarities argue for a high degree of functional conservation between orthologues.

**14-3-3 Regulation**

Understating the functional regulation of 14-3-3 proteins will allow us to appreciate how and why they are misexpressed in various disease pathologies and the potential implications that altered expression of these master regulators has in these states. The 14-3-3 proteins are regulated by a diverse set of events. They are substrates for phosphorylation themselves and further go on to become binding partners for phosphorylated ligands. The regulation at this level has been intensely studied. One of the major gaps in the field, beyond their posttranslational regulation, is to determine how 14-3-3 proteins themselves are regulated. To begin to appreciate the need to identify the transcriptional regulation of these isoforms, it is advantageous to understand the major roles they these master regulators partake in the cell.

***Post-translational Regulation of 14-3-3 monomers***

Once expressed and translated, the function of 14-3-3 proteins is tightly regulated by phosphorylation dependent interactions. One such interaction involves two momomeric 14-3-3 molecules. These dimeric units can exist as either homo-or hetero-dimers of multiple isoforms whose interaction is negatively regulated by phosphorylation [91-93]. For example, when phosphorylated at serine 58, the zeta isoform is unable to from a stable dimer [93,94]. However, in the unphosphorylated state, dimer formation occurs resulting in the ability of 14-3-3ζ to generate dynamic interactions with client proteins (Figure 1.6).

***Phosphorylation dependent (and independent) regulation of 14-3-3 binding to client proteins***

A second layer of control regulated via phosphorylation exists on the client protein. Three well defined 14-3-3 recognition motifs have been characterized in 14-3-3 client proteins, termed mode 1 (RSXpS/TXP; where pS/T denotes a phosphorylated serine or threonine residue), mode 2 (RXFXpSXP; where F indicates aromatic amino acids), and mode 3 (pS/T($X_{1-12}$)-COOH, where X stands for any amino acid) [95-98]. Ligand phosphorylation of a serine or threonine residue within a conserved 14-3-3 motif is a signal for 14-3-3 binding. In addition, 14-3-3 can also associate with some proteins in a phosphorylation-independent manner, including the telomerase reverse transcriptase protein, TERT and the bacterial encoded cytotoxin, exoenzyme S [82,88,89,99].

***Recognition of phosphorylated clients by 14-3-3 proteins***

Recognition of the phosphorylated 14-3-3 motif on a client protein is accomplished by the cup like region found within a 14-3-3 monomer, termed the amphipathic groove. The inner concave surface of the 14-3-3 structure contains a region of hydrophobic amino

acids on one side with charged polar residues on the other, including K49, R56 and R127 [100]. These residues are mostly conserved among 14-3-3 family members, suggesting their functional importance to the molecule [96,100-102]. Further, mutational analysis and structural studies of the tau and zeta isoforms strongly support the involvement of these conserved residues in client protein binding [103-106]. This highly conserved amphipathic groove within all 14-3-3 proteins forms the primary contact sites for client proteins. Additionally, this region is the main part of the molecule currently being targeted for drug development. Targeting small molecules to the amphipathic groove of 14-3-3 results in disruption of client protein interaction. Albeit, this impairs client binding to all isoforms, the importance of which will be eluted to in the following sections.

**Outcome of 14-3-3 binding to client proteins**

With the determination of the 14-3-3/client-protein interaction so well defined, the next question becomes how 14-3-3 binding affects the function of its client protein within the cell. 14-3-3 proteins bind to well over 200 ligands that function in diverse cellular processes (see [107] for review). Since 14-3-3 proteins have no enzymatic activity of their own it is best to look at the function that they elicit on their bound ligands. Studies of 14-3-3 client protein interactions have grouped the mechanism of action of 14-3-3 binding into three well-defined consequences to the bound ligand, which are not mutually exclusive.

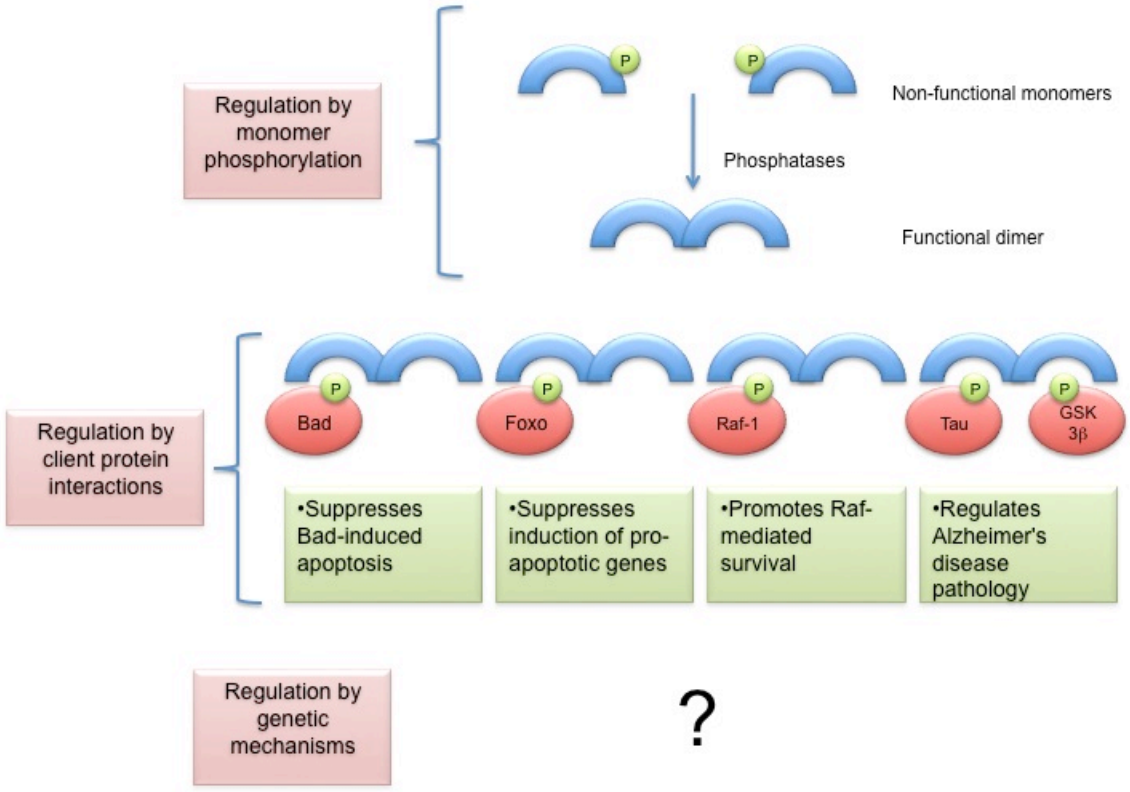


**Figure 1.6 Regulatory mechanisms governing 14-3-3 function.** Currently two modes of regulation for 14-3-3 protein have been well studied. Regulation of 14-3-3 monomers via phosphorylation can impair 14-3-3 function. Once dimerized, 14-3-3 proteins become binding partners for over 200 cellular substrates. Bind to 14-3-3 molecules elicits a cellular response. Typically this response is survival promoting. Studies to determine the genetic component to 14-3-3 regulation are currently underrepresented in the scientific community.

***14-3-3 binding changes the localization of a protein***

First, 14-3-3 binding can lead to altered cellular locations of its client protein. This scenario has been well described for the pro-apoptotic signaling molecule, Bad. Bad is a member of the BH3-only subfamily of proteins that functions at the mitochondria membrane to elicit a mitochondria-mediated apoptotic response [63]. Bad induced apoptosis is engaged when Bad is bound to the anti-apoptotic BH3 molecules, Bcl-$X_L$ and Bcl-2 [63,108-111]. In this way the anti-apoptotic functions of Bcl-$X_L$ and Bcl-2 are inhibited. Binding of Bad to Bcl-$X_L$ and Bcl-2 is regulated via phosphorylation of Bad. When phosphorylated within its 14-3-3 binding motif at serine 136, Bad becomes a target for 14-3-3 binding [112]. Upon binding to 14-3-3, Bad is sequestered away from the mitochondria into the cytosol where it no longer interacts with Bcl-2 or Bcl-$X_L$, leading to the release of these anti-apoptotic proteins. Highlighting the importance of 14-3-3 mediated re-localization of its client proteins. This first scenario is seen for many other 14-3-3 ligands, including the death inducing transcription factors Foxo and Yap that are both sequestered away from their cis regulatory elements on DNA when bound to 14-3-3 [113-117]. As such, elevations in 14-3-3 proteins can lead to enhanced survival signaling based on their ability to inhibit the function of pro-apoptotic proteins such as Bad, Foxo and Yap.

***14-3-3 binding can alter enzymatic function of the client***

A second function of 14-3-3 proteins is their ability to alter intrinsic catalytic activity of the target. One such example is the exoenzyme S (ExoS) cytotoxin, secreted by the gram-negative bacteria *Pseudomonas aeruginosa* [88]. This toxin contributes to the infection this opportunistic pathogen causes in immunocompromised individuals. ExoS

has two primary enzymatic activates. Rho GTPase protein activity is confined within the N-terminal domain while the C-terminal region has ADP-ribosylation activity towards small GTP-binding proteins such as RAS family members. Expression of the C-terminal ADP-ribosylation region alone results in cell death, further clarifying the cytotoxic role of the ADP-ribosylation activity of ExoS. Activation of ADP-ribotransferase activity of ExoS has been tightly coupled to the interaction of ExoS with the 14-3-3 family of proteins. In fact both *in vitro* and *in vivo* data support the notion that ExoS relies on 14-3-3 as an activating cofactor. Further, mutations of key residues with in the ExoS binding site, for 14-3-3 result in diminished ADP-ribosylation activity of ExoS and show impaired virulence in a mouse pneumonia model [89,106]. The investigation of 14-3-3 dependent activation of a bacterial encoded cytotoxin determined a novel role for 14-3-3 proteins in their ability to act as cofactors to alter enzymatic function. Other examples of proteins whose enzymatic function is altered upon 14-3-3 binding include the pro-survival signaling molecule Raf-1, and the enzyme involved in the conversion of serotonin to melatonin in the pinealocytes, serotonin-N-acetyltransferase (AANAT) [88,103,118-120].

***14-3-3 binding contributes to altered protein-protein interactions***

In addition to sequestering interacting proteins and acting as enzymatic modulators, 14-3-3 proteins can also bridge multiple proteins together into a complex. Because 14-3-3 proteins function as dimers in the cell, two amphipathic grooves are available for binding to client proteins (one on each monomer). Therefore each monomer can bind to an independent client bringing two into close proximity with each other.

We focus on the role of 14-3-3ζ in Alzheimer's disease to illustrate this function. Alzheimer's is the most common form of dementia that can be attributed to the formation of neurofibrillary tangles or aggregates in the brains of these patients. In Alzheimer's the scaffolding of tau to glycogen synthase kinase 3β (GSK3β) is found to be one of the causative reasons for aggregate formation [121]. Scaffolding of tau protein to GSK3β is accomplished by 14-3-3ζ [122]. In this case, 14-3-3ζ is fundamental for the formation of these two molecules into the microtubule-associated tau phosphorylation complex. This complex has been found to be indispensable for tau induced phosphorylation that accumulates in Alzheimer's disease. In the absence of 14-3-3ζ, the ability of the proteins to come together and function is abrogated implicating 14-3-3ζ as a key component in Alzheimer disease pathology [122]. The adapter function of 14-3-3 proteins is also evident with Raf-1 proteins, which are bridged to BCR, PKC-z or A20 through 14-3-3 [123,124].

**Cellular survival functions associated with 14-3-3**

The ability of 14-3-3 proteins to regulate over 200 cellular ligands via the aforementioned mechanisms suggests a prominent role for 14-3-3 proteins in the cell. A functional relevance for 14-3-3 proteins in enhancing cell survival has been well established. First, 14-3-3 proteins aid in the activation of pro-survival molecules such is the case for Raf-1. Although complex due to multiple 14-3-3 binding sites, it is accepted that 14-3-3 binding to Raf-1 is necessary for Raf-1 activation (see[125] for review). Additionally, 14-3-3 binding contributes to the inactivation of cell cycle regulatory proteins such as $p27^{Kip1}$ and $p21^{WAF1}$ [126-128]. Both p21 and p27 are phosphorylated by Akt, which then generates 14-3-3 binding sites. When bound to 14-3-3 both proteins are excluded from the nuclear compartment and cannot act to inhibit cell cycle progression. Finally, the function of

proteins involved in inducing apoptosis is impaired when they are complexed with 14-3-3. This is most notably seen for Apoptosis Signal Regulating Kinase 1 (ASK1), which when bound to 14-3-3 can no longer phosphorylate its downstream targets MKK3/6 and MKK4/7 leading to suppression of ASK1-induced apoptosis [129].

Based on the above functions of 14-3-3 proteins, it is suggested that loss of 14-3-3 proteins or impaired 14-3-3 client protein interactions, should lead to cell death. Indeed this is the case and has been proven both directly and indirectly. Induction of cell death is observed when the 14-3-3 binding mutant, K49E, is overexpressed in cell culture [129]. This mutant has been reported to act as a dominant negative based on the fact that 14-3-3 proteins function as dimers [93,100,103]. When the K49E mutant is overexpressed, it is thought to interact with endogenous 14-3-3 proteins rendering them "inactive". A more direct assessment of the role that 14-3-3 proteins play in cell survival is seen when a peptide inhibitor of 14-3-3 is expressed [130]. The peptide disrupts endogenous 14-3-3 client protein binding by competing with the clients for 14-3-3 binding. Thus in the presence of the peptide, the client proteins are liberated from 14-3-3 and apoptosis is induced. These both imply a prominent role for 14-3-3 proteins in maintaining cell survival in the cell. It further supports that elevated 14-3-3 protein levels in the cell can activate growth and survival pathways while decreased 14-3-3 protein loads may act to suppress growth. Thus, identification of the mechanism involved in maintaining a proper level of 14-3-3 proteins is important for potential targeted therapies aimed at controlling 14-3-3 levels.

**Transcriptional and translational regulation of 14-3-3 proteins**

The cell-based activity of 14-3-3 proteins is attributed to their interaction with a large number of client proteins involved in multiple cellular functions as mentioned above. As such, changes in 14-3-3 protein levels can have a major impact on cellular function. The events leading to changes in 14-3-3 protein levels suggest the possibility of transcriptional regulation, translational regulation or a combination there of. However, up until now, of the seven 14-3-3 isoforms, sigma is the only one that has been well studied at this level.

Unlike the other six isoforms, 14-3-3σ behaves as a tumor suppressor whose levels are reduced in a multitude of human epithelial cancers including head-and-neck, squamous cell carcinomas, oral carcinomas, bladder carcinomas, lung cancers, and hepatocellular carcinomas [131-136]. Most intensely studied in breast cancer, Vercoutter-Edouart et al. used a proteomics approach to show that 14-3-3σ is only visible in normal breast epithelial cells but not in breast tumor tissue [137]. In a separate study, the mRNA of sigma was found to be undetectable in 45 out of 48 primary breast carcinomas [138]. It was determined that gene silencing in these tumors occurs at an epigenetic level due to hypermethylation of the CpG island within the promoter of *sfn*, the gene encoding 14-3-3σ. Demethylation of the promoter with 5-aza-2'-deoxycytidine decreased the promoter methylation with subsequent increases in transcript. Conversely to the epigenetic silencing of *sfn*, the p53 transcription factor is involved in inducing *sfn* gene expression [139]. A functional p53 binding site 1.8 kilobases upstream of the *sfn* transcriptional start site was identified. In response to DNA damage, p53 is recruited to the promoter resulting in gene activation leading to G2-M arrest. Again attesting to the tumor

suppressive nature of this gene. These and other studies of 14-3-3σ expression suggest a mode of regulation at the genomic and transcriptional level of this specific isoform.

Little is known about the regulation of the expression of the remaining six isoforms. It seems likely that they too will contain transcriptional and translational components, however research supporting this notion has been lacking. Indeed, both the promoter and the 5'UTRs (untranslated regions) of each of the isoforms are quite divergent. Moreover, *in silico* databases predict rather large CpG islands in the promoters and/or 5'UTRs for all the genes encoding 14-3-3 isoforms (Table 1.1). Further, both the beta and zeta isoforms express multiple transcript variants that may add another layer of complexity to their regulation. To support this regulation, Qi et. al. show that the mRNA levels of the oncogenic 14-3-3 isoforms, β, γ, σ, θ, ε and ζ are found in abundance in lung cancer biopsies relative to normal tissue[140]. More specifically, the genes encoding 14-3-3 β, γ, σ, and τ were elevated in 11, 10, 13 and 8 of the 14 biopsies examined, respectively. Therefore, the possibility exists for both epigenetic and transcriptional regulation for the remaining isoforms including mRNA stability and altered translation efficiencies. This becomes increasing more important as the independent role for 14-3-3 isoforms in disease pathology is established.

**Role of 14-3-3 in disease**

As master regulators in the cell, aberrant 14-3-3 levels have been correlated with a wide variety of diseases. For example, the zeta isoform alone has been identified in protein aggregates in neurodegenerative diseases such as Alzheimer's, Creutzfeldt-Jacob's and Huntingtin's [141-145]. These three diseases all present with a misfolded protein response. For example, in Huntingtin's, there is an accumulation of polyglutamine expanded

huntingtin proteins that form high-molecular weight, insoluble aggregates in effected neurons. When 14-3-3ζ (but not β nor η) was knocked-down in effected neurons, aggregate formation was abolished [142]. The pathology of knocking down 14-3-3ζ in the brains of a model system has not yet been established. It is postulated that a because a reduction in huntingtin aggregate formation can lead to suppression of the pathology of this disorder that perhaps a loss of 14-3-3ζ may do the same. It seems likely that since 14-3-3 proteins interact with and inhibit proteins involved in the misfolded protein response such as ASK1, that elevations in 14-3-3 could indeed lead to unchecked protein aggregates as is the case with the above aforementioned neurodegenerative diseases. Further, due to the very hydrophobic amphipathic groove of the 14-3-3 molecule, direct interactions with the hydrophobic misfolded proteins could also lead to disease forming aggregates. Although research supporting this notion is not complete, it seems quite clear that 14-3-3ζ plays a prominent role in these diseases and that regulating 14-3-3ζ protein levels may be one means to control aggregate formation.

More recent studies have identified a negative correlation between 14-3-3ζ protein levels and disease free survival in breast and head-and-neck/oral squamous cell carcinomas (HNOSCC) [146,147]. Further, elevated 14-3-3ζ proteins are evident in, lung, prostate, stomach, liver and uterine cancers [140,148-150]. Although the research supporting the correlation and/or contribution to tumorigenesis is incomplete, it seems likely that there will be a role for multiple14-3-3 isoforms in this deadly disease. Indeed, overexpression of 14-3-3β causes MAPK-dependent tumor formation in nude mice, while overexpression of 14-3-3τ leads to an enhanced growth rate of tumor cells [151,152]. Further, 14-3-3ζ is necessary for anchorage-independent growth, which is a hallmark of

cancer cells [153]. These data and others suggest a role for individual 14-3-3 isoforms in the development and maintenance of cancer and are guiding researchers towards the design of novel therapeutics aimed at targeting individual isoforms.

**Targeting 14-3-3 for therapeutic development**

The broad function of the 14-3-3 proteins in cell survival signaling, and the inverse-correlative studies between elevated 14-3-3 protein levels and disease free survival, make targeting 14-3-3 proteins promising for therapeutic intervention. Current efforts are focused on disrupting 14-3-3 client protein interaction. As one could imagine, impinging on 14-3-3 client interactions would liberate pro-apoptotic proteins such as Bad and Ask1, while suppressing the activities of pro-survival proteins such s Raf-1. Further, proteins involved in cell cycle checkpoint such as p21 and p27, would be allowed to freely translocate to the nucleus and control unwanted cellular amplification.

Although this approach is promising, developing isoform specific inhibitors at the protein-protein interaction level is challenging. Due to the high degree of amino acid identity, generation of molecular probes to one isoform will most likely block the remaining six [130]. To gain a better understanding of the possibility to develop isoform specific inhibitors or activators, a clear understanding of the genetic regulation of the individual isoforms is necessary. The zeta isoform has been shown to play an important role in tumorigenesis and neurodegenerative disease. Its upregulation has been correlated with poor survival in both populations [147]. Thus, identification of regulatory mechanisms that control zeta expression may lead to novel zeta-specific targeting strategies for the development of new therapeutics. My research focusing on the transcriptional regulatory mechanism governing 14-3-3ζ expression are outlined in Chapter 3. Multiple transcripts

were identified in this study. A transcriptional mode of regulation dependent on expression of a dominant transcript whose expression is regulated by CREB family members was a major finding. Therefore a brief overview of the family follows.

## CREB/ATF family of transcription factors

### Identification

The cyclic AMP response element binding protein (CREB) was identified in 1987 through its ability to bind to an 8 bp inverted palindromic sequence, now termed CRE, or cyclic AMP response element (TGACGTCA) [154]. Montminy et al. determined that CREB binding to this highly conserved palindrome could control cyclic-AMP (cAMP) induced expression of the neuronal hormone, somatostatin [155]. Since that time multiple spliced isoforms of CREB have been characterized in both mouse and human (see figure 1.7 for an example). Two of these, $\alpha$, and $\Delta$, are equal in their expression and are ubiquitously expressed. They can bind the CRE sequence with no difference in their activity, including a third minor product, beta that is missing the first 40 amino acids. Two years after CREB was characterized, the activating transcription factor-1 (ATF-1) was identified and found to bind the adenovirus early promoters E2, E3 and E4 at sites with a similar sequence to those bound by CREB [156]. Later CREB, ATF-1 and the cAMP response modulator (CREM) were grouped into one of six ATF/CREB subgroups based on amino acid and domain similarity (Figure 1.7).

### Protein structure

CREB and its family members, ATF-1 and CREM, contain a number of functional domains required for their transcriptional activation and/or repression (figure 1.7). First

is the basic leucine zipper domain (bZIP). This domain, which is found in other members of the bZIP superfamily, including cFos, cJun, cMyc and C/EBP, mediates dimerization through salt bridges and hydrogen-bonds between CREB family members [157]. Nucleotide base recognition is carried out by the basic region, which contains two extended a-helices rich in basic residues including the invariant basic-domain residues Asn293 and Arg301 [158]. While the bZIP and basic domains mediate dimerization and nucleotide recognition respectively, the remaining domains serve to facilitate interactions with coactivators and components of the transcriptional machinery. The most abundant CREB isoforms, α and Δ, contain two glutamine rich domains (Q1 and Q2) that flank the kinase inducible domain (KID) [159,160]. The critical residue (S133) resides in the KID [160]. Stimuli induce phosphorylation at S133 results in recruitment of coactivators such as CREB-binding protein (CBP) and its homologue p300 [160]. Binding of the coactivators to CREB family members is believed to function as the trigger for gene expression. Indeed, CREB is activated in the absence of stimuli as well [161]. The Q2 region interacts with basal transcriptional machinery to induce stimuli-independent gene activation.

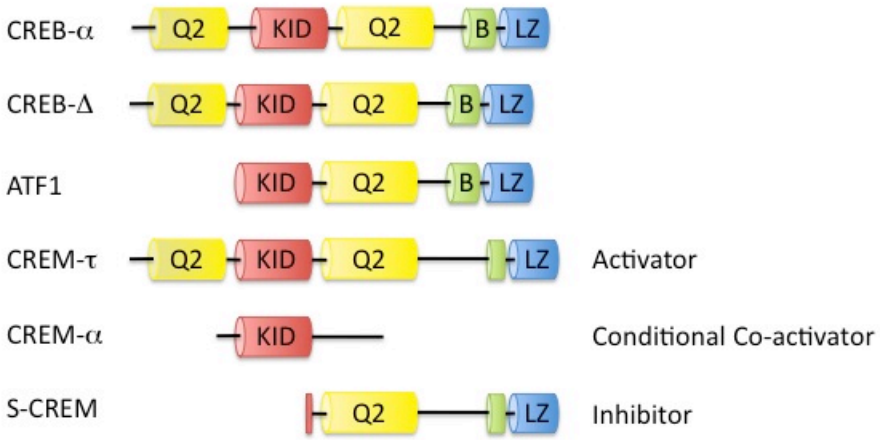


**Figure 1.7 Representation of CREB family members.** Q2, glutamine rich domain; KID, kinase inducible domain; B, basic domain; LZ, leucine zipper domain.

**Signaling to CREB and ATF Family Members**

CREB family members are considered prototypical stimulus-induced transcription factors. In fact CREB was the first transcription factor identified that was regulated by stimulus-induced post-translation modification [162]. The main activating stimulator for CREB is cAMP. Binding of ligands to external receptors results in either activation or inhibition of cAMP-dependent pathways ultimately effecting cAMP-target gene transcription. One of the major activating kinases downstream of cAMP is protein kinase A (PKA) [163,164]. Binding of cAMP to two PKA regulatory subunits releases the catalytic subunits of PKA enabling them to phosphorylate target proteins [165]. Some of the activated PKA subunits translocate to the nucleus where they directly phosphorylate members of the CREB family (at S133 on CREB for example) [166]. Phosphorylated CREB becomes a target for coactivator binding and subsequent expression of cAMP-induced genes [162]. Although the cAMP-PKA complex is the most reported activator of CREB family members, over 300 stimuli and multiple kinases can result in phosphorylation of CREB, including TNFα [162].

**Functions downstream of CREB**

Most of the literature focuses on the role of CREB in the brain ranging from development to plasticity to disease. Elevated CREB in the brain is thought to aid in neuronal survival, long-term memory potentiating and to protect the brain following ischemic insult [167]. One mechanism by which it protects the brain is through the expression of neuroprotective genes such as the anti-apoptotic protein Bcl-2 [168]. As discussed in the previous section, Bcl-2 is an anti-apoptotic molecule that can suppress Bad-induced apoptosis. As such treatments aimed at ischemic precondition are being considered.

This therapy results in increased levels of activated CREB (p-S133) leading to elevations in Bcl-2, which results in decreased caspase-3 activation [167]. Although CREB-related therapies may be promising for brain protection and endogenous neurogenesis, similar elevation in these pro-survival genes beyond the brain can result in tumorigenesis. Indeed this is the case with CREB family members.

**CREB family members in oncogenesis**

While CREB traditionally plays a role in glucose homeostasis, and learning and memory in the brain, its activation can be triggered in other tissues in response to growth factors and mitogenic signaling [162]. Signals such as insulin-like growth factor, hypoxia, and survival signals activate pro-survival pathways such as MEK/ERK, AKT, and Ras-dependent signaling pathways, which participate in the induction of CREB [162]. Indeed a direct role for both ATF-1 and CREB in promoting oncogenesis has been established [169-172].

ATF-1 and CREB were both found to be upregulated in human melanoma [169]. Jean et al., show reduced tumorigenicity and metastatic potential in nude mice only when cells overexpressed either a dominant negative form of CREB (KCREB) or when an antibody to ATF-1 were used in this xenograft model [170,171]. Clinical relevance for elevated CREB in oncogenesis also exists. Acute leukemic patients typically present with upregulated levels of CREB [173,174]. This elevation is associated with CREB induced gene amplification that leads to a inverse correlation between elevated CREB levels and less favorable prognosis in these patients. These reports suggest a role for ATF-1 and CREB in tumor cell survival and in their ability to activate pro-survival genes. However specific cancer-causing targets of CREB and ATF-1 are still being identified.

The majority of tumors that have elevated CREB develop from melanocytes or are of myeloid origin. A similar pattern in *ywhaz* transcript level is observed in hematopoiesis. Suggesting the possibility that CREB could be a potential candidate for controlling 14-3-3ζ expression in these tissues. Indeed the work in Chapter 3 describes a functional CRE element located in the promoter for *ywhaz*, the gene encoding 14-3-3ζ. Mutation of this element caused a reduction in activation from the promoter of *ywhaz*. Furthermore, 14-3-3ζ protein levels were decreased following ATF-1 silencing.

# Chapter 2: Inhibition of IKK-NF-κB signaling pathway by EF24, a novel monoketone analogue of curcumin

Andrea L Kasinski, Yuhong Du, Shala L Thomas, Jing Zhao, Shi-Yong Sun, Fadlo R. Khuri, Cun-Yu Wang, Mamoru Shoji, Aiming Sun, James P. Snyder, Dennis Liotta, and Haian Fu

Andrea Lynn Kasinski contributed to the design and execution of major experiments described in this chapter except for cell viability assay (SLT and JZ) and nuclear translocation experiments (YD).
Experimental design, data analysis and manuscript preparation was shared by A.L.K. and H.F..
Regents were provided by S.Y.S., F.R.K., C.Y.W., M.S., A.S., J.P.S, and D.L..

# Inhibition of IKK–NF-κB signaling pathway by EF24, a novel monoketone analogue of curcumin

Andrea L Kasinski, Yuhong Du, Shala L Thomas, Jing Zhao, Shi-Yong Sun, Fadlo R. Khuri, Cun-Yu Wang, Mamoru Shoji, Aiming Sun, James P. Snyder, Dennis Liotta, and Haian Fu

Graduate Programs in Genetics and Molecular Biology (A.L.K), and in Molecular and Systems Pharmacology (S.L.T), Departments of Pharmacology (Y.D., J.Z., H.F.), Hematology & Oncology (S.Y.S, F.R.K, M.S.), and Chemistry (A.S., J.S., D.L.), and Emory Chemical Biology Discovery Center (Y.D, A.S., J.S., D.L., H.F.), Emory University, 1510 Clifton Road, Atlanta, GA 30322; Division of Oral Biology and Medicine (C.Y.W), UCLA Dentistry, Los Angeles, CA 90095

## Abstract

The nuclear factor kappa-B (NF-κB) signaling pathway has been targeted for therapeutic applications in a variety of human diseases such as cancer. A number of naturally occurring substances, including curcumin, have been investigated for their actions on the NF-κB pathway because of their significant therapeutic potential and safety profile. A synthetic monoketone compound termed EF24 was developed from curcumin and exhibited a potent anticancer activity. Here we report a mechanism by which EF24 potently suppresses the NF-κB signaling pathway through direct action on the I-κB kinase (IKK). We demonstrate that: (i) EF24 induces death of lung, breast, ovarian, and cervical cancer cells with a potency about 10 times higher than curcumin; (ii) EF24 rapidly blocks the nuclear translocation of NF-κB with an $IC_{50}$ of 1.3 μM compared with curcumin with an $IC_{50}$ of 13 μM; (iii) EF24 effectively inhibits TNFα-induced I-κB phosphorylation and degradation, suggesting a role of this compound in targeting IKK; and (iv) EF24 indeed directly inhibits the catalytic activity of IKK in an *in vitro* reconstituted system. Our study identifies IKK as an effective target for EF24 and provides a molecular explanation for a superior activity of EF24 over curcumin. The effective inhibition of TNFα-induced NF-κB signaling by EF24 extends the therapeutic application of EF24 to other NF-κB-dependent diseases, including inflammatory diseases such as rheumatoid arthritis.

## Introduction

Curcumin, isolated from the rhizomes of the plant *Curcma longa* L, is the major component of the spice curry. This compound, freely available in the human food supply, is associated with numerous therapeutic benefits including chemoprevention and chemotherapy in cancer, anti-inflammatory, antioxidant, and antiviral activities [175-178]. In addition, the pharmacological safety of curcumin is evident by its consumption for centuries at levels up to 100 mg/day by people in certain countries [179]. These beneficial properties have attracted numerous efforts for the development of curcumin as a safe therapeutic agent [18,180]. Recent therapeutic efficacy against pancreatic cancer in a phase II clinical trial further supports the use of curcumin as a lead for the development of a new class of anticancer agents [181]. Unfortunately, due to the low potency and poor absorption characteristics of curcumin, its clinical potential remains to be limited [19]. However, curcumin represents an ideal lead compound for further chemical modification and optimization [5,6].

In an attempt to retain curcumin's favorable medicinal properties and safety profile, while increasing its potency, computer-assisted topological searches of the NCI database were carried out to identify lead analogs. Two such analogs incorporating a monoketone were identified and exhibited improved cytotoxic effect over curcumin [5]. These results stimulated a more thorough search for easily prepared and readily functionalized analogs with improved potency. The strategy adopted is captured by the following manipulation of curcumin. Two carbons and an oxygen were removed from the center of the molecule to produce a monoketone, terminal ring substituents were varied, and an extensible heterocyclic six-membered ring including the ketone was

installed (see Figure 2.1 for an example). Approximately 100 analogs were tested. A subset of 10 was further evaluated in the 60 panel of NCI cancer cell lines and in several in vitro anti-angiogenesis screens [5]. EF24 (Figure 2.1) surfaced as one of the top candidate compounds. EF24 has shown to induce apoptosis in cancer cells and inhibit the growth of human breast tumors in a mouse xenograft model with relatively low toxicity and at a dose much less than that of curcumin [5,6]. Studies with various cancer cells have suggested a model that EF24 impairs cell growth by inducing G2/M arrest followed by induction of apoptosis, which is accompanied by caspase-3 activation, phosphatidylserine externalization, and an increased number of cells with a sub-G1 DNA content [6]. However, the cell signaling pathways that mediate the EF24 effect remain to be elucidated. This study examines the effect of EF24 on a key survival pathway in lung cancer cells mediated by the NF-kB transcription factor.

NF-κB is maintained in an inactive state in the cytoplasm by the inhibitor of kappa B (Iκ-B), which masks the nuclear localization signal of NF-κB. Phosphorylation of Iκ-B by the inhibitor of kappa B kinase (IKK), via the canonical NF-κB pathway, results in subsequent ubiquitination of Iκ-B and proteasomal degradation. It is this degradation of Iκ-B that liberates NF-κB, allowing its localization to the nucleus and the transcriptional activation of its target genes. Although imperative for normal physiological processes, aberrant activation of NF-κB contributes to deregulated growth, resistance to apoptosis, and propensity to metastasize observed in many cancers [182,183]. The NF-κB effect is in part due to the upregulation of NF-κB -controlled genes that promote survival function of tumor cells, including c-myc, Bcl-xL, and members of IAP (Inhibitor of Apoptosis) family of genes. In addition, many anticancer agents can induce

the activation of NF-κB, resulting in reduced therapeutic efficacy [78]. Thus, agents that effectively impair the NF-κB pathway are expected to have significant therapeutic potential.

In this report, we identify the molecular mechanism of action of EF24. We show that treatment with EF24 results in a marked decrease in cellular viability. The dose necessary to reduce viability correlates well with that needed for EF24 to impair the nuclear translocation of NF-κB and to inhibit IKK. EF24 is at least 10 times more potent than curcumin and represents a lead compound for further therapeutic development of a new generation of natural product-derived anticancer agents.

## Materials and Methods

*Materials* –Curcumin was purchased from Alfa Aesar and its structural analog, namely EF24 (3,5-bis(2-flurobenzylidene)piperidin-4-one), was prepared as previously reported [5]. Both compounds were dissolved in DMSO with a stock concentration of 10 mM. TNFα (Sigma-Aldrich Chemicals, St Louis, MO) was resuspended in water to a final concentration of 10 μg/ml. Glutathione S-transferase-I-κBα (1-54) was purified from expression plasmid as previously described [184]. Antibodies against pS32-I-κBα and I-κBα were purchased from Cell Signaling (Beverly, MA). Antibodies against IKKα and IKKβ were purchased from Imgenex (San Diego, CA ). Antibodies to Raf-1, and secondary antibody conjugates, HRP-goat anti-mouse and HRP-goat anti-rabbit antibodies, were purchased from Santa Cruz Biotechnology (Santa Cruz, CA)

*Cell Cultures* – Cells were maintained in either in RPMI (A549, H157, H460, Calu-1, H358, PC3, 1A9, MDA-MB231), or DMEM (HeLa) with 10% fetal bovine serum (FBS) and penicillin/streptomycin in a 37°C incubator with 5% $CO_2$. For Western blot analysis, unless otherwise noted, cells were lysed in 1% NP-40 lysis buffer (1% Nonident P-40, 10 mM Hepes [N-2hydroxyethylpiperazine-N'-2-ethanesulfonic acid], pH 7.4, 150 mM NaCl, 5 mM NaF, 2 mM $Na_3VO_4$, 5 mM $Na_4P_2O_7$, 10 μg/ml aprotonin, 10 μg /ml leupeptin, 1 mM phenylmethylsulfonyl fluoride (PMSF).

*Cytotoxicity Assay* - Cells were plated at 5,000 cells/well in 96-well plates. They were treated with test agents in triplicate in the following day and further incubated for 48 hr

before viability assay was carried out. The sulforhodamine B assay was performed to evaluate cell viability and to obtain the $IC_{50}$ values [185,186]. It measures cellular protein content in order to determine cell density. The mean value and standard error for each treatment were determined and the cell viability index relative to control (untreated) was calculated. The $IC_{50}$ is defined as the concentration of agents that decrease viability by 50% in a total cell population (cell viability index = 0.5) as compared to control cells (cell viability index = 1) at the end of the incubation period.

*High content analysis of NF-kB subcellular translocation* - A549 cells were plated in 96-well plates (Becton Dickinson Labware, Franklin Lakes, NJ) at 10,000 cells/90 $\mu$l/well and grown for 20 hr. Test compounds were added to each well and incubated at 37°C. All samples were performed in triplicates. The cells were stimulated with TNFα as indicated. Reactions were terminated by washing the plates with ice-cold phosphate-buffered saline (PBS) followed by fixation with paraformaldehyde (2%, 100 $\mu$l) for 30 min at room temperature. Cells were permeabilized with Triton X-100 (0.1%, 100 $\mu$l) for 20 min, washed three times with PBS, and blocked with BSA (1%, 100 μl) for 1 hr. Rabbit anti-p65 NF-κB antibody (Santa Cruz biotechnology, Inc., Santa Cruz, CA) was added and incubated overnight at 4°C. Cells were washed three times in PBS and incubated with goat anti-rabbit IgG with conjugated Alexa Fluor 488 (50 $\mu$l; Molecular Probes, Inc., Eugene, OR) along with Hoechst 33342 (1 $\mu$g/ml; Promega, Madison, WI). After washing with PBS, cells were imaged with the ImageXpress 5000 with the filter set for FITC ( Ex: 490 nm, Em: 525 nm and dichroic mirror at 505 nm) and DAPI ( Ex: 350 nm; Em: 479 nm with dichroic mirror at 400 nm) (Molecular Devices, Sunnyvale, CA).

The images were quantified and analyzed using MetaXpress software (Molecular Devices). "Translocation Enhanced" module was used for the NF-κB translocation analysis. The nucleus was defined by Hoechst 33342 staining. The levels of NF-κB translocation were calculated and expressed as the difference between average fluorescence intensity in nucleus and in cytoplasm (Nuc – Cyt). After stimulating with TNFα, the inhibitory effect of test compounds on TNFα induced NF-κB translocation was expressed as % of fluorescence intensity difference (Nuc-Cyt) in the control wells (TNFα only) after subtracting background (no TNFα treatment). Data shown are average values from triplicate samples.

*Western Blotting* – Cells were lysed in NP-40 buffer (1.0% NP-40, 10 mM Hepes, pH 7.4, 150 mM NaCl, 5 mM NaF, 2 mM $Na_3VO_4$, 5 mM $Na_4P_2O_7$, 10 $\mu$g/ml aprotinin, 10 $\mu$g/ml leupeptin, 1 mM PMSF). Equal volumes of cell lysate were subject to electrophoresis on SDS-PAGE (12.5%). Proteins were then electrotransfered to a nitrocellulose membrane (GE water and Process Technologies, Trevose, PA ) as described previously [129]. Membranes were blocked in a solution of 5% non-fat dry milk in TBS-T buffer (20 mM Tris pH 7.6, 500 mM NaCl, 0.5% Tween-20) for 30 min followed by incubation with primary antibody for at least two hours. The membrane was then washed and treated with the corresponding horseradish peroxidase-conjugated anti-mouse immunoglobulin [Ig] or anti-rabbit Ig as indicated. Immunodetection was performed using West Pico (Pierce, Rockford, IL) or West Dura (Pierce) followed by imaging on Kodak's Image Station 2000R (New Haven, CT).

*Immunoprecipitation* – Cells were seeded in 150 mm plates to approximately 70% confluency one day before treatment. Cells were treated with increasing doses of EF24 or curcumin with or without TNFα as indicated and lysed in 1% NP-40 lysis buffer at 4°C. Lysates were clarified by centrifugation (14,000 rpm, 10 min, 4°C). Cytoplasmic extracts were immunoprecipitated with an anti-IKKα antibody (Imgenex, San Diego, CA) at 4°C overnight. Protein G Sepharose beads (50% slurry; Pharmacia) in lysis buffer were added to each reaction the following day and incubated for an additional two hours. Protein G beads were then gently spun down and washed two times with NP-40 lysis buffer and one final time with the kinase assay buffer (50 mM Hepes, pH 7.4; 20 mM $MgCl_2$; 2 mM DTT)). The immunocomplexes were used for IKK kinase assays.

*Kinase assays* – (***a***) IKK immunocomplex assay. Immunoprecipitated complexes were added to kinase reaction buffer containing [$\gamma$-$^{32}$P]ATP (20 μCi with 10 μM unlabeled ATP), and glutathione S-transferase (GST)-I-κBα (residues 1-54; 5 μg) in a total volume of 25 μl and incubated at 30°C for 30 min. Reactions were stopped by boiling the kinase solution in a 6 X SDS sample buffer for 5 min. The samples were resolved on SDS-PAGE (12.5%). The top portion of the gel was transferred and immunoblotted with anti-IKKβ antibody while the bottom portion was stained with Coomassie Blue dye (0.05%). Radiolabeled phosphate incorporation into GST- I-κBα was assessed by the PhosphoImager and quantified with the ImageQuant software (Molecular Dynamics, Sunnyvale, CA). (***b***) *In vitro* recombinant IKKβ assay. Activated recombinant IKKβ in MOPS buffer (8 mM MOPS-NaOH, pH 7.0, 200 μM EDTA, 15 mM $MgCl_2$) (Upstate Cell Signaling Solutions, Lake Placid, NY;) was used to assess the direct effect of EF24

or curcumin on the kinase. The test compounds were incubated in the presence of 40 ng of IKKβ for 15 minutes at room temperature. The addition of Mg-ATP cocktail (15 mM $MgCl_2$, 100 μM ATP, 8 mM MOPS-NaOH, pH 7.0, 5 mM β-glycero-phosphate, 1 mM EGTA, 200 nM sodium orthovanadate, 200 nM DTT) purified GST- I-κBα (5 μg) and [γ-$^{32}$P]ATP (0.5 μCi) in a final volume of 25 μl started the reaction which was allowed to proceed at 30°C for 15 min. Reactions were terminated and processed as described in (*a*). In addition, the radiolabeled GST-I-κBa protein bands were excised for quantification with a scintillation counter (Beckman LS 6500, Beckman Coulter, Fullerton, CA). For competition assays, total ATP was varied while the ratio of [γ-$^{32}$P]ATP to cold ATP remaining constant in the reaction. Test compounds and ATP were incubated in the presence of IKKβ (20 ng) at room temperature. At various time-points within the linear range of the enzyme, the reaction was terminated by spotting assay mixture (5 μl) onto P81 phosphocellulose paper (Whatman). The filters were washed three times with phosphoric acid (0.75%) and once with acetone. Radioactivity was determined by liquid scintillation counting.

## Results

### EF24 exhibits a more potent cytotoxic effect than curcumin

To evaluate the potency of EF24 in comparison to its parent compound curcumin, we carried out cell viability tests with the SRB assay on a panel of lung cancer cells (Figure 2.2). Treatment of cells with both EF24 and curcumin led to a significantly decreased viability. Dose-response studies revealed that the $IC_{50}$ of EF24 was in the range of 0.7 to 1.3 μM for various cell lines as summarized in Table 2.1 (Figure 2.2). Under the same treatment condition, the $IC_{50}$ for curcumin ranged from 15 – 20 μM. These data indicate a more potent cytotoxic effect of EF24 over curcumin for lung cancer cells. This study was extended to include ovarian, breast, prostate, and cervical cancer cells. A similar trend was observed with EF24 exhibiting an $IC_{50}$ at least 20 fold lower than curcumin for each cell line, respectively, with the exception of PC3 (10-fold lower) (Table 2.1). These results are consistent with previous reports and demonstrate that this monoketone analog of curcumin, EF24, has a much-improved cytotoxic activity over the parent compound [5,6].

### High content analysis (HCA) revealed an effective EF24 action in blocking nuclear translocation of NF-κB

In order to understand the mechanism of action of EF24 for its improved bioactivity, we examined its effect on the NF-κB signaling pathway, which is suggested to be targeted by curcumin [187,188]. The NF-κB transcription factor mediates a critical survival mechanism in lung cancer cells. To monitor the activation status of NF-κB, we employed a HCA approach to visualize the dynamic movement of the NF-κB p65 subunit between the

cytoplasm and nucleus under various experimental conditions. The p65 subunit in A549 cells was detected with an immunofluorescent probe and its movement was captured through an automated fluorescence microscopy (Figure 2.3). To validate the HCA assay and to establish experimental conditions for testing the EF24 effect, we initially utilized a known NF-κB activator, TNFα, to manipulate the NF-κB movement [189]. While the majority of the p65 subunit was detected in the cytoplasm, the addition of TNFα (10 ng/ml) resulted in complete translocation of the p65 protein into the nucleus as indicated by overlapping p65 green fluorescent signal with DAPI stained blue nuclear signal (Figure 2.3a). Time course and dose-response experiments were carried out to establish an $EC_{50}$ for TNFα (1.5 ng/ml), which was used to set the subsequent experimental conditions (Figure 2.3b). To examine whether EF24 has any effect on the NF-κB pathway, A549 cells were pretreated with EF24 before TNFα was added to cause predominant nuclear translocation of NF-κB. Strikingly, EF24 pretreatment retained the NF-κB in the cytoplasm even when the amount of TNFα used completely relocated the p65 subunit to the nucleus. Curcumin showed a similar effect albeit with much higher concentration in order to achieve an effect as EF24 (Figure 3.3). Quantification of captured images under various experimental conditions led to the establishment of dose-response curves, which gave rise to an $IC_{50}$ of 1.3 μM and 13 μM for EF24 and curcumin, respectively (Figure 3.3c). The ten fold difference in blocking the NF-κB translocation activity between EF24 and curcumin as revealed by the quantitative HCA is consistent with their difference in cytotoxicity against lung cancer cells. It is likely that EF24 induces cell death in part through interfering with the NF-κB-mediated survival signaling.

**EF24 inhibits TNFα-induced I-κB phosphorylation and subsequent degradation**

When in the cytoplasm, NF-κB is associated with I-κB as an inactive protein complex. Nuclear translocation of NF-κB requires dissociation of I-κB, which is controlled by phosphorylation of I-κB at S32 and S36 and the subsequent degradation induced by various extracellular signals including TNFα [190]. It is possible that EF24's effect on nuclear translocation of NF-κB is through its action on I-κB phosphorylation and/or degradation. To test this model, we first established conditions to monitor the status of I-κB phosphorylation and degradation that takes into account their transient nature. A549 cells were treated with TNFα. Phosphorylation of I-κB was visible within three minutes of treatment and reached a high level in approximately seven minutes. It was sustained for an additional six minutes (Figure 3.4a). I-κB phosphorylation was followed by its degradation. Degradation was most notably detected after 20 minutes of treatment with TNFα while the control protein, Raf-1, remained stable during the entire course of the test. Based on these observations, cells were treated with TNFα for 10 min for detecting I-κB phosphorylation and for 20 min for monitoring I-κB stability in subsequent experiments.

To examine the effect of EF24 on I-κB stability, A549 cells were pretreated with EF24 (5 μM) or curcumin (5 or 50 μM) followed by stimulation with TNFα. As shown in Figure 3.4b, TNFα alone rapidly induced I-κB degradation while pretreatment with EF24 (5 μM) for only 10 min was able to effectively block the TNFα effect, showing accumulated I-κB even in the presence of TNFα. However, curcumin required a much higher concentration (50 μM) and a longer period of time (60 min) in order to achieve a

level of inhibition similar to EF24. As a control, Raf-1 remained stable during these experimental conditions, suggesting a specific effect of TNFα on I-κB.

Because phosphorylation of I-κB precedes its degradation, we next examined the effect of EF24 on TNFα-induced phosphorylation of I-κB. A549 cells were pretreated with EF24 or curcumin for 30 min before the addition of TNFα (10 min). Cells were harvested for probing the status of I-κB phosphorylation with a phosphor-specific antibody, pS32- I-κB (Figure 3.4c). EF24 inhibited TNFα-induced I-κB phosphorylation in a dose dependent manner with an $IC_{50}$ about ten fold less than that of curcumin (Figure 3.4d). These results suggest that EF24 antagonizes the nuclear translocation of NF-κB through its inhibitory action on the phosphorylation of I-κB and its subsequent degradation. In support of a selective role of EF24 in inhibiting the I-κB kinase signaling, further experiments showed that EF24 is unable to inhibit TNFα induced activation of JNK and ERK (Figure 3.S1).

**EF24 directly inhibits the IKKβ kinase activity**

Because phosphorylation of I-κB is catalyzed by IKK in the canonical NF-κB signaling pathway, the above results imply a more potent EF24 action over curcumin on the IKK protein complex. To examine whether EF24 and curcumin differentially target the cellular IKK complex for effective NF-κB inhibition, we monitored the kinase activity of IKK upon compound treatment and compared the efficacy of EF24 and curcumin. A549 cells were pretreated with increasing doses of either a compound or vehicle for one hour before the addition of TNFα (10 ng/ml, 10 min). Cells were lysed and heterotrimeric

IKK complexes were immunopreciritated with an antibody to IKKα. The kinase activity of the immunoprecipitated IKK complex was determined by its ability to phosphorylate recombinant GST-I-κB. While pretreatment of cells with EF24 was able to completely neutralize TNFα-activated IKK complex activity, pretreatment with curcumin required a much higher dose to achieve a similar effect (Figure 3.5). Although this cell-based immunocomplex kinase assay allows the detection of permeabilized compound effect on intracellular IKK complex activity, it is unable to distinguish a direct effect of compound on a specific kinase from an indirect effect. It is possible that EF24 directly targets the IKKβ activity, a well defined kinase for I-κB. To test this notion, a reconstituted *in vitro* kinase assay was employed with recombinant IKKβ and other defined components in the reaction. Increasing concentrations of EF24 or curcumin were incubated with active recombinant IKKβ for 15 minutes prior to the addition of substrate, GST-I-κB, and [γ-$^{32}$P]ATP. Incorporation of radiolabeled $^{32}$P to GST-I-κB was detected by radiography and quantified by scintillation counting of excised GST-I-κB protein bands (Figure 3.6). It is striking that EF24 effectively inhibited the ability of IKKβ to phosphorylate its physiological substrate I-κB, with an estimated $IC_{50}$ of 1.9 μM. Interestingly, EF24 also impaired the autokinase activity of IKKβ with a similar potency (data not shown). These data strongly support a direct role of EF24 in the inhibition of IKKβ. Curcumin however, shows a much weaker effect on IKKβ in the *in vitro* kinase assay with an apparent $IC_{50}$ of above 20 μM (Figure 3.6). It is clear that the structural change of curcumin to EF24 has drastically enhanced its inhibitory effect on IKKβ catalytic activity. Thus, this *in vitro* kinase assay with recombinant IKKβ reveals IKKβ as a direct target of EF24.

Further kinetics studies showed both a decrease in *K*m and *V*max when EF24 was

present in the IKKβ kinase assay, however Linweaver-Burk plots are not parallel (Figure 3.S2 and data not shown). This suggests that EF24 may be acting as a mixed-type inhibitor with respect to ATP. These data further strengthen our conclusion that EF24 directly acts on and inhibits IKKβ.

## Discussion

The monoketone analog of curcumin, EF24, has been shown to induce cell cycle arrest and apoptosis in a number of cancer cell lines with potency much higher than curcumin. Consistent with previous reports, EF24 exhibited $IC_{50}$ values 10-20 times lower than that of curcumin in a panel of non-small cell lung cancer cells with different genetic background as well as in ovarian, cervical, breast, and prostate cancer cells. However, the molecular mechanism that underlying the enhanced therapeutic efficacy remains to be defined. Here we present evidence that supports a direct action of EF24 on the NF-κB survival signaling pathway. The amount of EF24 required for suppression of lung cancer A549 cell growth has been correlated with its ability to prevent the nuclear translocation of p65 subunit of NF-κB, to block I-κB phosphorylation and its subsequent degradation, and to inhibit the catalytic activity of the IKK protein complex (Figure 3.7). Curcumin exhibited at least ten times lower potency in all of the above assays. Importantly, in an *in vitro* reconstituted kinase assay, EF24 has been shown to inhibit the kinase activity of IKKβ. Thus, direct targeting of IKKβ and its mediated survival signaling may partially explain the improved therapeutic potency of EF24 over curcumin.

Although the NF-κB signaling pathway has been implicated as one of the curcumin targets, a direct inhibitory effect of curcumin on the catalytic activity of a purified IKK protein has not been shown [191,192]. Our research identifies EF24 as a new chemical class of IKKβ inhibitors derived from the natural product curcumin. However, whether EF24 serves as a irreversible inhibitor of IKKβ requires further investigation. With the recognition of a new IKKβ inhibitor, EF24 may serve as a lead compound for further chemical optimization in search for more potent and efficacious IKKβ inhibitors

[193]. It should be noted that curcumin has been reported to be an inhibitor of a number of other kinases as well, in particular protein kinase C, epidermal growth factor receptor tyrosine kinase and mTOR serine/threonine kinase [187]. It remains to be determined whether EF24 may be active against other kinases. At this point, we have ruled out the possibility that EF24 acts as a general inhibitor of TNFα signaling by monitoring the phosphorylation status of two additional downstream targets of the TNFα pathway, JNK and ERK1/2. Neither of these kinases were found to be suppressed when EF24 was present (Figure 3.S1).

Why is EF24 a more effective inhibitor of IKKβ than curcumin? This question cannot be answered definitively in the present work, but a possible explanation can be outlined based on structural differences and the commonly accepted mechanism of kinase inhibition. Curcumin exists in the enol form both in the solid state and in solution [194,195]. In addition, in the crystal lattice, the molecule adopts an extended planar form that spans 19 Å in the longest direction (i.e. H---H). The X-ray structure of EF24, depicts a nonplanar molecule with a propeller arrangement of the terminal phenyl rings that incorporates a reasonable degree of flexibility and a long dimension of 15 Å (Snyder, J. P. and Sun, A. unpublished). Assuming that both curcumin and EF24 occupy at least partially the ATP binding site of IKKβ kinase as the origin of their inhibition, the shorter and more flexible EF24 would appear to be more adaptable to the globular binding pocket. For comparison, we refer to roscovitine, a compound that potently blocks a number of cyclin-dependent kinases [196]. Roscovitine is a nonplanar flexible molecule with a long dimension of 14 Å in a low energy conformation. The properties match those of EF24 and suggest that a compact and potentially mobile kinase ligand is best suited to the

ATP site. The mixed-type competitive inhibitor of EF24 with respect to ATP partially supports this notion. Ultimately, this hypothesis can be tested by determination of the X-ray structures of curcumin and EF24 bound to IKKβ.

The NF-κB pathway has been found to be activated in lung cancer, with various chemotheraputic regiments adding to already elevated NF-κB activation in tumors and representative cell lines [197,198]. Lung cancer A549 cells may have developed certain dependency on upregulated NF-κB pathway for sustained survival. This mechanism may involve upregulated NF-κB controlled survival genes, such as Bcl-XL and IAP. Thus, inhibition of IKKβ and its mediated NF-κB signaling by EF24 likely leads to the suppression of survival mechanism and the induction of cells death. Additionally, it has been reported that upregulated NF-κB also has a transcription independent function through suppression of tumor suppressor gene PTEN expression [199]. Activated p65 in nucleus has been shown to sequester the transcriptional coactivators CBP/p300, leading to the suppression of PTEN expression. PTEN is a negative regulator of Akt, a major survival kinase in A549 cells[200]. In addition to inhibiting NF-κB-controlled expression of survival genes, EF24-mediated IKK inhibition may result in the release of p65-sequestered CBP/p300 and the subsequent activation of PTEN. In support of our model, Selvendiran et al demonstrated that EF24 induces the expression of PTEN in ovarian cancer cells, which mediates EF24-triggered G2/M cell cycle arrest and apoptosis [201].

Because the IKK protein complex plays a vital role in cellular responses to many environmental signals under both physiological and pathological conditions, IKK inhibitors are known to have significant therapeutic values [193]. It is expected that the

EF24 class of agents may not only have a role as potential cancer therapeutics, but may also have important applications in various IKK/NF-κB dysregulated autoimmune and inflammatory diseases, including rheumatoid arthritis.

## Reference


1. Levi, M.S., Borne, R.F. & Williamson, J.S. A review of cancer chemopreventive agents. *Curr Med Chem* **8**, 1349-62 (2001).

2. Cheng, A.L. et al. Phase I clinical trial of curcumin, a chemopreventive agent, in patients with high-risk or pre-malignant lesions. *Anticancer Res* **21**, 2895-900 (2001).

3. Commandeur, J.N. & Vermeulen, N.P. Cytotoxicity and cytoprotective activities of natural compounds. The case of curcumin. *Xenobiotica* **26**, 667-80 (1996).

4. Osawa T, S.Y., Inayoshi M, Kawakashi S. Antioxidative activity of tetrahyrocurcuminids. *Biosci Biotechnol Biochem* **59**, 1609-12 (1995).

5. Satoskar, R.R., Shah, S.J. & Shenoy, S.G. Evaluation of anti-inflammatory property of curcumin (diferuloyl methane) in patients with postoperative inflammation. *Int J Clin Pharmacol Ther Toxicol* **24**, 651-4 (1986).

6. Anand, P., Kunnumakkara, A.B., Newman, R.A. & Aggarwal, B.B. Bioavailability of curcumin: problems and promises. *Mol Pharm* **4**, 807-18 (2007).

7. Aggarwal, S. et al. Curcumin (Diferuloylmethane) Downregulates Expression of Cell Proliferation, Antiapoptotic and Metastatic Gene Products Through Suppression of I{kappa}B{alpha} Kinase and AKT Activation. *Mol Pharmacol* (2005).

8. Dhillon N et al. Phase II clinical trial of curcumin in patients with advanced pancreatic cancer. *Journal of Clinical Oncology, 2006 ASCO Annual Meeting Proceedings* **24**, 14151 (2006).

9. Shoba, G. et al. Influence of piperine on the pharmacokinetics of curcumin in animals and human volunteers. *Planta Med* **64**, 353-6 (1998).

10. Adams, B.K. et al. Synthesis and biological evaluation of novel curcumin analogs as anti-cancer and anti-angiogenesis agents. *Bioorg Med Chem* **12**, 3871-83 (2004).

11. Adams, B.K. et al. EF24, a novel synthetic curcumin analog, induces apoptosis in cancer cells via a redox-dependent mechanism. *Anticancer Drugs* **16**, 263-75 (2005).

12. Richmond, A. Nf-kappa B, chemokine gene transcription and tumour growth. *Nat Rev Immunol* **2**, 664-74 (2002).

13. Rayet, B. & Gelinas, C. Aberrant rel/nfkb genes and activity in human cancer. *Oncogene* **18**, 6938-47 (1999).

14. Nakanishi, C. & Toi, M. Nuclear factor-kappaB inhibitors as sensitizers to anticancer drugs. *Nat Rev Cancer* **5**, 297-309 (2005).

15. Mercurio, F. et al. IKK-1 and IKK-2: cytokine-activated IkappaB kinases essential for NF-kappaB activation. *Science* **278**, 860-6 (1997).

16. Rubinstein, L.V. et al. Comparison of in vitro anticancer-drug-screening data generated with a tetrazolium assay versus a protein assay against a diverse panel of human tumor cell lines. *J Natl Cancer Inst* **82**, 1113-8 (1990).

17. Skehan, P. et al. New colorimetric cytotoxicity assay for anticancer-drug screening. *J Natl Cancer Inst* **82**, 1107-12 (1990).

18. Zhang, L., Chen, J. & Fu, H. Suppression of apoptosis signal-regulating kinase 1-induced cell death by 14-3-3 proteins. *Proc Natl Acad Sci U S A* **96**, 8511-5 (1999).

19. Lin, J.K. Molecular targets of curcumin. *Adv Exp Med Biol* **595**, 227-43 (2007).

20. Singh, S. & Khar, A. Biological effects of curcumin and its role in cancer chemoprevention and therapy. *Anticancer Agents Med Chem* **6**, 259-70 (2006).

21. Rothe, M., Sarma, V., Dixit, V.M. & Goeddel, D.V. TRAF2-mediated activation of NF-kappa B by TNF receptor 2 and CD40. *Science* **269**, 1424-7 (1995).

22. Beg, A.A., Finco, T.S., Nantermet, P.V. & Baldwin, A.S., Jr. Tumor necrosis factor and interleukin-1 lead to phosphorylation and loss of I kappa B alpha: a mechanism for NF-kappa B activation. *Mol Cell Biol* **13**, 3301-10 (1993).

23. Bharti, A.C., Donato, N., Singh, S. & Aggarwal, B.B. Curcumin (diferuloylmethane) down-regulates the constitutive activation of nuclear factor-kappa B and IkappaBalpha kinase in human multiple myeloma cells, leading to suppression of proliferation and induction of apoptosis. *Blood* **101**, 1053-62 (2003).

24. Deeb, D. et al. Curcumin sensitizes prostate cancer cells to tumor necrosis factor-related apoptosis-inducing ligand/Apo2L by inhibiting nuclear factor-kappaB through suppression of IkappaBalpha phosphorylation. *Mol Cancer Ther* **3**, 803-12 (2004).

25. Karin, M. NF-kappaB and cancer: Mechanisms and targets. *Mol Carcinog* **45**, 355-61 (2006).

26. Mague, J.T., Alworth, W.L. & Payton, F.L. Curcumin and derivatives. *Acta Crystallogr C* **60**, o608-10 (2004).

27. Payton, F., Sandusky, P. & Alworth, W.L. NMR study of the solution structure of curcumin. *J Nat Prod* **70**, 143-6 (2007).

28. Meijer, L. & Raymond, E. Roscovitine and other purines as kinase inhibitors. From starfish oocytes to clinical trials. *Acc Chem Res* **36**, 417-25 (2003).

29. Mukhopadhyay, T., Roth, J.A. & Maxwell, S.A. Altered expression of the p50 subunit of the NF-kappa B transcription factor complex in non-small cell lung carcinoma. *Oncogene* **11**, 999-1003 (1995).

30. Wang, C.Y., Mayo, M.W. & Baldwin, A.S., Jr. TNF- and cancer therapy-induced apoptosis: potentiation by inhibition of NF-kappaB. *Science* **274**, 784-7 (1996).

31. Vasudevan, K.M., Gurumurthy, S. & Rangnekar, V.M. Suppression of PTEN expression by NF-kappa B prevents apoptosis. *Mol Cell Biol* **24**, 1007-21 (2004).

32. Stambolic, V. et al. Negative regulation of PKB/Akt-dependent cell survival by the tumor suppressor PTEN. *Cell* **95**, 29-39 (1998).

33. Selvendiran, K. et al. EF24 induces G2/M arrest and apoptosis in cisplatin-resistant human ovarian cancer cells by increasing PTEN expression. *J Biol Chem* **282**, 28609-18 (2007).

## Footnotes

This work was supported in part by grants from NIH (R01 GM53165 to HF., P01 CA116676 to FRK, HF, and SS) and Emory URC. FRK, SS, and HF are GCC Distinguished Scholars. HF is a GRA Distinguished Investigator. YD is Emory Drug Development and Pharmacogenomics Academy Fellow and recipient of Emory Head and Neck cancer SPORE career development award (P50 CA128613). SLT is a recipient of AAAS/Packard Fellowship and Emory FACE program fellow.

## Figure legends

***Figure 2.1. Structures of curcumin and its analog EF24***

***Figure 2.2. EF24 shows more potent cytotoxic effect than curcumin on cancer cells***. Cells were grown in 96 well plates and were treated with EF24 or curcumin as indicated for 48 hr. Cell viability was assessed by the SRB method and expressed as % control (DMSO). Results with a panel of lung cancer cells are shown in panel ***a***: A549, H358 (lung adenocarcinoma); H460 (large cell carcinoma); H157 (squamous cell carcinoma); Calu-1 (lung epidermoid carcinoma). Panel ***b*** represents results with breast (MDA-MB231), cervical (HeLa), prostate (PC3), and ovarian (1A9) cancer cell lines.

***Figure 2.3. EF24 impairs TNFα induced NF-κB nuclear translocation.*** A549 cells were grown in 96-well plates and treated with TNFα or control (DMSO) for 30 min before sample processing for the detection of NF-κB as described in Materials and Methods (Upper two rows of ***a***). The induction of NF-κB nuclear translocation by TNFα was quantified as shown in ***b*** with an apparent $EC_{50}$ of 1.5 ng/ml. The effect of EF24 or cucumin treatment (30 min) on TNFα induced nuclear translocation of NF-κB was shown in the lower two rows in (***a***) and quantified as shown in (***c***).

***Figure 2.4. EF24 blocks TNFα-induced I-κB degradation and phosphorylation***. (***a***) A549 cells were treated with TNFα (10 ng/ml). Whole cell lysates were prepared at indicated times and analyzed for the phosphorylation state of I-κB with anti-pS32 antibody via Western blotting (Upper panel). Then, antibodies on the membrane were stripped and the membrane re-probed for total I-*κ*B with antiserum against I-*κ*B (Middle panel). Raf-1 was used as a control (Lower panel). (***b***) A549 cells were pretreated for various times with EF24 (5 μM), curcumin (5 μM or 50 μM) prior to the addition of TNFα. Cells were cultured in the presence of TNFα (10 ng/ml) for an additional 20 minutes, lysed and analyzed for total I-*κ*B levels by Western blot (*Upper panels*). Raf-1 was used as a control (*Lower panels*). (***c***) A549 cells were pretreated with compounds (EF24 or curcumin) as indicated for 30 minutes. TNFα was added to induce I-*κ*B phosphorylation. Cell lysates were prepared after 7 min of treatment and used for probing pS32-I-κB followed by probing total I-*κ*B with Western blots. Intensity of cross-reacting material bands on Western blots was estimated with a Kodak imaging system. The phosphorylation levels of I-κB at S32 are normalized to total I*κ*B and expressed relative to control sample with DMSO treatment (***d***).

***Figure 2.5. EF24 inhibits the kinase activity of endogenous IKK complex*** A549 cells were pretreated with EF24 or curcumin at indicated doses for one hr followed by TNFα (10 ng/ml) stimulation for 10 min. Cell lysates were prepared for immunoprecipitation of the IKK complex with an antibody raised against IKKα. The isolated IKK complex was used in an in vitro kinase assay with GST-I-κB as a substrate. Samples were resolved on

a SDS-PAGE and stained for total I-κB protein with Coomassie Blue (Middle panel, ***a***). The gel was dried to reveal radiolabeled I-κB with PhosphoImager (upper panel, ***a***). The amount of IKKβ in the immuno-complex used in each reaction was revealed by Western blot. As a negative control, the inactive IKK complex without TNFα treatment is shown in left lane. Quantified result from ***a*** is plotted relative to vehicle control (***b***).

***Figure 2.6. EF24 inhibits IKKβ kinase activity in a reconstituted system.*** Recombinant IKK*β* was incubated with increasing concentrations of EF24 (***a***) or curcumin (***b***) for 15 min. Addition of Mg/[$\gamma$-$^{32}$P] cocktail with purified GST-I-κB started the reactions, which were continued for 15 min at 30°C. Proteins were separated by SDS-PAGE and processed for radiolabeled GST-I-κB (*upper panel*s), total GST-I-κB (*middle panels*), and IKKβ (*lower panels*) as described in legend to Fig. 5. Controls include reactions without IKKβ (lane 1) or without I-*κ*B (lane 2).

***Figure 2.7. Working model for the EF24 mode of action.*** EF24 efficiently blocks the cytokine-induced nuclear translocation of NF-κB, which is important for cell survival and inflammation signaling. This EF24 activity is at least in part due to its inhibitory effect on I-κB degradation and possibly through a direct inhibitory effect on the kinase activity of IKKb.

***Supplemental Figure S1: EF24 is not a broad spectrum TNF-alpha inhibitor.*** A549 lung cancer cells were pretreated with increasing doses of EF24 or DMSO vehicle (veh) for 30 minutes. Cells were then stimulated with 10ng/ml of TNF-alpha for 20 minutes followed by lysis. Proteins were separated on SDS-PAGE gels and transferred to nitrocellulose membrane followed by subsequent immunoblotting with phosph-JNK antibody. Antibodies were removed using Restore Western Blot Stripping Buffer (Thermo Scientific, Rockford, IL) and reassessed with anti-JNK. This procedure was repeated with antibodies to the phosphorylated forms of ERK (p-p44/p42), and total ERK (p44/p42).

***Supplemental Figure S2: EF24 acts as a mixed-type inhibitor with respect to ATP*** Michaelis-Menten plots were generated by varying [ATP] at a constant [GST-I-κB] of 6.6 $\mu$M. Reactions (25 $\mu$l) were performed that allowed incubation with inhibitor and ATP at 23 °C for 15 min followed by addition of GST-I-κB. Time points were taken within the linear range of enzyme and were graphed against incorporation of $^{32}$P (pmol GST-I-κB /min). Twenty nanograms of IKKβ were used in the assay. Slopes were used to record the initial rate *v* as picomoles of phosphate transferred to GST-I-κB during the reaction period. The curves shown were obtained by fitting the data to a rectangular hyperbolic curve according to the Michaelis-Menten equation and are graphed relative to fmoles of GST-I-κB/min (■control, ●0.5mM EF24, ◆1mM EF24, ▲2.5mm EF24). The derived apparent $Km_{(ATP)}$value is 1.9 mM for IKKβ in the absence of inhibitor.

**Table 2-1**: Cytotoxicity of curcumin and EF24 against a panel of cancer cell lines

| **Cell Line** | **$IC_{50}$ (μM)** | |
|---|---|---|
| | **EF24** | **Curcumin** |
| **1A9** (ovarian) | 0.44 ± 0.09 | 9.85 ± 1.20 |
| **HeLa** (cervical) | 1.23 ± 0.88 | 26.9 ± 7.0 |
| **A549** (lung) | 1.31 ± 0.01 | 19.75 ± 4.03 |
| **H358** (lung) | 0.66 ± 0.09 | 14.9 ± 3.1 |
| **H460** (lung) | 0.79 | 16.9 |
| **H157** (lung) | 0.77 ± 0.06 | 19.55 ± 6.71 |
| **Calu-1**(lung) | 1.03 ± 0.14 | 18.1 ± 2.46 |
| **MDA-MB231** (breast) | 1.03 ± 0.40 | 26.55 ± 3.18 |
| **PC3** (prostate) | 2.07 | 23.7 |

$IC_{50}$ values derived from Figure 2.2 are given as the average of at least two separate experiments. $IC_{50}$: concentration at which cell growth is inhibited by 50%.

**Figure 2.1**

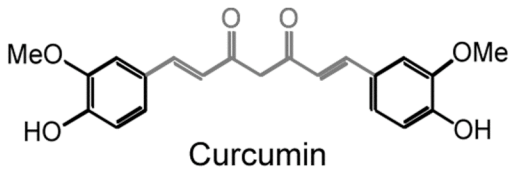


Curcumin

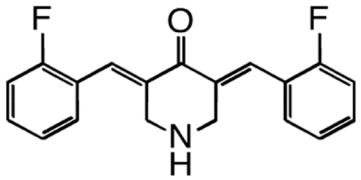


EF24

**Figure 2.2**

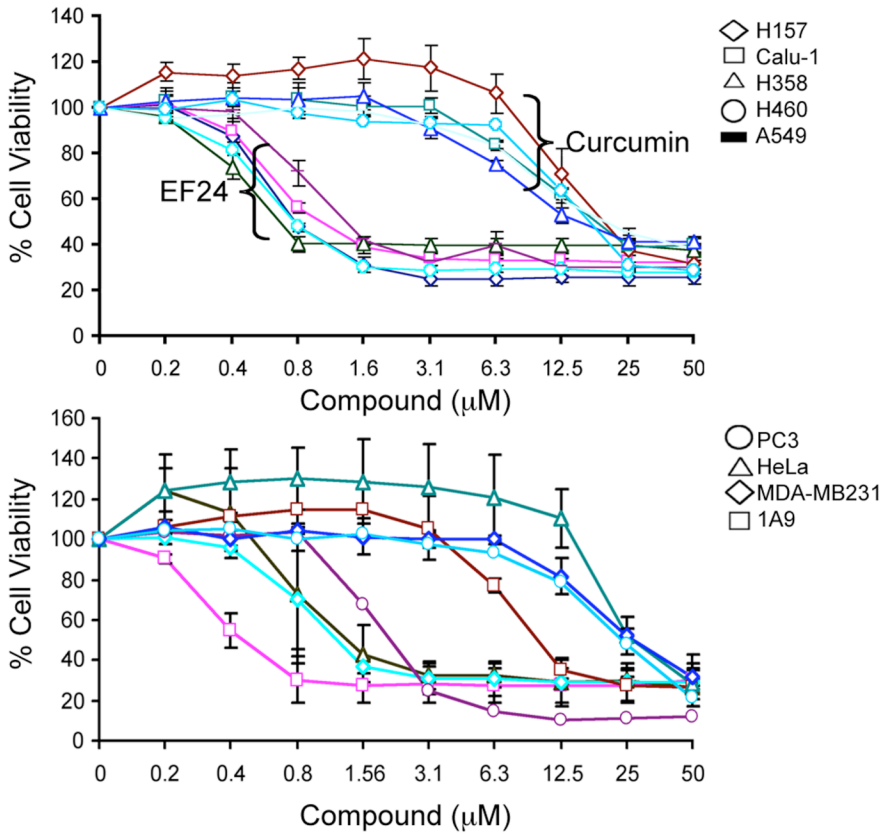
% Cell Viability
Compound (μM)
H157
Calu-1
H358
H460
A549
Curcumin
EF24
PC3
HeLa
MDA-MB231
1A9

**Figure 2.3**

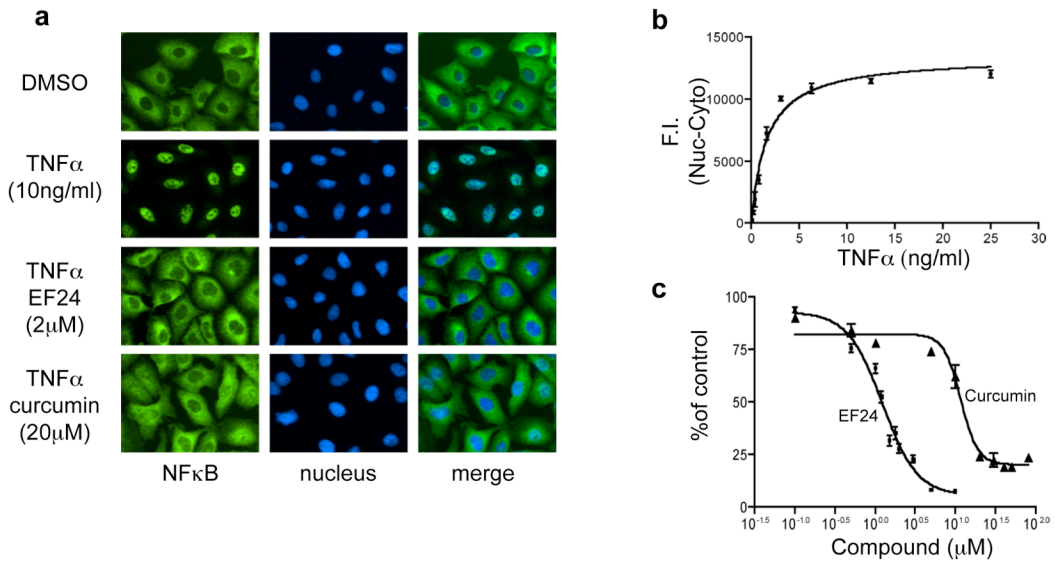
a
DMSO
TNFα (10ng/ml)
TNFα EF24 (2μM)
TNFα curcumin (20μM)
NFκB
nucleus
merge
b
F.I. (Nuc-Cyto)
15000
10000
5000
0
0
5
10
15
20
25
30
TNFα (ng/ml)
c
%of control
100
75
50
25
0
EF24
Curcumin
Compound (μM)

**Figure 2.4**

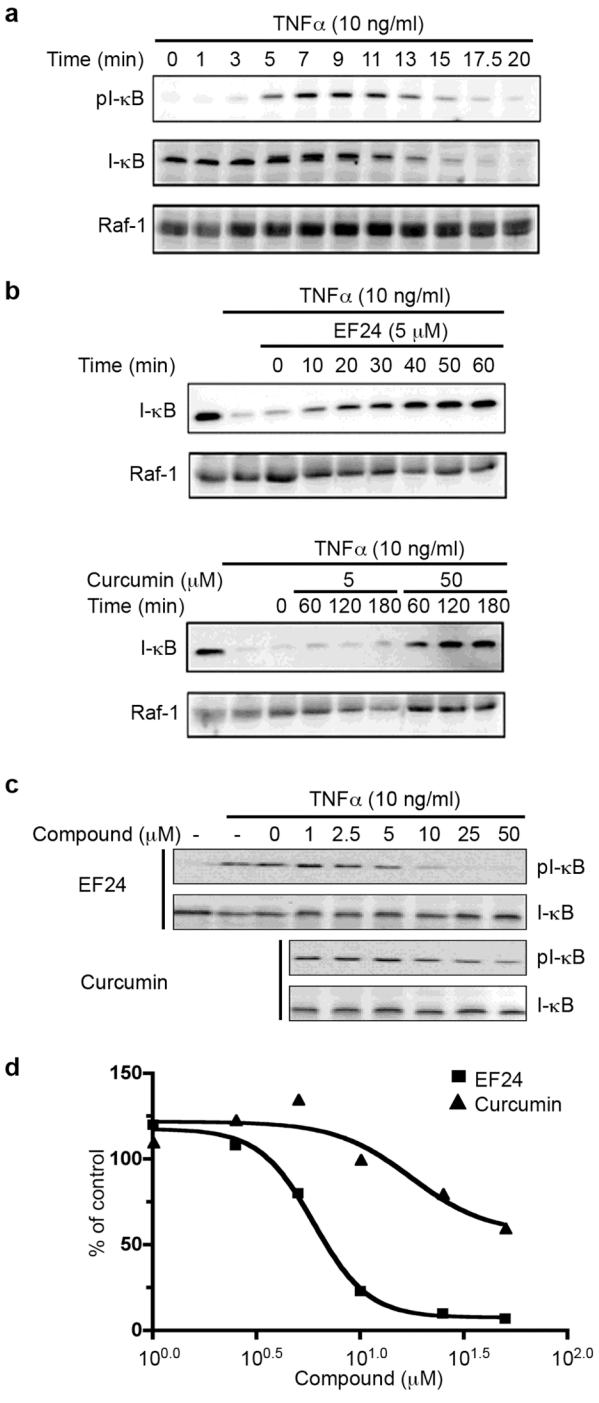
a
TNFα (10 ng/ml)
Time (min) 0 1 3 5 7 9 11 13 15 17.5 20
pI-κB
I-κB
Raf-1
b
TNFα (10 ng/ml)
EF24 (5 μM)
Time (min) 0 10 20 30 40 50 60
I-κB
Raf-1
TNFα (10 ng/ml)
Curcumin (μM) 5 50
Time (min) 0 60 120 180 60 120 180
I-κB
Raf-1
c
TNFα (10 ng/ml)
Compound (μM) - - 0 1 2.5 5 10 25 50
EF24
pI-κB
I-κB
Curcumin
pI-κB
I-κB
d
EF24
Curcumin
% of control
150
100
50
0
10^0.0
10^0.5
10^1.0
10^1.5
10^2.0
Compound (μM)

**Figure 2.5**

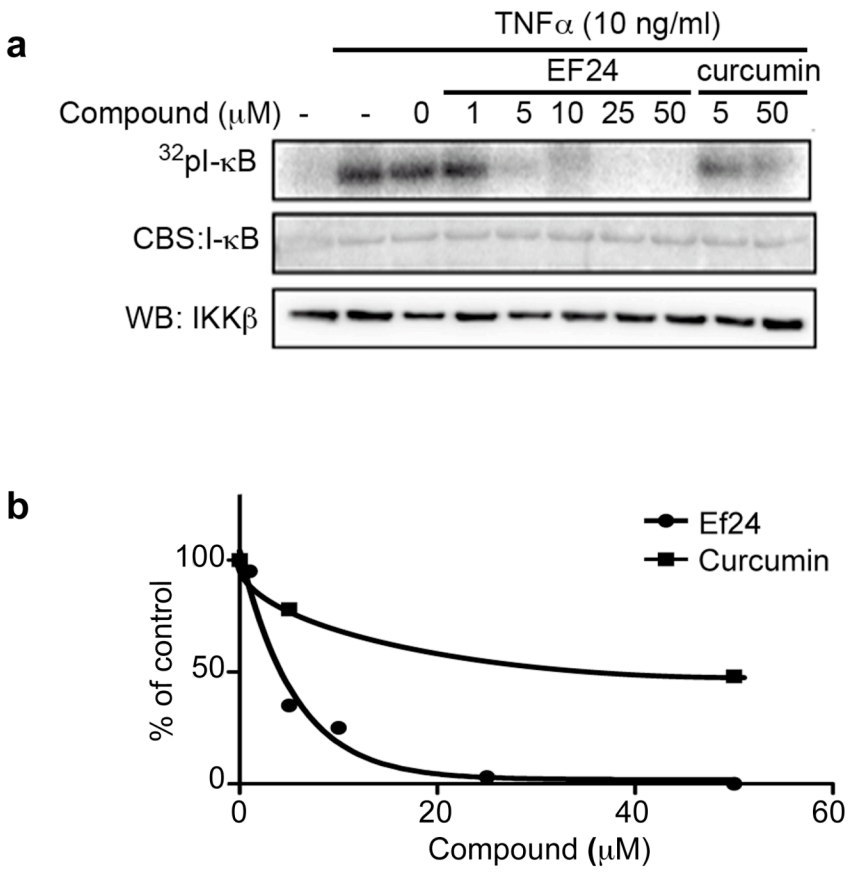
a
TNFα (10 ng/ml)
EF24
curcumin
Compound (μM) - - 0 1 5 10 25 50 5 50
32pI-κB
CBS:I-κB
WB: IKKβ
b
Ef24
Curcumin
% of control
100
50
0
0
20
40
60
Compound (μM)

**Figure 2-6**

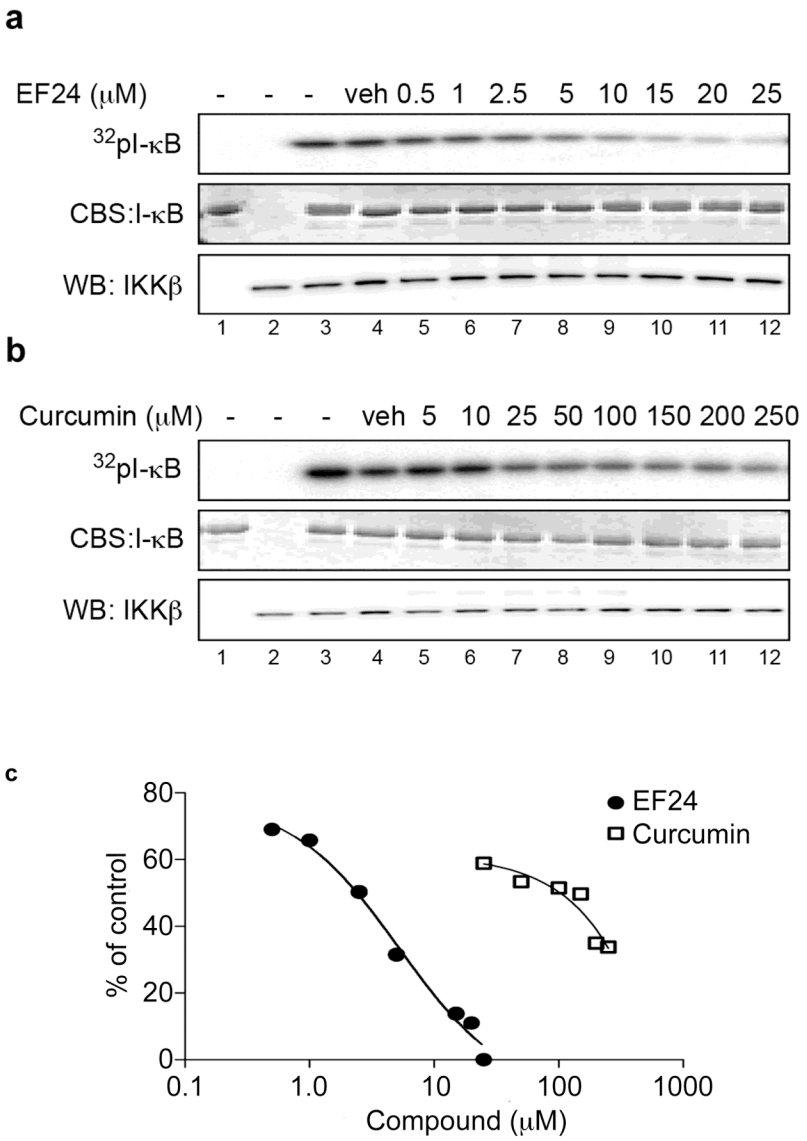
a
EF24 (μM) - - - veh 0.5 1 2.5 5 10 15 20 25
32pI-κB
CBS:I-κB
WB: IKKβ
1 2 3 4 5 6 7 8 9 10 11 12
b
Curcumin (μM) - - - veh 5 10 25 50 100 150 200 250
32pI-κB
CBS:I-κB
WB: IKKβ
1 2 3 4 5 6 7 8 9 10 11 12
c
EF24
Curcumin
% of control
0
20
40
60
80
0.1
1.0
10
100
1000
Compound (μM)

**Figure 2.7**

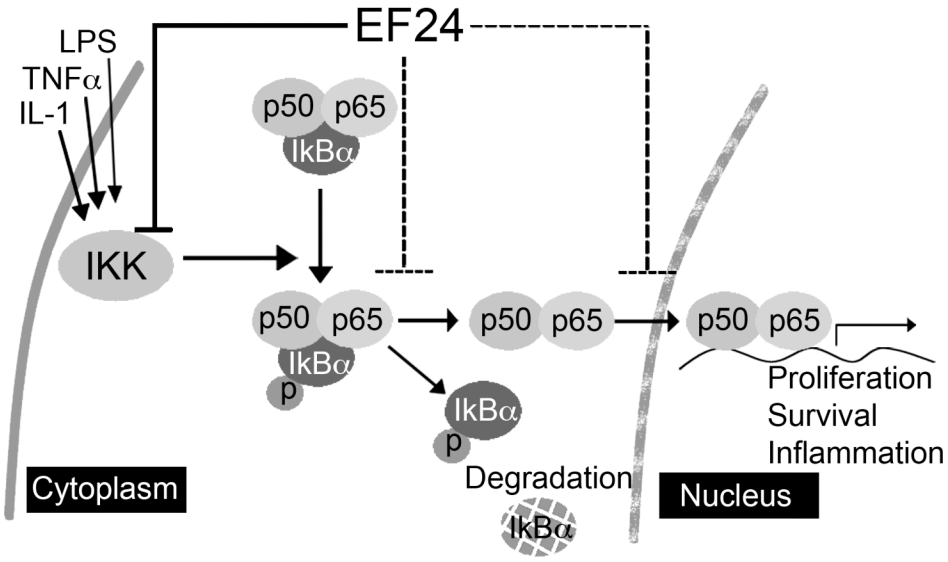
EF24
LPS
TNFα
IL-1
p50
p65
IkBα
IKK
p50
p65
IkBα
p
p50
p65
p50
p65
IkBα
p
Degradation
IkBα
Cytoplasm
Nucleus
Proliferation
Survival
Inflammation

**Figure 2-S1**

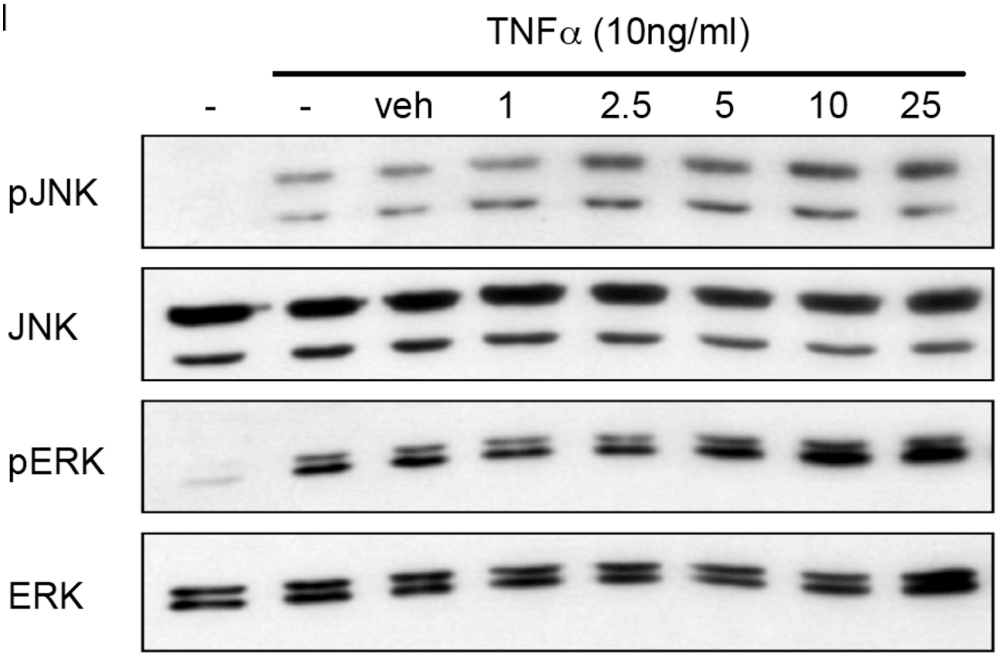

**Figure 2-S2**

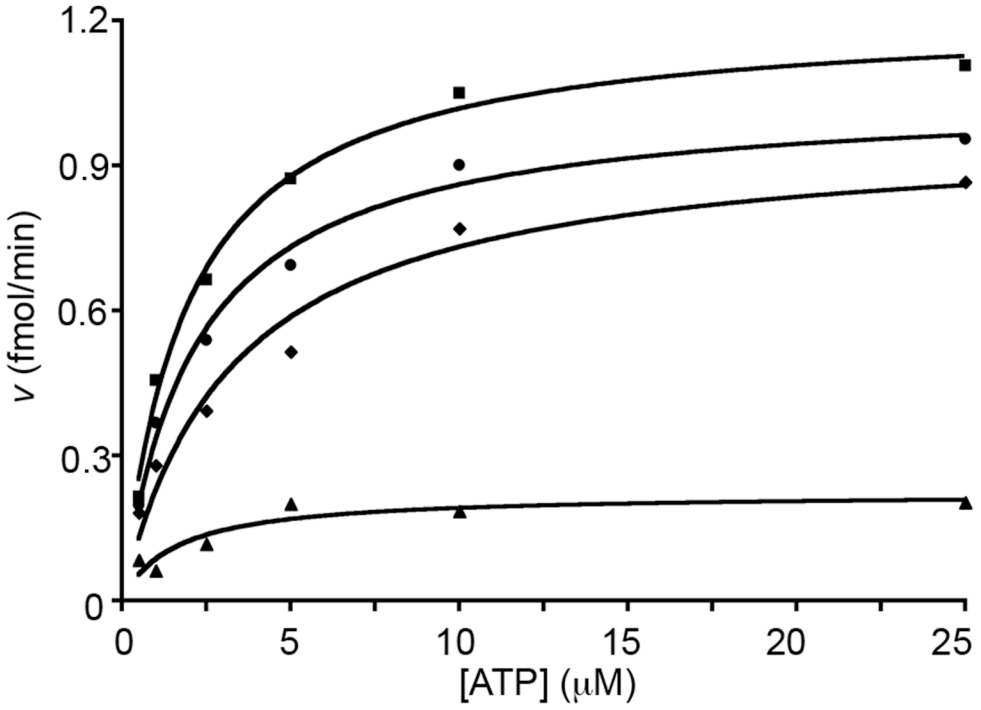

# Chapter 3: Transcriptional regulation of *ywhaz*, the gene encoding 14-3-3ζ

All work was performed by Andrea Kasinski

# Transcriptional regulation of *ywhaz*, the gene encoding 14-3-3ζ

Andrea Kasinski and Haian Fu

Graduate Programs in Genetics and Molecular Biology (A.L.K), Departments of Pharmacology (H.F.), and Emory Chemical Biology Discovery Center (H.F.), Emory University, 1510 Clifton Road, Atlanta, GA 30322

## Abstract

Atypical expression of oncogenic 14-3-3 proteins is positively correlated with tumor progression. The underlying cause of the aberrant protein levels seen in these tumors remains a mystery for six of the seven 14-3-3 isoforms; however gene duplication as well as a transcriptional component have been suggested. Unfortunately, little work has been done to support these hypotheses. In this study we describe the genetic structure and determined a novel signaling mechanism that induces transcription of *ywhaz*, the gene encoding 14-3-3ζ. A total of five transcript variants were identified and their expression confirmed in a panel of cell lines. Each of the variants revealed expression levels that were different between each other and between cell-lines. Although all five variants encode for the same protein, their unique signature is contained within their varied 5' untranslated region (UTR). This region controlled the efficiency of translation to varying degrees that was dependent on each of the five independent 5'UTR. Expressed sequence tag (EST) database mining and in-vitro rapid-amplification of cDNA ends (RACE) identified one variant that represents >80% of the expressed transcripts. This same variant is the most efficiently translated as well. Analysis of the proximal promoter of this variant determined a functional CRE element. It was identified that both CREB and ATF-1 can bind the CRE element in-vitro; however chromatin-immunoprecipitation (ChIP) data show a more favorable binding by ATF-1 under TNF-α stimulating conditions. Further, silencing of ATF-1 caused a marked reduction in two of the five transcripts resulting in decreased 14-3-3ζ protein levels. These data suggest a novel mechanism for the transcriptional regulation of a major pro-survival gene by ATF-1.

## Introduction

The 14-3-3 proteins are a family of acidic, dimeric, small proteins found in all eukaryotes examined. There are seven highly conserved isoforms (β, γ, ε, η, σ, τ, and ζ) encoded by seven distinct genes in mammals, all of which act as master regulators in the cell. They function in various aspects of cell survival signaling by contributing to cell cycle progression, the onset of differentiation and senescence, proliferation, and transformation [82]. The ability to control such events depends on the phosphoserine/phosphothreonine-binding of a 14-3-3 dimer to over 200 known client proteins. The majority of 14-3-3 ligands contain one of three well-defined binding motifs (RSXpS/TXP, RXFXpS/TXP, or pS/T($X_{1-12}$)-COOH, where pS/T, F and X denote a phosphorylated serine or threonine residue, an aromatic amino acid and any amino acid, respectively) [95-98] . However, ligands have been identified that can bind 14-3-3 in a phosphorylation-independent manner as well. These binding events lead to alterations in client protein sub-cellular localization (eg. Bad, Cdc25), the modification of enzymatic function (eg Raf-1, serotonin-N-acetyl transferase, Chk1, and Wee1), and/or the formation of dynamic multi-protein complexes (Raf-Bcr and Raf-A20) [103,118-120,123,124,202,203].

The majority of the work in the field has focused on how 14-3-3 proteins regulate other proteins. Very little attention has been given to how 14-3-3 proteins themselves are regulated. What is known, is that many 14-3-3 family members including 14-3-3β and ζ can undergo post-translational modification by phosphorylation [93,94]. Modification at this level can disrupt 14-3-3 dimer formation which is found to be necessary for subsequent client protein interaction. Indeed, 14-3-3 proteins function as hetero- and homodimers with particular heterodimeric pairs having specificity and/or affinity for individual client

proteins. As such, the amount of each individual isoform in the cell can dictate successive events. Intrinsically, alterations of 14-3-3 proteins due to mutation or expression of specific isoforms can result in global changes in the cell.

The ability of 14-3-3 dimers to bind to and regulate oncogenic proteins and tumor suppressors such as Raf-1 and Bad, respectively point to a role for 14-3-3 proteins in cancer. Of the seven isoforms, six "canonical" members are referred to as oncogenic. The only isoform with clear tumor suppressive properties is 14-3-3σ, which is silenced in the epithelial cells of a sub-set of breast cancer leading to decreased genomic instability [138]. As one of the only isoforms intensely studied at the genomic level, it was determined that gene silencing in these tumors occurs at an epigenetic level due to methylation of a CpG island within the promoter of *sfn*, the gene encoding the 14-3-3σ protein. Additionally, a functional binding site for the tumor-suppressor, p53 is present in the promoter of 14-3-3σ [139]. In response to DNA damage, p53 is recruited to the promoter resulting in gene activation leading to G2-M arrest.

Although little is known about the transcriptional contribution of the remaining six isoforms, it seems likely that they will contain a genetic component to their regulation. Various groups have shown that gene amplification and increased transcript levels of the canonical isoforms are present in cancers and may contribute to protein elevations. For example, Qi et al. provide evidence for increased transcript levels of multiple 14-3-3 isoforms in lung cancer, while a separate group determined that gene amplification may be one mechanism leading to elevated 14-3-3ζ levels [140,147]. Further, putative CpG islands are found in the genes for all 14-3-3 isoforms although their functionality has not yet been tested. Both the promoter and the 5'UTRs of each of the

isoforms are also quite divergent, suggesting that individual family members may have a second level of control at the transcriptional level. Further, multiple transcript variants have been identified for both 14-3-3β and ζ that may add another layer of complexity to their regulation.

In this report we choose to focus on the genetic organization and regulation of *ywhaz*, the gene encoding 14-3-3ζ. The correlation of 14-3-3ζ with tumorigenesis is quite clear and understanding the transcriptional contribution to this regulation may be an opportunity for the design of isoform specific14-3-3 targeted therapies. In this study, we identified a total of 5 transcript variants each of which contains a different 5'UTR. The UTR's are differential in their ability to translate the protein. Moreover we identify that of the five variants, one is expressed the highest at the transcriptional level and most readily translated. This particular variant is controlled by a CRE element found with in the proximal promoter of the gene. We further show that ATF-1 and CREB bind to the putative CRE element in vitro and that ATF-1 binds the endogenous promoter. Likewise, knockdown of ATF-1, diminished 14-3-3ζ protein levels with specific reductions seen in two of the five transcript variants. This suggests a novel mechanism for 14-3-3ζ regulation and is the first report to look at transcriptional mechanisms controlling one of the oncogenic 14-3-3 family members.

## Materials and Methods

*Cell lines* - HeLa and Hek-293 cells were grown in DMEM while PC3, DU145, LnCap, Colo205, MCF7, A549 and H358 cells were grown in RPMI. All cells culture medium was supplemented with 10% FBS, 100 units/ml of penicillin and 100 μg/ml of streptomycin. BEAS and HBEC cells were maintained in keratinocyte medium supplemented with 20 ug/ml bovine pituitary extract and 0.1 ng/ml of human recombinant epidermal growth factor. All cell lines were grown at 37°C in 5% $CO_2$ and passed every 3-4 days.

*Cloning and generation of luciferase constructs* - Constructs used to assay translation efficiency were generated as follows. Oligos containing a T7 promoter sequences with HindIII overhangs were annealed together and ligated into the HindIII site of pGL3 (Promega). These oligos also contained an internal EcoRI site that would later be used for cloning in the 5'UTR sequences. Directionality of T7 insert was confirmed by plasmid isolation followed by sequencing. This new vector was given the name, T7-pGL3.

The following primer pairs were used to amplify the specific 5'UTRs for subsequent cloning into T7-pGL3:

1a forward 5'-AGAGGAATTCTTTCTCCTTCCCCTTCTTCCGGGCT-3'

1a reverse 5'-CTCTCCATGG**GACTGGATGTTCT**TTTTATCTCCTAGAAGC-3'

1b forward 5'-AGAGGAATTCGTCCCCTCGCGCAGTCACCGAG-3'

1b reverse 5'-CTCTCCATGG**GACTGGATGTTCT**GCTGGCTCGG-3'

1c forward 5'-AGAGGAATTCGTTTGACGTCATCGTGCGTGTGGTGC-3'

1c reverse 5'-CTCTCCATGG**GACTGGATGTTCT**GTGTCCGGAGTG-3'

1e forward 5'-AGAGGAATTCGACACAGATCCGCCATGACAAAGGAGGAGA-3'

1e reverse 5'-CTCTCCATGG**GACTGGATGTTCT**GACTTGAGACGTC-3'

Underlined sequences in forward and reverse primers represent EcoRI, and NcoI sites, respectively. The bold sequence in the reverse primers is shared between all 5'UTRs. This is the sequence preceding the start methionine in exon 2. Amplification of each of the 5'UTR sequences was accomplished using the following primer pair combinations: 1a, 1a forward and 1a reverse; 1b, 1b forward and 1b reverse; 1bc, 1b forward and 1c reverse; 1c, 1c forward and 1c reverse; 1e, 1e forward and 1e reverse. The template used for amplification was a cDNA prep prepared from HeLa cells. PCR amplifications were performed using Pfu polymerase from Stratagene. Reactions were set-up per manufacturers directions with the following PCR cycles and amplification temperatures. Initial denaturing at 95°C for two minutes followed by 30 cycles of 95° - 30 sec, 58°C for 30 sec, 72°C for 45 sec, with one final extension at 72°C for 10 minutes. PCR products were digested with EcoRI and NcoI in PCR reaction buffer supplemented with 1X EcoRI NEB buffer. Digested PCR fragments were gel purified and directionally ligated into EcoRI/NcoI digested T7-pGL3.

Generation of constructs used for *ywhaz* 1c promoter studies began with cloning the largest fragment into pGL4.10 (Promega). Using a previously generated *ywhaz* luciferase construct, the proximal 1c promoter was cut out with SacII. This fragment was treated with Klenow and ligated into EcoRV digested pGL4.10. This new construct,

pALK31, contains 806 nt upstream of the putative transcriptional start site for exon 1c. To generate the truncations, pALK31 was first digested with SacI, and SmaI. This fragment was cloned back into the parent pGL4.10 to generate pALK33, which contains 593 nt upstream of exon 1c. The -72 construct, pALK34, was generated by digestion of pALK31 with SacI, and AatII. The purified fragment was ligated into pGL4.10. The remaining constructs were generated by PCR. All forward and reverse primers contained a SacI, and NheI site, respectively for subsequent cloning back into pGL4.10.

*Luciferase assays* - HeLa cells were seeded in 12-well plates at $1x10^5$ cells/well. The following day, cells were transfected with 150 ng of test firefly vector, and 20 ng of renilla control vector using Fugene-HD. Twenty-four hours after transfection, cells were lysed with 100 µl of passive lysis buffer (Promega). Ten micorliters of lysate were analyzed for luciferase activity using the Dual Luciferase Kit (Promega). Data are represented as firefly relative to renilla.

*RNA isolation and first-strand cDNA synthesis* - Total RNA was isolated from cells grown to approximately 80% confluency in 100 mm culture dishes using Qiagens RNeasy kit as described by manufacturer. Concentrations were determined by taking the absorbance at 260 nM . Five µg of total RNA were reverse transcribed using the first-strand cDNA synthesis kit (Invitrogen). Subsequent amplification of cDNA was done by either real-time-RT-PCR, or by semi-quantitative-PCR for primer sets that exhibited non-specific amplification.

*Real-time reverse transcription PCR* - Power SYBR Green (Applied Biosystems) was used for amplification per manufacturers instructions. Briefly, 2 μl of cDNA was added to a 20 μl reaction containing 1X Power SYBR Green master mix with transcript specific primers. Amplification and quantification was performed on the BioRad iQ5. Cycles were conducted with fluorescence intensity measurements acquired at the end of each round of amplification following the extension. Melting profiles confirmed the presence of a single product.

*Semi-quantitative PCR* - For primer pairs that exhibited non-specific bands after PCR amplification, semi-quantitative PCR was used to assess amplification. For these experiments a 50 μl PCR reaction was set-up. Beginning at cycle twenty and every five subsequent cycles, 10 μl of reaction was removed following the extension step. This was done in order to catch the amplification within the linear range. Products were resolved on agarose gels, imaged, and quantified by densotometry.

*Northern blot* - Two μg of total RNA from each cell line was resolved on a formaldehyde gel. RNAs were transferred to Hybond-N membrane by upward transfer overnight and crosslinked using a UV stratlinker. Radioactive probes to the various *ywhaz* exons were generated and hybridized to Northern blots. Signals were obtained by overnight exposure

of the probed membrane to phosphoimaging screens and subsequent scanning on the Typhoon (Molecular Devices).

*Nuclear preparation and fractionation* - Nuclear preparations were prepared essentially as described (Shapiero et al. DNA volume 7, Number 1, 1988, pg 47-55). HeLa cells were grown in 100-150 mm plates to approximately $1x10^9$ cells. After two washes with PBS, cells were resuspended in 5 x packed cell volume (PCV) of hypotonic buffer (10 mM HEPES, pH 7.9, 0.75 mM spermidnie, 0.15 mM spermine, 0.1 mM EDTA, 0.1 mM EGTA, 1 mM DTT, 10 mM KCl inhibitors). Cells swelled on ice for 10 minutes followed by pelleting at 300 x g for 10' at 4°C. Two times the original PCV of hypotonic buffer was added to the pellet and transferred to a Dounce homogenizer. Cytoplasmic membranes were broken with 10 strokes of the tight pestle after which 0.1 PCV of sucrose restore buffer (67.5% RNase free sucrose, 50 mM HEPES, pH 7.9, 0.75 mM spermidine, 0.15 mM spermine, 10 mM KCl, 0.2 mM EDTA, 1 mM DTT) was immediately added. The homogenate was centrifuged 30 seconds at 16,000 x g to pellet nuclei. Three mls of nuclear resuspension buffer (20 mM HEPES, pH 7.9, 0.75 mM spermidine, 0.15 mM spermine, 0.2 mM EDTA, 2 mM EGTA, 2 mM DTT, 25% glycerol)/1 x $10^9$ cells were added to the pellet. Resuspended nuclei were rocked for 30 minutes at 4°C followed by centrifugation for 90 minutes at 150,000 x g at 4°C. The supernatant containing the nuclear proteins was transferred to a clean tube and 0.33 g/ml of solid ammonium sulfate was added to facilitate protein precipitation. After the ammonium sulfate went into solution, tubes were rocked for 20 minutes in the cold room. The precipitated nuclear proteins were pelleted via centrifuged at 85,000 x g for 20

minutes at 4°C. Pellets were redissolved in 1 ml of nuclear dialysis buffer (20 mM HEPES, pH 7.9, 20% glycerol, 100 mM KCl, 0.2 mM EDTA, 0.2 mM EGTA, 2mM DTT)/$10^9$ cells and were dialyzed twice for 90 minutes against >200 volumes of nuclear dialysis buffer. Protein concentrations were determined by biorads protein assay and nuclear extracts were stored at -80°C.

*Heparin purification* - Crude nuclear preparations from HeLa cells (20 mg) were loaded onto a Heparin-agarose column. The column was washed with 10 volumes of loading buffer. Elutions were performed over a 1M gradient of NaCl collected in 0.5 ml fractions. Three μl of each of the fractions were subject to binding activity by EMSA.

*EMSAs* - The following sense and complementary anti-sense oligos were used to generate probes and competitors for EMSA:

CRE wild type 5'-TAGCAGCGTTGAATATCATCGTGCGTGT-3'

CRE mutant 5'-TAGCAGCGTTGAATATCATCGTGCGTGT-3' .

For radioactive probe generation, wild-type oligos were labeled with [$\gamma$-$^{32}$P]ATP. Following labeling, free unincorporated ATP was removed using Qiagens nucleotide removal kit. Sense and antisense oligos were combined, heated to 94°C and slowly cooled to room temperature to allow for annealing. Double stranded probes were separated from single stranded oligos on PAGE and subsequently purified. Radioactively purified probes were used in combination with nuclear extract to assess binding. In short,

10 μg of purified extract was added to each well of a 96-well plate containing 30,000 cpm of EMSA probe in the presence of buffer. Plates were rocked at room temperature for 1 hour to induce binding. For supershift assays, 5 μg of each respective antibody was added at the beginning of the 1-hour incubation period. The following antibodies were used: anti-Atf-1 (#sc-243), anti-Atf-1 (#sc-270), anti-Atf-1 (#sc-60), anti-Prep-1(#sc-6245) and anti-Creb (#9197). Seventeen μl of each reaction was loaded on 5% PAGE and separated at 175 volts in the cold room for ~2.5 hours. Gels were fixed, dried and exposed to phosphoimaging screens overnight followed by scanning on the Storm (Molecular Dynamics) for further analysis using Image Quant.

*Streptavidin agarose pull down assays* - Biotinylated oligos containing the *ywhaz* CRE region were synthesized and annealed together

(CRE wild type 5'-TAGCAGCGTTGAATATCATCGTGCGTGT-3'

CRE mutant 5'-TAGCAGCGTTGAATATCATCGTGCGTGT-3').

Oligos, streptavidin-conjugated beads and 400 μg of nuclear extract were incubated overnight in the cold room to induce binding. The following day, complexes were precipitated and resolved on 12% SDS-PAGE. Proteins were transferred to nitrocellulose membranes and probed with antibodies to CREB and ATF-1 to determine degree of protein binding to each of the oligos.

*Chromatin Immunoprecipitation* - HeLa cells were seeded at 2 x $10^7$ cells one day before ChIP. Following appropriate treatments, a final concentration of 1% formaldehyde was added directly to the tissue culture medium. Cells were rocked at room temperature for 10 minutes followed by washing with cold PBS. To remove the cells from the culture dish, a rubber policeman was used to scrape the cells in a small volume of PBS. Cells were centrifuged at 3,000 x g for 5 minutes and washed two times with PBS and resuspended in 1 ml of cell lysis buffer (5 mM PIPES, pH 8.0, 85 mM KCl, 0.5% NP-40, 10 mg/L aprotin, 10 mg/L leupeptin, 1 mM PMSF). Cells incubated on ice for 5 minutes and were pelleted at 3,000 x g for 5 minutes. This was repeated a second time. Pellets were resuspended in 0.5 ml of nuclei lysis buffer (50 mM Tris, Ph 8.1, 10 mM EDTA, 1% SDS, 10 mg/L aprotin, 10 mg/L leupeptin, 1 mM PMSF). Sonication was performed that included three cycles of 4 seconds on, 6 seconds off for a total of 50 seconds/cycle at an amplitude of 15%. Precipitates were centrifuged out and the degree of sonication was determined by crosslink reversal, DNA precipitation, and agarose gel analysis of the sheared fragments.

Immunoprecipitation of bound proteins was performed overnight in 950 ml of IP dilution buffer (0.01% SDS, 1.1% Trition X-100, 1.2 mM EDTA, 16.7 mM Tris, pH 8.1, 167 mM NaCl) containing 50 μl of purified chromatin and 5 μg of antibody per sample. The following antibodies were used: anti-Atf-1 (#sc-243), anti-Creb (#9197), and anti-NF-κB (p65). Immune complexes were recovered with 60 μl of protein A beads. Samples were washed with 1 ml each of IP dilution buffer 2X, TSE-500 (0.1% SDS, 1% Triton X-100, 2 mM EDTA, 20 mM Tris, pH 8.1, 500 mM NaCl) 2X, LiCl/detergent wash (100 mM Tris, pH 8.1, 500 mM LiCl, 1% NP-40, 1% deoxycholic acid) 2X and TE

buffer (10 mM Tris, pH 8.1, 1 mM EDTA) 2X. Each wash was performed for 10 minutes with rotation at 4°C. Beads were vortexed in 250 μl of IP elution buffer (50 mM $NaHCO_3$, 1% SDS) followed by rotation at room temperature for 15 minutes. The supernatant was saved and the elution step was repeated one additional time. Crosslink reversal was achieved by adding 20 μl of 5 M NaCl to each sample with an overnight incubation at 65°C. Proteins were digested with proteinase K and DNA was recovered with phenol-cholorform iso-amyl alcohol extraction and ethanol precipitation. Pelleted DNA was resuspended in 30 μl of water and 3 μl were used in subsequent real-time PCR amplification. The amount of immunoprecipitated DNA was normalized to 1/30 of the input chromatin. Primer sequences are as follows:

I-κB forward, 5'-GACGACCCCAATTCAAATCG-3' and

I-κB reverse 5'-TCAGGCTCGGGGAATTTCC-3'

*ywhaz* CRE forward, 5'-GAAGCCGAGCGGGGTGGGAGGAGT-3' and

*ywhaz* CRE reverse 5'-GGCGGCGGACGGACGGGCTCAG-3' .

*Western blotting* - Cells were lysed in 1%-NP-40 lysis buffer (1% NP-40, 10 mM HEPES, pH 7.45, 150 mM NaCl, 10 mg/L aprotin, 10 mg/L leupeptin, 1 mM PMSF). Lysates were clarified by centrifugation, and resolved on 12% SDS-PAGE. Proteins were transferred to nitrocellulose membranes and probed with antibodies against the indicated protein.

*shRNA knockdown* - Short hairpin RNA constructs were obtained from Open Biosystems. One day prior to transfection, HeLa cells were seeded in 6-well plates at 2 x $10^5$ cells/well. The following day, 2 μg of each construct were transfected into HeLa cells using Fugene HD per manufacturers instructions. The cells not expressing the shRNA were removed by negative selection in 1μg/ml of puromycin. Five days following the initial transfection, total RNA or protein was extracted from the cells and analyzed for gene specific knockdown.

*Sequence alignment* - Alignment of human, rhesus, mouse, rat, dog, horse, armadillo, elephant, opossum, platypus and tetradon at the ywhaz locus was performed using the UCSC genome browser http://genome.ucsc.edu/ [204].

## Results

### 14-3-3 zeta is encoded from at least five different transcript variants

The gene that encodes for 14-3-3ζ, *ywhaz*, is found on chromosome 8 and spans just over 35 kilobases. Six exons have been reported for this gene with the first exon lying entirely within the 5' untranslated region (Figure 3.1a). Prior to our work, two transcript variants for this gene were described each with an independent exon 1 (Figure 3.1b). To determine if additional variants for this gene existed, we utilized RNA-ligase-mediated-(RLM)-RACE. This technique can determine the 5' transcriptional start sites as well as the relative abundance of individual transcripts in an mRNA pool. We were able to confirmation expression of the two previously reported variants and identified two novel ones by this technique (Figure 3.1b). An additional variant was later identified as a splice variant containing both exon 1b and 1c. This variant was found as a higher molecular weight band on a gel after reverse transcription (RT)-PCR (Figure 3.2). Following its purification and sequencing it was determined to be a fifth *ywhaz* variant.

Northern Blot analysis combined with real-time reverse-transcription PCR of total RNA isolated from a panel of cell lines confirmed the expression of all five transcript variants (Figure 3.3). Expression levels were shown to change between cell lines as well as between transcript variants. Interestingly, there is an inverse correlation in four of five transcript variants between the prostate cancer lines with the more highly metastatic PC3 having the highest expression compared to the moderately metastatic DU145 and LnCap (Figure 3.3b). This is most evident with transcript variant 1c.

### *ywhaz* variant 1c is the most dominant variant identified

While multiple transcripts of 14-3-3ζ have been identified through this work the contribution of each to the overall expression of 14-3-3ζ is lacking. We chose to examine two important characteristics that are important for the ultimate level of 14-3-3ζ protein expressed in the cell. One entails the relative mRNA expression levels of the different transcripts. It is likely that one or more of these transcripts may be playing a larger role than the others based on the abundance of message produced. Furthermore, the sequences contained within the different 5'UTRs will be evaluated for their ability to efficiently induce translation of the gene.

Each of the transcript variants encodes for the same protein. The start methionine resides in exon 2 and all the variants identified in this study share exons 2 through 6 (Figure 3.1). The inconsistencies between different transcripts reside in exon 1 which encompasses the majority of the 5' UTR. The ability of a protein to be translated efficiently depends on the sequence within the 5' UTR of the message. To test the function of the individual UTR's on translation efficiency, each of the five UTR's was cloned upstream of a luciferase reporter vector fusing the ATG for *ywhaz* with the ATG for the luciferase gene. Transcript levels for *luciferase* and *renilla* were monitored from 12 through 36 hours to confirm equal expression. All 5'UTRs had near equal levels of *luciferase* transcript levels relative to *renilla*, suggesting that changes in luciferase activity were due to alteration in translation and were not because of inconsistencies in message levels (Figure 3.4). At each of the time-points, the relative level of luciferase protein level was determined. Of the five different UTR's, the variant containing exon 1c had the most luciferase activity with the splice variant containing both exons 1b and 1c

having a slightly reduced level of activity (Figure 3.4b and c). Both variants 1a and 1b were relatively equal in their translation efficiency, while variant 1e suppressed translation from the luciferase vector. These data suggests that the UTR's contained within the different transcript variants function to control protein translation. Further, variant 1c is translated at the highest rate.

To determine if any of the transcripts were more abundantly expressed, we first looked *in-silico* at the expressed sequences tags (EST) deposited in the UCSC Genome Database. Although all five variants were identified, of the 265 EST's in the repository, greater than 75% began with exon 1c (Figure 3.5a). The remaining 25% were mostly variants beginning with 1a or 1b. Only one represented the splice variant from 1b to 1c. To confirm this finding in vitro, 5'-RLM-RACE was employed. As alluded to in the previous section this technique allowed us to determine the relative abundance of the transcript variants in a given mRNA pool. We choose to utilize both HeLa and MCF7 cells for this analysis. Based on our cell line expression data, HeLa and MCF7 contained dissimilarities in expression levels of the different variants as analyzed by real time-RT-PCR. In this small screen of 77 clones, we first determined similar percentages of each variant in both cell lines analyzed. If the abundance of isolated and sequenced RLM-RACE clones was increased, it is speculated that the mRNA pool from MCF7 cells would present with a higher percentage of transcripts containing exon 1c based on the RT-PCR results. Secondly, and more importantly, our experimental findings supported the EST database results, where the majority of the clones that were pulled out of the screen were ones that represented variant 1c (Figure 3.5b). This screen identified all variants except for the splice variant containing exons 1b and 1c. This particular

transcript was also found to be the least represented in the EST database as well (1/265). There is a slight elevation in the amount of variant 1e represented in our RLM-RACE screen with a similar decrease seen for variant 1b when compared to the EST database search. However, the variant for 1c was found to be the most highly represented transcript in both methods.

### Identification of a CRE regulatory region in the proximal promoter for variant 1c

The 5'UTR contained in transcript 1c allowed for the greatest efficiency in translation and this particular variant was identified as the most highly expressed as determined from both the EST database and from our experimental data. We therefore began to determine the cis-regulatory regions necessary for expression from its proximal promoter. The first 593 base pairs of the proximal promoter were cloned upstream a luciferase reporter vector and truncations of the promoter region were generated. Indeed, expression from the full vector (-593) was greater than 170 fold over the control vector suggesting the possibility of multiple regulatory regions within this sequence (Figure 3.6). In particular, when the truncated reporters were evaluated, two regions stood out that contained cis-activating regulatory sequences. A large decrease in luciferase reporter activity was apparent between the -166 and -85 construct with a second cis activating sequence contained between -85 and -72. To determine if any regions within these sequences were highly conserved, we performed a comparative genomics study on both regions. Although a high degree of nucleotide similarity exists, we were able to determine a well-conserved region that retained all the nucleotides down to *Tetraodon nigroviridis* (Figure 3.7). The conserved residues were that of an 8 bp palindromic sequences that is most

similar to a cyclic-AMP-response-element (CRE) (refer to Figure 3.1 for location within *ywhaz*).

**A putative CRE element is necessary for basal activation from the 14-3-3 promoter**

CRE elements are typically found as an 8-bp palindromic sequence (TGACGTCA); however, a truncated, albeit less active, half palindrome is also functional. The central CG dinucleotide in the 8-bp palindrome is determined to be necessary for expression of CRE target genes. We sought to determine if the CRE element that was identified by comparative genomics was indeed a functional element. The critical GC dinucleotide within the palindrome was mutated to TA in three independent reporter vectors, including a reporter containing an additional 213 nucleotides further upstream (-806) (Figure 3.8a). Mutation of these two key base pairs within the promoter sequence of all three reporters reduced activity by greater than 70%, suggesting that the CRE element is indeed functional in our in vitro setting (Figure 3.8b). The mutated reporter containing a larger portion of the 5'UTR (-806), retained a bit more activity than the other smaller reporters (-593, and -453). Although the change is slight, it is significant and suggests that there may be additional activating regions contained within the 213 base pairs of the -806 construct that lead to the additional 5% in activity.

**Nuclear proteins bind the CRE element in vitro**

Because the putative CRE element was responsible for basal promoter activity, an electrophoretic mobility shift assay (EMSA) was used to identify if any nuclear factors could bind the sequence in vitro. A 28-base pair DNA probe containing sequence surrounding the 14-3-3ζ-CRE region was generated and assayed for its ability to shift in the presence of crude nuclear extract obtained from HeLa cells. Shifting of the probe

suggests binding of nuclear complex to the DNA sequence. Nondenaturing polyacrylamide gel electrophoresis revealed at least 4 independent CRE specific complexes (Figure 3.9, lane 1). All four complexes were deemed specific as they could be competed away by an excess of unlabeled probe (Figure 3.9, compare lane 1 to lanes 2 and 3). The specificity of this interaction was further evaluated by including an unlabeled competitor engineered with a mutation within the CRE element. This mutant could not compete with the radioactively labeled wild-type probe for binding, implying that the complexes seen in our EMSA are dependent on an intact CRE element (Figure 3.9, lanes 4 and 5).

In an attempt to separate and concentrate the different nuclear factors for further analysis, 20 mg of purified nuclear protein was bound to a heparin agarose column. Proteins were eluted over a salt gradient and subjected to EMSA analysis to identify fractions containing CRE binding activity. As evident in Figure 3.10a, the fractionation technique separated the shifted complexes into two major groups. One group was contained within fraction #s 48-52 and a second in fraction #s 56-60. These independent fractions (48-52, and 56-60) were pooled in an attempt to further characterize the proteins that bound the 14-3-3ζ probe. Competition assays were done as in 3.10a to determine the specificity of each of these pooled fractions with respect to the CRE element. Again we found that both pooled fractions contained complexes that bound to the wild-type CRE element, as inclusion of excess mutant sequence was unable to disrupt complex formation on the radioactively labeled wild-type probe (Figure 3.10b).

**ATF-1 and CREB bind to the CRE element *in vitro***

CREB and CREB family members (ATF-1 and CREM) are basic leucine zipper domain (bZIP) transcription factors that bind CRE elements as both heter- and homo-dimers of each other acting to induce or repress target genes. Our luciferase experiments identified a functional CRE element within the promoter for 14-3-3ζ. Likewise a probe encompassing this element shifted in our EMSA, therefore it seemed likely that CREB or one of the CREB family members may bind to this element. To test this model, supershift experiments were performed on the semi-purified heparin pooled fractions. We saw no apparent shift when antisera against CREB or CREB family members was used in EMSA supershift analysis on pooled fractions 48-52 (Figure 3.11a). However, both CREB and ATF-1 were identified in multiple complexes found in fractions 56-60 (Figure 3.11b). Lane 2 (crude extract) and 8 (heparin fractions 56-60) showed shifts of all three major bands with antisera against CREB, CREM and ATF-1. Since our nuclear preparation was generated from HeLa cells, CREM was not further evaluated as it is known to have little to no expression in HeLa cells and therefore is probably not contained in any of the complexes. Supershifts with a CREB specific antibody identified CREB in two of the three complexes (Figure 3.11b, lanes 3 and 9) while ATF-1 was identified as a component in all of the major complexes (lanes 4, 5, 10 and 11). An antibody to Prep-1 served as a negative control and showed no apparent shift in any of the bands from either pooled fraction (Figures 3.11a and 3.11b, lanes 6 and 12). This defines the possibility that an ATF-1/CREB heterodimer may be acting in one complex while an ATF-1 homodimer or an ATF-1 heterodimer with a yet to be identified

additional factor may be contained in a separate complex. The identification of the CREB independent factors found in fractions 48-52 has yet to be determined.

To further confirm the binding of CREB and ATF-1 to the wildtype CRE element a streptavidin pulldown assay (SAPD) was employed. For this analysis, biotinylated *ywhaz* oligos that spanned the CRE element were generated. These oligos (either wild-type of CRE mutant) were annealed and bound to streptavidin beads. After incubating the oligo-bound beads with nuclear extract, beads were pulled down and precipitated proteins were resolved by SDS-PAGE. A single antibody that recognizes both CREB and ATF-1 was used to assay for the abundance of these two proteins in the pulldown. Figure 3.12 reveals that although both proteins were contained within the nuclear extract utilized in this assay (lane 1), both CREB and ATF-1 were enriched when beads containing the wildtype sequence were used for the pulldown relative to mutant bound beads. This data confirmed the EMSA findings, that CREB and ATF-1 can bind the wild-type CRE element of *ywhaz in-vitro*.

To determine if both of these factors could indeed occupy the CRE element in vivo, chromatin immunoprecipitation (ChIP) was used to test for CREB and/or ATF-1 binding to the endogenous *ywhaz* promoter in cell culture. Antisera against neither CREB nor ATF-1 immunoprecipitated *ywhaz*-CRE promoter DNA under the basal conditions tested.

**ATF-1 is recruited to the endogenous *ywhaz* promoter after stimulation with TNF-α**

Since neither CREB nor ATF-1 was found to occupy the endogenous CRE element during normal culture conditions, we sought to determine if binding could be induced by

stimulation. Previous reports suggest that both factors can be recruited to promoters after stimulation with TNF-α. Based on the ability of TNF-α to activate an apoptotic response it seemed likely that one mechanism by which cancers cell may act to evade TNF-α induced apoptosis would be to counter balance this response by inducing pro-survival factors such as 14-3-3ζ. Indeed this is the case in many cancer cells that are subject to pro-apoptotic stimuli where survival pathways, such as the nuclear-factor kappa B (NF-κB), are activated in response to TNF-α. To determine if the *ywhaz* promoter acted in a similar fashion with respect to CREB and ATF-1, we repeated the ChIP experiment after exposure to TNF-α. HeLa cells were cultured with 10 ng/ml of TNF-α for 0,1 or 2 hours, followed by ChIP. As anticipated TNF-α activated our positive control, NF-κB, which was found to bind a previously identified κB site in the promoter of the inhibitor of kappa B (I-kB), while neither CREB nor ATF were present at this promoter (Figure 3.13a). As it relates to the 14-3-3ζ promoter, antisera against ATF-1 and to a lesser extent CREB immunoprecipitated significantly more promoter DNA after stimulation (Figure 3.13b). These results are consistent with earlier reports where ATF-1 and CREB are phosphorylated in their kinase inducible domain after TNF-α treatment and subsequently recruited to CRE elements.

**Silencing of ATF-1 decreased 14-3-3 zeta expression**

Mutations of the CRE element decreased activity of the *ywhaz* promoter in reporter assays (Figure 3.6). Since both CREB and ATF-1 can bind this element, we next wanted to determine the requirement of ATF-1 and CREB in controlling endogenous 14-3-3 zeta expression in cells. To address this, short haripin RNAs (shRNA) targeting CREB or ATF-1 were expressed in HeLa cells. To circumvent the possibility of non-transfected

cells confounding our data analysis, cells were put under selection for 4 days prior to protein or mRNA extraction. The vectors used in this study produced a polycistronic transcript containing both the shRNA and the transcript encoding GFP, as such, we were able to monitor shRNA expression. Essentially, GFP fluorescence was indicative of shRNA expression in the same cells. Four days after the cells were put into selection, greater than 85% expressed detectable levels of GFP, which confirmed that shRNA expression in these cells was achieved. Longer time points resulted in complete cell death presumably due to ATF-1 knockdown, as control lines still proliferated. Therefore, the remaining experiments were conducted five days after shRNA transfection. Western blot analysis determined that ATF-1 knockdown resulted in reduced 14-3-3ζ protein levels (Figure 3.14a). ATF-1 levels fell to modest levels in cells transfected with construct III, while expression of the other two shRNA vectors resulted in marked reduction in ATF-levels. Unfortunately, neither of the shRNAs directed at CREB produced adequate knockdown of CREB protein (data not shown). Expression of neither an empty vector nor an shRNA generated against GAPDH could produce similar results suggesting that the 14-3-3ζ reduction was specific for ATF-1 knockdown.

**ATF-1 regulates expression of *ywhaz* transcript variants 1c and 1e**

Although we have determined that ATF-1 is important for the maintenance of 14-3-3ζ protein levels, the transcriptional contribution to this needs to be determined. As such, similar knockdown experiments were performed. The relative levels of the five transcript variants were determined by semi-quantitative PCR. Expression levels for both transcript variants 1c and 1e were reduced in cells overexpressing shRNA to ATF-1, while no apparent change in the transcript levels for the remaining three variants was observed

(figure 3.14b). Suggesting that ATF-1 controls expression of *ywhaz* from two transcript variants, one of which is the most abundant variant identified.

## Discussion

Although the research supporting the contribution of the14-3-3 family of proteins to tumor formation is still in its infancy, there certainly is an inverse correlation between 14-3-3 protein levels and cancer free survival. Imunohistological studies have determined aberrant levels of 14-3-3 proteins in various tumors where elevations tend to correlate with tumor severity [205-207]. As such, targeting these pro-survival master regulators for therapeutic development is an intense focus of the field; however many of these efforts are aimed at inhibiting 14-3-3 client protein interactions. As all seven family members share a remarkable degree of amino acid conservation, targeting one isoform is challenging at this level. Additionally, knockout studies in yeast suggest that a certain amount of functional 14-3-3 protein is necessary for normal cellular growth and proliferation [87]. Therefore a more direct approach would be to target these isoforms individually. This is supported by recent findings suggesting independent functions for the individual 14-3-3 isoforms. For example, knockdown of 14-3-3γ alone resulted in Bax and Bad induced apoptosis, while the contribution of 14-3-3ζ to anchorage independent growth was recently elucidated [153,208]. This emphasizes the importance of isoform independent cellular functions and the inability of the remaining isoforms to compensate for each other. Underscoring the need to better understand the regulation of the individual isoforms, which may offer an opportunity for therapeutic development through isoform specific inhibitors. In this current study we show the genomic contribution of *ywhaz* to 14-3-3ζ expression. We present here for the first time the transcriptional regulation of this pro-survival 14-3-3 isoform. At least five different transcript variants have been identified through this study, three of which have not yet

been reported in any peer reviewed publication. Furthermore, one of the transcripts, variant 1c, is the most dominant in its message levels and it translation efficiency. Finally, we show that the CREB family of transcription factors controls this major variant.

The CREB family of transcription factors binds to CRE elements in the promoter and enhancers of multiple genes. In fact, more than 6,300 CRE elements have been identified in the human genome; however the functionality of all of these has not yet been elucidated. In our study we show the CRE element within the proximal promoter of *ywhaz* is indeed functional, as mutations in the element result in a marked reduction in reporter activity (figure 3.6). Indeed the expression of CREB and ATF-1 change during the progression of human tumors. CREB protein levels positively correlate with the metastatic potential of melanoma cells and although ATF-1 is not identified in normal human melanocytes, it is easily identifiable in metastatic melanoma [169-171,209,210]. Based on our findings, correlative studies would suggest that tumors in which overexpressed CREB and ATF-1 have been identified should present with aberrant levels of 14-3-3ζ. This correlation is indeed present, as determined by expression profiling results available *in silico*. In fact, in the majority of microarray profiles examined, positive correlations exist between *ywhaz* and CREB family members (UCSC Genome Database, microarray expression data). An additional member of the 14-3-3 family also showed a similar profile in this database. This particular isoform, 14-3-3ε harbors a putative CRE element within its promoter as well. The function of this element has not been confirmed however it is possible that CREB family members may control the expression of multiple 14-3-3 family members. Our knockdown data suggest that although there is a modest

amount of total 14-3-3 protein loss that can be attributed to reduction in 14-3-3ζ, we cannot rule out the possibility that other isoforms may be directly or indirectly effected by this KD approach (Figure 3.14a). Importantly, not all 14-3-3 protein is lost, suggesting that ATF-1 cannot regulate expression of all 14-3-3 isoforms.

Both CREB and ATF-1 are upregulated in multiple cancers; therefore, it seems likely that TNF-α stimulation of these transcription factors may be one mechanism by which cancerous cells can evade TNF-α-induced apoptosis. Indeed, we see targeted binding of ATF-1 and CREB to the *ywhaz* in the presence of TNF-α. Although this data is preliminary it suggests that CREB and/or ATF-1 may act to induce activation of this pro-survival gene leading to a reduction in TNF-α-induced apoptosis. This suggests that a novel therapeutic approach to tumors with elevations in 14-3-3ζ may be to use a CREB family member inhibitor to sensitize cells to TNF-α treatment.

## References


1. Fu, H., Subramanian, R.R. & Masters, S.C. 14-3-3 proteins: structure, function, and regulation. *Annu Rev Pharmacol Toxicol* **40**, 617-47 (2000).
2. Muslin, A.J., Tanner, J.W., Allen, P.M. & Shaw, A.S. Interaction of 14-3-3 with signaling proteins is mediated by the recognition of phosphoserine. *Cell* **84**, 889-97 (1996).
3. Yaffe, M.B. et al. The structural basis for 14-3-3:phosphopeptide binding specificity. *Cell* **91**, 961-71 (1997).
4. Ganguly, S. et al. Melatonin synthesis: 14-3-3-dependent activation and inhibition of arylalkylamine N-acetyltransferase mediated by phosphoserine-205. *Proc Natl Acad Sci U S A* **102**, 1222-7 (2005).
5. Coblitz, B., Wu, M., Shikano, S. & Li, M. C-terminal binding: an expanded repertoire and function of 14-3-3 proteins. *FEBS Lett* **580**, 1531-5 (2006).
6. Lopez-Girona, A., Furnari, B., Mondesert, O. & Russell, P. Nuclear localization of Cdc25 is regulated by DNA damage and a 14-3-3 protein. *Nature* **397**, 172-5 (1999).
7. Lee, J., Kumagai, A. & Dunphy, W.G. Positive regulation of Wee1 by Chk1 and 14-3-3 proteins. *Mol Biol Cell* **12**, 551-63 (2001).
8. Obsil, T., Ghirlando, R., Klein, D.C., Ganguly, S. & Dyda, F. Crystal structure of the 14-3-3zeta:serotonin N-acetyltransferase complex. a role for scaffolding in enzyme regulation. *Cell* **105**, 257-67 (2001).
9. Morrison, D.K., Heidecker, G., Rapp, U.R. & Copeland, T.D. Identification of the major phosphorylation sites of the Raf-1 kinase. *J Biol Chem* **268**, 17309-16 (1993).
10. Thorson, J.A. et al. 14-3-3 proteins are required for maintenance of Raf-1 phosphorylation and kinase activity. *Mol Cell Biol* **18**, 5229-38 (1998).
11. Tzivion, G., Luo, Z. & Avruch, J. A dimeric 14-3-3 protein is an essential cofactor for Raf kinase activity. *Nature* **394**, 88-92 (1998).
12. Braselmann, S. & McCormick, F. Bcr and Raf form a complex in vivo via 14-3-3 proteins. *EMBO J* **14**, 4839-48 (1995).
13. Vincenz, C. & Dixit, V.M. 14-3-3 proteins associate with A20 in an isoform-specific manner and function both as chaperone and adapter molecules. *J Biol Chem* **271**, 20029-34 (1996).
14. Woodcock, J.M., Murphy, J., Stomski, F.C., Berndt, M.C. & Lopez, A.F. The dimeric versus monomeric status of 14-3-3zeta is controlled by phosphorylation of Ser58 at the dimer interface. *J Biol Chem* **278**, 36323-7 (2003).
15. Powell, D.W. et al. Proteomic identification of 14-3-3zeta as a mitogen-activated protein kinase-activated protein kinase 2 substrate: role in dimer formation and ligand binding. *Mol Cell Biol* **23**, 5376-87 (2003).
16. Ferguson, A.T. et al. High frequency of hypermethylation at the 14-3-3 sigma locus leads to gene silencing in breast cancer. *Proc Natl Acad Sci U S A* **97**, 6049-54 (2000).
17. Hermeking, H. et al. 14-3-3 sigma is a p53-regulated inhibitor of G2/M progression. *Mol Cell* **1**, 3-11 (1997).

18. Qi, W., Liu, X., Qiao, D. & Martinez, J.D. Isoform-specific expression of 14-3-3 proteins in human lung cancer tissues. *Int J Cancer* **113**, 359-63 (2005).
19. Neal, C.L. et al. 14-3-3zeta overexpression defines high risk for breast cancer recurrence and promotes cancer cell survival. *Cancer Res* **69**, 3425-32 (2009).
20. Karolchik, D. et al. The UCSC Genome Browser Database. *Nucleic Acids Res* **31**, 51-4 (2003).
21. Cao, L. et al. Identification of 14-3-3 protein isoforms in human astrocytoma by immunohistochemistry. *Neurosci Lett* **432**, 94-9 (2008).
22. Matta, A., Bahadur, S., Duggal, R., Gupta, S.D. & Ralhan, R. Over-expression of 14-3-3zeta is an early event in oral cancer. *BMC Cancer* **7**, 169 (2007).
23. Fan, T. et al. Up-regulation of 14-3-3zeta in lung cancer and its implication as prognostic and therapeutic target. *Cancer Res* **67**, 7901-6 (2007).
24. van Heusden, G.P., van der Zanden, A.L., Ferl, R.J. & Steensma, H.Y. Four Arabidopsis thaliana 14-3-3 protein isoforms can complement the lethal yeast bmh1 bmh2 double disruption. *FEBS Lett* **391**, 252-6 (1996).
25. Ajjappala, B.S. et al. 14-3-3 gamma is stimulated by IL-3 and promotes cell proliferation. *J Immunol* **182**, 1050-60 (2009).
26. Li, Z. et al. Down-regulation of 14-3-3zeta suppresses anchorage-independent growth of lung cancer cells through anoikis activation. *Proc Natl Acad Sci U S A* **105**, 162-7 (2008).
27. Jean, D. & Bar-Eli, M. Targeting the ATF-1/CREB transcription factors by single chain Fv fragment in human melanoma: potential modality for cancer therapy. *Crit Rev Immunol* **21**, 275-86 (2001).
28. Jean, D. & Bar-Eli, M. Regulation of tumor growth and metastasis of human melanoma by the CREB transcription factor family. *Mol Cell Biochem* **212**, 19-28 (2000).
29. Jean, D., Harbison, M., McConkey, D.J., Ronai, Z. & Bar-Eli, M. CREB and its associated proteins act as survival factors for human melanoma cells. *J Biol Chem* **273**, 24884-90 (1998).
30. Xie, S. et al. Dominant-negative CREB inhibits tumor growth and metastasis of human melanoma cells. *Oncogene* **15**, 2069-75 (1997).
31. Yang, Y.M., Dolan, L.R. & Ronai, Z. Expression of dominant negative CREB reduces resistance to radiation of human melanoma cells. *Oncogene* **12**, 2223-33 (1996).

## Figure Legends

***Figure 3.1. Representation of ywhaz, the gene encoding 14-3-3ζ, and its transcript variants.*** **(A)** Genomic locus for ywhaz. Five different first exons are indicated as 1a, 1b, 1c, 1d and 1e. Right-hand arrow represents the start methionine. Putative CRE element is depicted as a downward arrow within the intron preceding exon 1c. The number of nucleotides contained within each of the introns and exons is labeled below each respective feature. **(B)** Transcripts that were confirmed to be expressed. Transcript variants beginning with exon 1a and 1c were previously reported. The remaining three variants are novel to this study.

***Figure 3.2. Reverse transcription-PCR amplification reveals an additional transcript variant for ywhaz.*** **(A)** Representation of location of primer pairs used of reverse transcript PCR. Right arrows indicate forward primers used in this study, while a left arrow spanning the boundary of exon 4 and 5 depicts the one reverse primer. **(B)** Transcript variants 1a, 1b and 1c were identified in mRNA pools from HeLa cells with a forward primer to the respective first exon and a reverse primer spanning the boundary of exon 4 and exon 5. A higher molecular weight product was amplified with the forward primer for exon 1b (arrow). All products were gel purified and sequenced and confirmed to be variants of *ywhaz*. The only splice variant identified contains both exon 1b and 1c followed by exon 2.

***Figure 3.3. Transcript variants are differentially expressed relative to one another as well as between cell-lines.*** Total RNA was isolated from a panel of cell lines. **(A)** A representative Northern blot of total RNA probed with cDNA to exons 1a, 1b, and 1c.

**(B)** RNA was reverse transcribed, amplified by real-time-RT-PCR and used to determine the relative expression of each of the five transcript variants. Data shown are relative to levels obtained from HeLa cell mRNA.

***Figure 3.4. The 5'UTR of ywhaz variant 1c dictates the highest efficiency in translation.*** Hela cells were transfected with luciferase reporter vectors for each of the 5'UTRs. Renilla control plasmid was used to normalize transcript levels and luciferase activity. Cells were lysed to determine luciferase activity and isolated for total RNA at 10, 28 and 35 hours post transfection. **(A)** Real-time-RT-PCR for firefly and renilla was performed on cDNA obtained from total RNA. *Firefly* transcript levels are graphed relative to *renilla*. **(B)** Isolated protein was assayed for luciferase activity as outlined in methods. Data are graphed as firefly relative to renilla control. **(C)** Data from (A) and (B) were combined are graphed as relative luciferase activity over the relative transcript levels for luciferase.

***Figure 3.5. ywhaz transcript variant 1c is the most highly expressed.*** **(A)** The total amount of ywhaz transcripts found in the UCSD Genome Database was determined to be 265. These were subdivided into ones belonging to the five different transcript variants and are graphed as percentages relative to the total. **(B)** RLM-RACE clones (77) were sequenced and grouped according to the exon that they began with. They are represented as the percent of clones sequenced that contained that particular variant.

***Figure 3.6. Two major cis-activating regions are identified in ywhaz transcript variant 1c.*** The proximal promoter for transcript variant 1c was cloned upstream of a luciferase reporter vector. Truncations of the promoter region were generated. These constructs

were transfected in combination with Renilla control vector into HeLa cells and assayed for their relative luciferase activity 24 hours later. Data are graphed as Firefly relative to Renilla over empty vector control and represent averages of three experiments +/- one standard deviation.

***Figure 3.7. A conserved CRE element identified within the promoter for ywhaz variant 1c***. The sequence between and surrounding the luciferase truncations (-72 and -85) was aligned from human to *tetradon*. Light grey nucleotides indicate loss of conservation. The grey box containing 100% sequence conservation contains the putative CRE element. Sequences were aligned using the UCSC Genome Bioinformatics Group Database.

***Figure 3.8. Two central nucleotides within the CRE element are necessary for basal expression from the promoter controlling variant 1c.*** **(A)** Schematic of the sequence surrounding the CRE element and the two-nucleotide mutation generated. **(B)** HeLa cells were transfected with one of three 1c constructs with or without CRE mutations engineered in them. Transfection efficiency was controlled for by co-expression of a Renilla reporter plasmid. Data are graphed as Firefly relative to Renilla over empty vector control and represent the average of three independent experiments +/- standard deviation. Percent loss of activity for each of the three mutated reporters is indicated.

***Figure 3.9. Nuclear proteins bind to the putative CRE element in vitro.*** EMSAs were performed using crude nuclear extracts prepared from HeLa cells. Extracts were incubated with a 28-nt-radioactively labeled probe surrounding the putative CRE element and were resolved on nondenaturing PAGE. 10 and 100 fold excess of either wildtype or

mutant competitor was added to determine specificity. Mutant competitor contained the same sequence as in Figure 3.8-A.

***Figure 3.10. Separation of active complexes over a heparin-agarose column.*** **(A)** Twenty mg of crude nuclear extract purified from HeLa cells was fractionated over a heparin-agarose column. Eluted fractions were obtained over a 1M NaCl gradient and assayed for their binding ability by EMSA. Multiple complexes were identified (arrows) that could be separated into two pools with peak EMSA activity. **(B)** Pooled fractions obtained from the previous EMSA analysis were subject to competition assays with either 10 or 100 fold excess of wildtype or mutant competitor as in Figure 3.9.

***Figure 3.1.1 CREB family members bind to the ywhaz promoter in vitro.*** EMSAs were performed using HeLa nuclear extract incubated with radioactive labeled probe as in Figure 3.9. Antisera included in the reaction include: 270, antisera to CREB, CREM and ATF-1; CR, antisera to CREB; 243, antisera to ATF-1; 60, antisera to ATF-1; P-1 antisera to Prep-1 (negative control). **(A)** EMSA supershift assay of both crude nuclear extract and fractions 48-52 obtained from heparin fractionation. No shifts are evident in the heparin-pooled lanes. **(B)** EMSA performed on crude nuclear extract and heparin pooled fractions 56-60. Shifts are evident with antisera against CREB and/or ATF-1. Arrows in both (A) and (B) represent the major complexes identified after heparin fractionation.

***Figure 3.12. CREB and ATF-1 bind the wildype CRE element.*** Nuclear extracts obtained from HeLa cells were incubated with streptavidin beads conjugated to wild type or mutant biotinylated oligos. Precipitated beads were washed extensively and bound

proteins were resolved on SDS-PAGE. Transfer of proteins to membranes was followed by probing with antisera against CREB and ATF-1. Both proteins were enriched for when wild type sequence-conjugated beads were used for precipitation.

***Figure 3.13. Binding of ATF-1 and CREB to the endogenous ywhaz promoter is induced following TNFα stimulation.*** HeLa cells were cultured in the presence or absence of TNF-α followed by isolation of chromatin. ChIP assays were performed using antisera against ATF-1, CREB, or NF-κB (p65). Immunoprecipitated DNA was amplified with primer sets to *ywhaz* and I-κB promoters and are represented as amplified product relative to product obtained from 1/30 the amount of input. **(A)** TNF-α induced binding of NF-κB to the I-κB promoter. **(B)** TNF-α induced binding of ATF-1 and CREB to the *ywhaz* promoter.

***Figure 3.14. ATF-1 regulated expression of 14-3-3ζ by transcript variants 1c and 1e.*** HeLa cells were transfected with three different shRNAs targeted to the 3'UTR of ATF-1 (I, II, and III). Five days following transfection protein or total RNA was isolated. **(A)** Proteins were fractionated by SDS-PAGE followed by immunoblotting. Antisera against CREB and ATF-1 were used to monitor knockdown. 14-3-3ζ and total 14-3-3 levels were determined first with zeta specific antisera followed by antisera against all 14-3-3 isoforms. Beta-actin protein levels serves as a loading control. Empty vector (-) and shRNA to GAPDH are negative controls **(B)** Total RNA was reverse transcribed. Amplification of *ywhaz* transcripts was carried out with transcript specific primers by semi-quantitative PCR followed by densitometry analysis. Data are graphed relative to β-actin transcript levels.

**Figure 3.1**

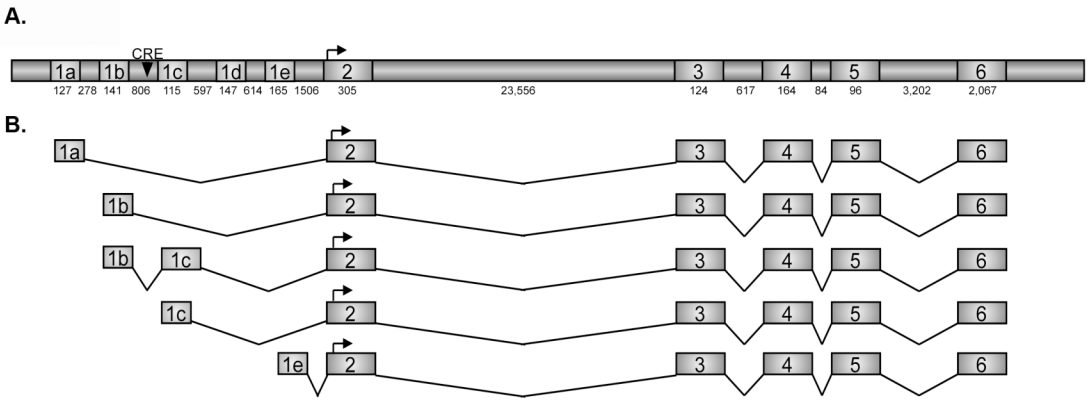
A.
CRE
1a
1b
1c
1d
1e
2
3
4
5
6
127 278 141 806 115 597 147 614 165 1506 305 23,556 124 617 164 84 96 3,202 2,067
B.
1a
1b
1c
1d
1e
2
3
4
5
6

**Figure 3.2**

**A.**

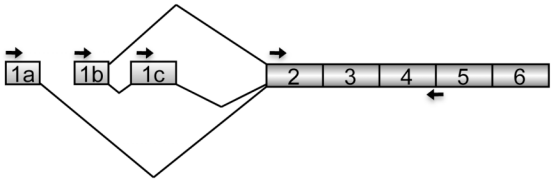


**B.**

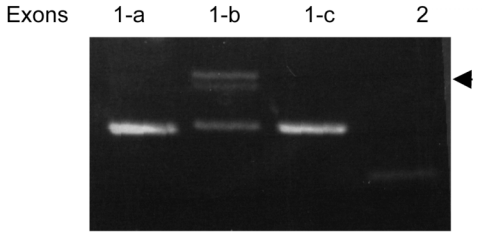

**Figure 3.3**

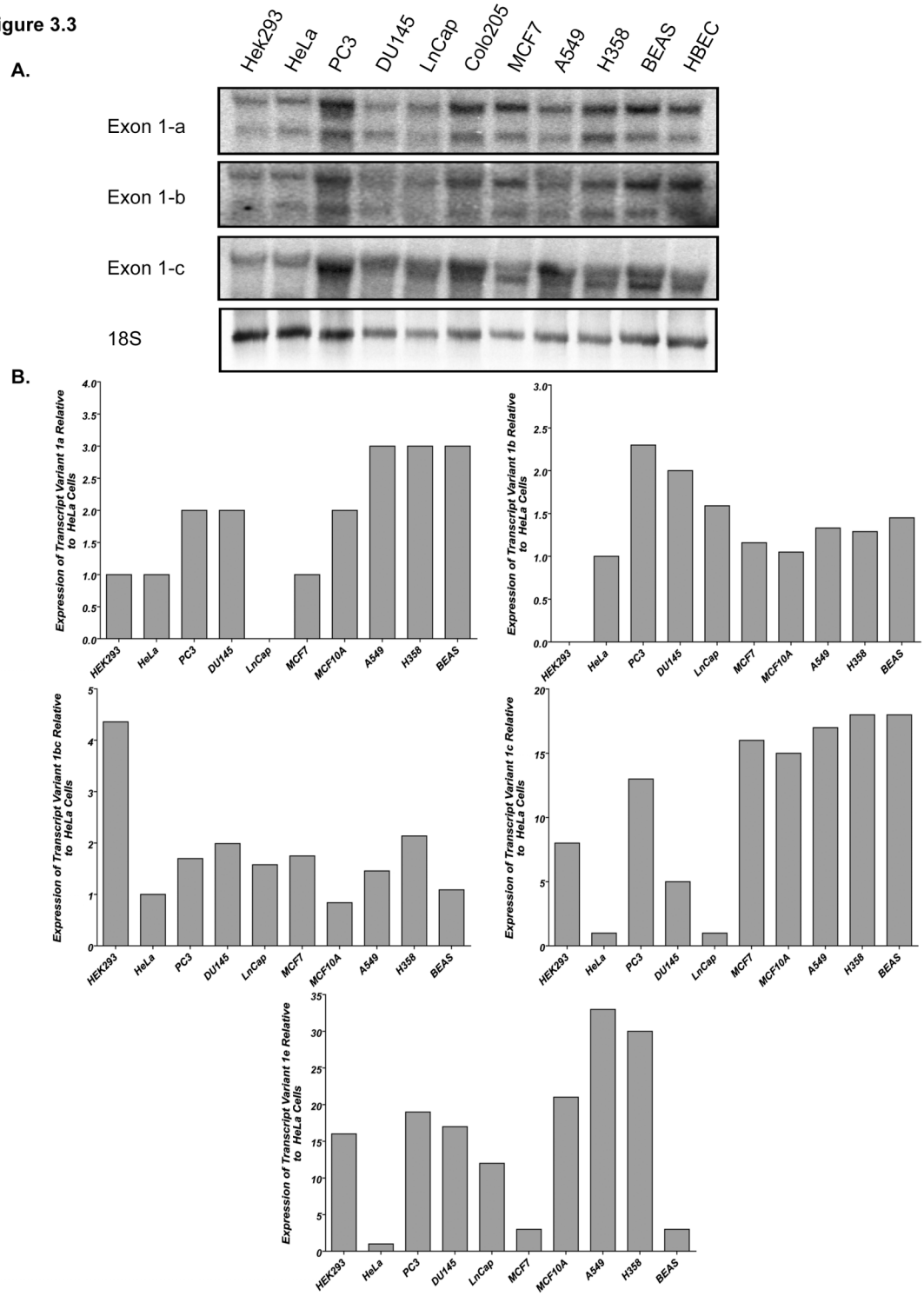
A.
Hek293
HeLa
PC3
DU145
LnCap
Colo205
MCF7
A549
H358
BEAS
HBEC
Exon 1-a
Exon 1-b
Exon 1-c
18S
B.
Expression of Transcript Variant 1a Relative to HeLa Cells
Expression of Transcript Variant 1b Relative to HeLa Cells
Expression of Transcript Variant 1bc Relative to HeLa Cells
Expression of Transcript Variant 1c Relative to HeLa Cells
Expression of Transcript Variant 1e Relative to HeLa Cells
HEK293
HeLa
PC3
DU145
LnCap
MCF7
MCF10A
A549
H358
BEAS

**Figure 3.4**

**A.**

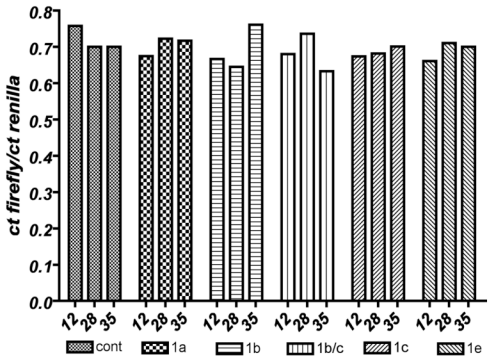


**B.**

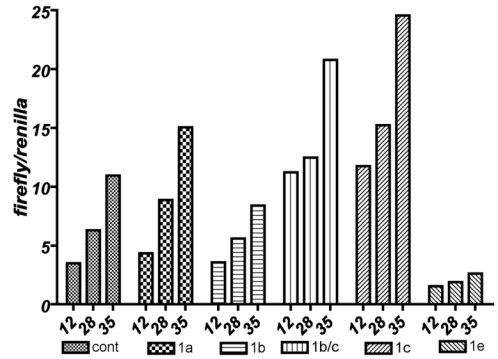


**C.**

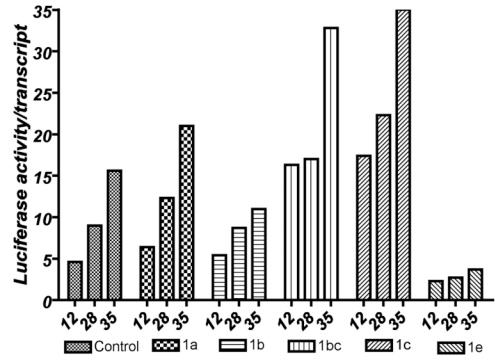

**Figure 3.5**

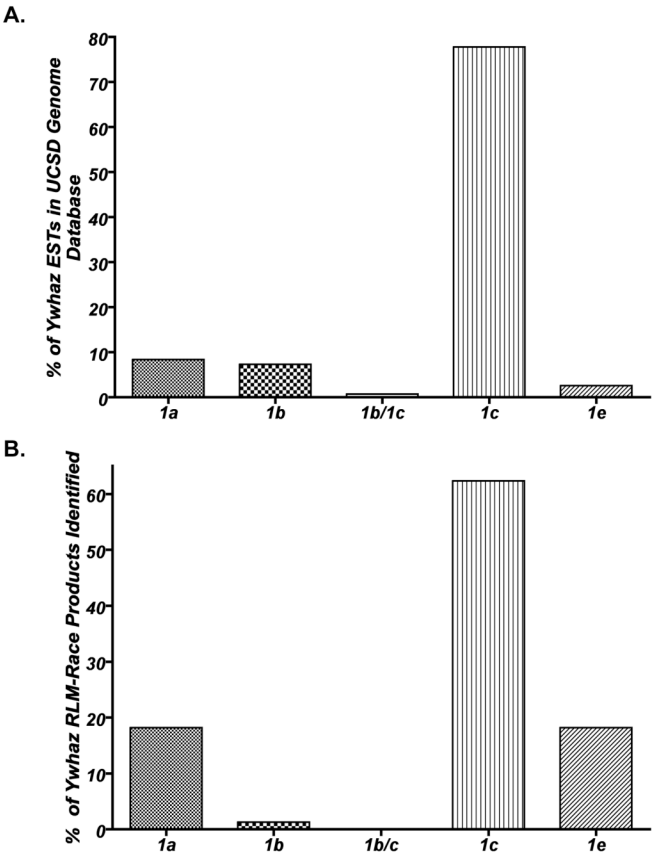
A.
% of Ywhaz ESTs in UCSD Genome Database
80
70
60
50
40
30
20
10
0
1a
1b
1b/1c
1c
1e
B.
% of Ywhaz RLM-Race Products Identified
60
50
40
30
20
10
0
1a
1b
1b/c
1c
1e

**Figure 3.6**

**A.**

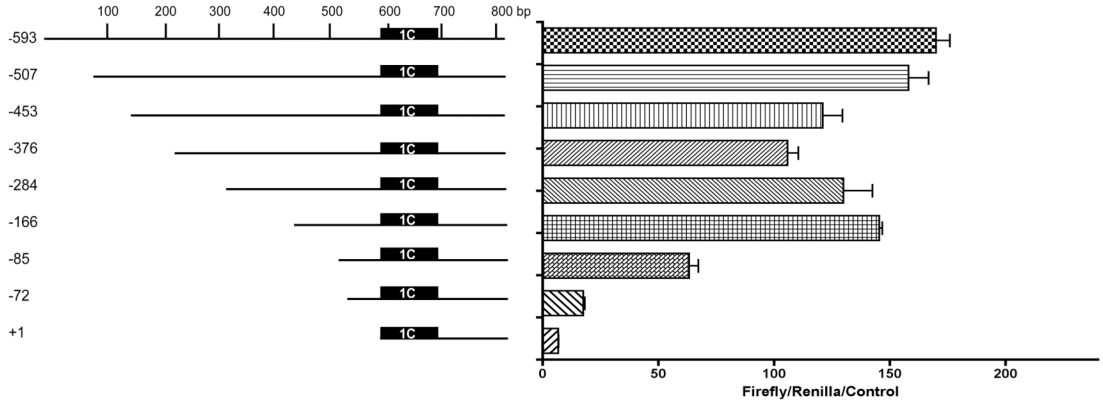
100
200
300
400
500
600
700
800 bp
-593
-507
-453
-376
-284
-166
-85
-72
+1
1C
0
50
100
150
200
Firefly/Renilla/Control

**Figure 3.7**


Human GCAGGGGCACCACACGCACGATGACGTCAAACGCTGCTATGGCAACCGTTGATTGGT
Rhesus GCAGGGGCACCACACGCACGATGACGTCAAACGCTGCTATGGCAACCGTTGATTGGT
Mouse GCAGGGGCACCACACGCACGATGACGTCAAACGCTGCTATGGCAACCGTTGATTGGT
Rat GCAGGGGCACCACACGCACGATGACGTCAAACGCTGCTATGGCAACCGTTGATTGGT
Dog GCAGGGGCACCACACGCACGATGACGTCAAACGCTGCTATGGCAACCGTTGATTGGT
Horse GCAGGGGCACCACACGCACGATGACGTCAAACGCTGCTATGGCAACCGTTGATTGGT
Armadillo GCAGGGGCACCACACGCACGATGACGTCAAACGCTGCTATGGCAACCGTTGATTGGT
Elephant GCAGGGGCACCAGACGCACGATGACGTCAAACGCTGCTATGGCAACCGTTGATTGGT
Opossum GCAGGGGCACCACACGCACGATGACGTCAAACGCTGCTATGGCAACCGCTGATTGGT
Platypus GCAGGGGCACCACACGCGCGATGACGTCAAACGGTGGTATGGCAACCGCTGATTGGT
Tetradon GCAGGGTCTCGCCGGGCACGCTGACGTCAGCGGTTGCCAGGGCAACC
CRE

**Figure 3.8**

**A.**

Wild-type 14-3-3ζ-CRE CAGCGTT**TGACGTCA**TCGTGC
Mutant 14-3-3ζ-CRE CAGCGTT**TGA**TA**TCA**TCGTGC

**B.**

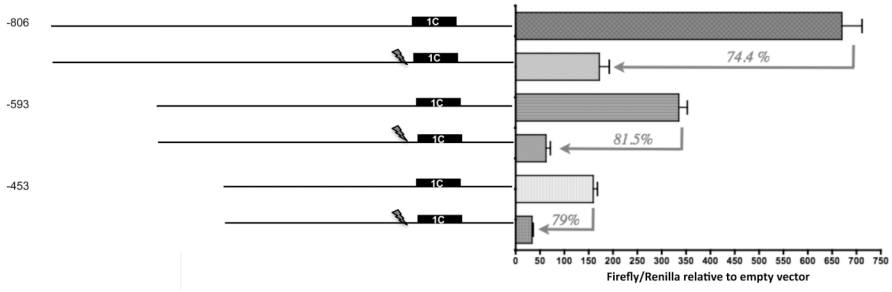

**Figure 3.9**

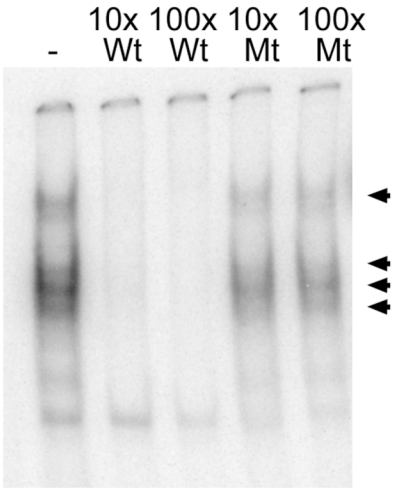

**Figure 3.10**

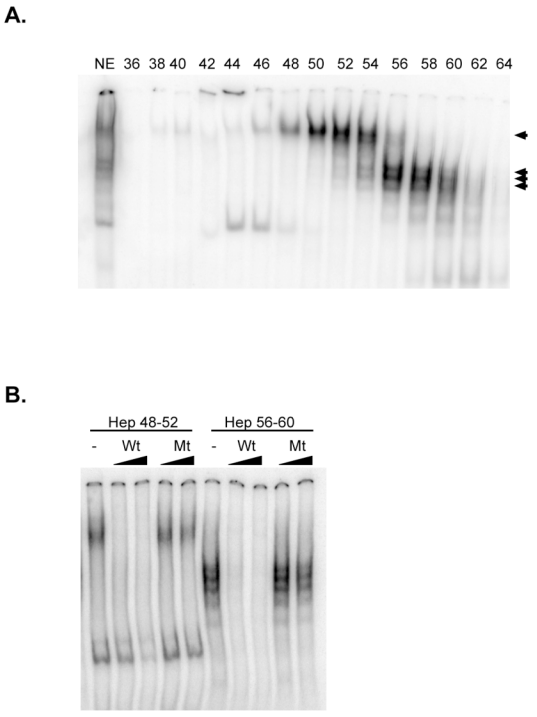
A.
NE 36 38 40 42 44 46 48 50 52 54 56 58 60 62 64
B.
Hep 48-52
Hep 56-60
- Wt Mt - Wt Mt

**Figure 3.11**

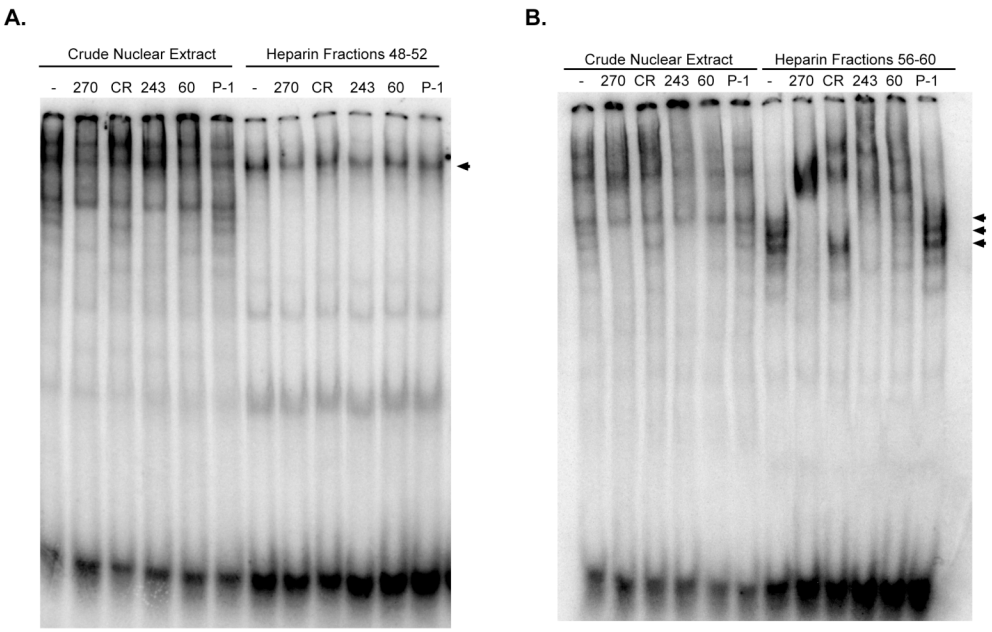
A.
Crude Nuclear Extract
Heparin Fractions 48-52
- 270 CR 243 60 P-1 - 270 CR 243 60 P-1
B.
Crude Nuclear Extract
Heparin Fractions 56-60
- 270 CR 243 60 P-1 - 270 CR 243 60 P-1

**Figure 3.12**

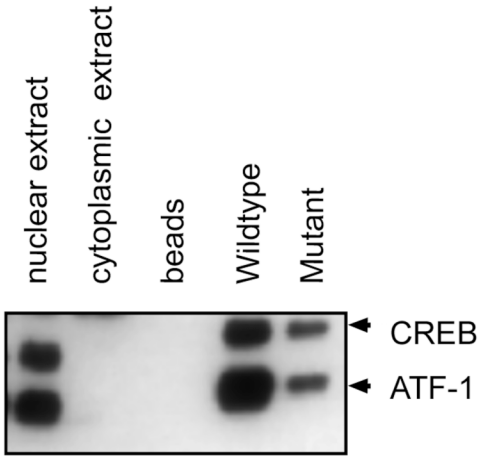
nuclear extract
cytoplasmic extract
beads
Wildtype
Mutant
CREB
ATF-1

**Figure 3.13**

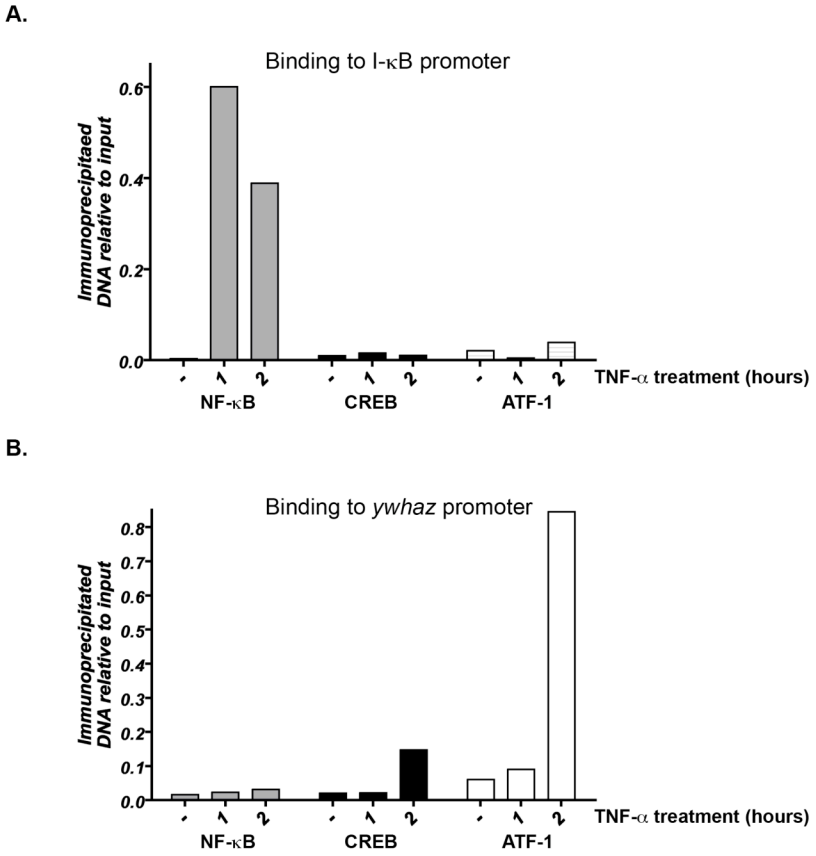
A.
Binding to I-κB promoter
Immunoprecipitaed DNA relative to input
0.6
0.4
0.2
0.0
- 1 2 - 1 2 - 1 2
TNF-α treatment (hours)
NF-κB
CREB
ATF-1
B.
Binding to ywhaz promoter
Immunoprecipitated DNA relative to input
0.8
0.7
0.6
0.5
0.4
0.3
0.2
0.1
0.0
- 1 2 - 1 2 - 1 2
TNF-α treatment (hours)
NF-κB
CREB
ATF-1

**Figure 3.14**

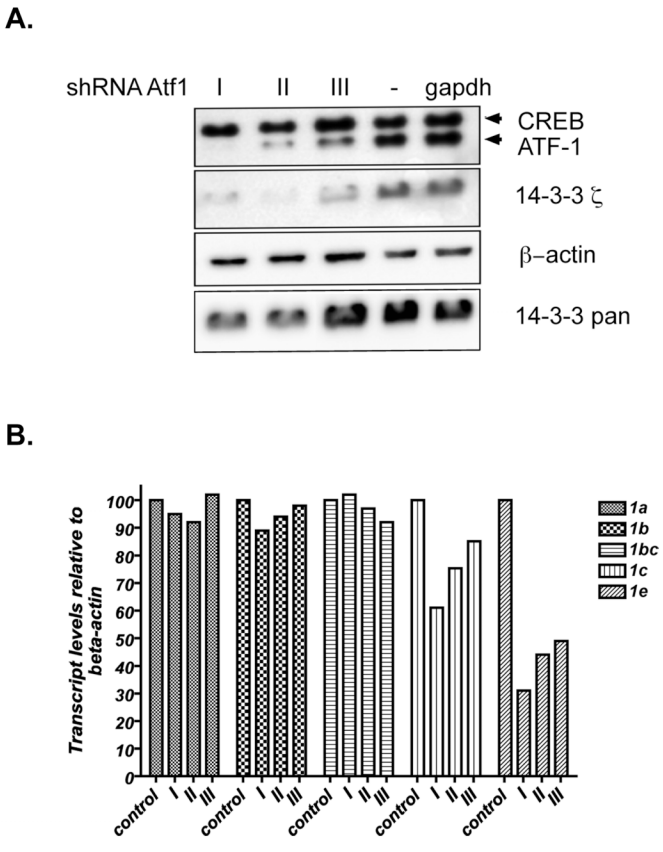
A.
shRNA Atf1 I II III - gapdh
CREB
ATF-1
14-3-3 ζ
β–actin
14-3-3 pan
B.
Transcript levels relative to beta-actin
100
90
80
70
60
50
40
30
20
10
0
control I II III control I II III control I II III control I II III control I II III
1a
1b
1bc
1c
1e

# Chapter 4: Discussion

**Discussion**

Each cancer can be viewed as a completely different disease. The reason for this is evident when analyzing gene signatures for different cancers. Microarray based techniques show very different expression pattern between tumors. Even metastatic tumors originating from the same parent tumor display differences in the genes that are necessary to sustain their growth and proliferation. As such, a great deal of effort has gone into the classification of tumors according their aberrant gene expression patterns, many of which are pro-survival and anti-apoptotic genes. Understanding how these genes are switched on and off in a tumor becomes imperative for treating these deadly diseases. Furthermore, many current therapies used in the clinic today are based solely on the phenotype that they elicit. Treatments are currently aimed at the final outcome of either tumor suppression or regression, opposed to targeting individual genes (or a subset) that are found to be elevated in that particular tumor. Although the results of this phenotype based approach looks promising in the beginning, many cells develop resistance to standard regiments. As such more directed therapies that hit individual proteins necessary for tumor growth are needed in the early stages of treatment. Two major things come to mind that are needed for such an approach. The first is to determine the signature for a particular tumor. In doing so we unravel the unique characteristics attributed to that particular tumor and learn about the genes that it requires to grow and proliferate. This avenue has taken off with the advent of the sequencing of the human genome. However, it is not enough to know that a certain gene is elevated or reduced. Not every gene has an approved molecular inhibitor that can be used for treatment. In addition to discovering

small molecule inhibitors targeting the aberrantly regulated protein, compound libraries can be screened for inhibitors of upstream regulatory proteins. Therefore, if we first understand how these genes are regulated via these upstream modulators, the treatment window expands. The work outlined in Chapter 3 of this dissertation does just that.

The 14-3-3 family of proteins show positive correlations with increased cancerous deaths. Experimental evidence supports a role for these proteins in growth and proliferation. Their elevated levels lead to enhanced proliferation through their interactions with multiple cellular ligands. Overall, 14-3-3 proteins act to suppress pro-apoptotic genes and increase the activity of genes important for survival. As such blocking the interaction of 14-3-3 with its clients is an area of intense investigation. Much of this is being accomplished through inhibitors that bind the amphipathic groove of 14-3-3 monomers. This seems promising, though evidence suggests that 14-3-3 proteins have independent cellular roles. Recent work has discovered that these homologous 14-3-3 proteins cannot compensate for the loss of a single member. Much of the homology between isoforms falls within the amphipathic groove of these proteins. Indeed a phospho-peptide generated with a 14-3-3 binding motif docks within the amphipathic groove of these molecules. Introducing it into cells suppressed all 14-3-3 isoforms from interacting with multiple clients. As many of the currently identified small molecule inhibitors bind to this region, they will lead to global 14-3-3-client protein inhibition. Side effects attributed to suppressing all seven family members are not fully understood at this time; however knockout studies suggest that at least one 14-3-3 member is required for sustained growth and proliferation in both yeast and fungi. Furthermore, 14-3-3σ is thought to have tumor-suppressive properties. It too would be

inhibited by this method and as a result may induce tumor progression. A way to circumvent this is to determine the underlying mechanism controlling the elevations in individual members. In this dissertation, 14-3-3ζ, an oncogenic member of the 14-3-3 family was studied at the genomic and transcriptional level to identify potential mechanisms leading to its elevation in tumors. The complexity of this isoform was much more appreciated following this study. Through this work, five different transcript variants were identified. One was shown to be more dominant than the rest. A member of the CREB family of transcription factors, ATF-1, controls the expression of this variant. Indeed ATF-1 is elevated in cancers and microarray profiling has determined that ATF-1 and 14-3-3ζ are expressed to near equal levels in a variety of tissues and cancers. Although the levels of the remaining isoforms still need to be evaluated individually in our ATF-1 silenced cells, the total level of 14-3-3 protein is not completely diminished. If the other isoforms are not affected, it now becomes possible to regulate 14-3-3ζ apart from disrupting the activities of the other six isoforms. ATF-1 inhibitors now become a tool for studying 14-3-3ζ in the laboratory. This also has served as a link to the potential role for why elevations in ATF-1 may be leading to carcinogenesis.

As aforementioned, the sequencing of the human genome followed by microarray analysis of tumor tissue has led to an appreciation of genes whose expression are altered in tumors. A lot of data surrounding this has been deposited into various databases. Once individual proteins are identified as having a causative role in tumorigenesis, the next and possibly more cumbersome task entails the design of molecular inhibitors to target these proteins. Although the technology exists for identifying tumor signatures, the design of

drugs to target causative proteins lags behind. The main reason for this is that many drugs are identified based on a forward pharmacological approach. Basically, drug use is dependent on the elicited phenotype and less on the molecular target of the compound. As such many of these compounds are pleiotropic, meaning that they have more than one cellular target. One can assume that this could be advantageous, such that tumors are unable to become resistant to the drug. However, because many of these targets go without being identified, we cannot be certain that they are helpful to the therapies being conducted. Researchers both in academia and in industry have shifted to identification of inhibitors by a more reverse approach. In this way, a target is identified and hundreds-of-thousands of compounds are screened for their ability to modulate the chosen target. This too seems like a very promising approach. What one forgets is that although many compounds may indeed act on the desired target, they most likely will also target other proteins in the cell. Therefore, where do we go from here? The main problem with drugs identified by both of these methods is the potential side effects leading to toxicity. These challenges have led researches to explore the use of natural products that present with limited toxicities for further drug development. Many of these have been used over centuries and as such have well documented safety profiles. The challenge to us is to determine the targets of these safe compounds such that they can be used appropriately and quite possible to suppress tumor growth based on the target they hit. My work evaluating the molecular mechanism of action of EF24 did just that. EF24, an analog of curcumin, had shown very promising anti-cancer roles in the laboratory. Both treatments of cell culture and in vivo model organisms suggest that this compound is both safe and effective. As EF24 has entered into Phase 0 clinical trials for head and neck cancer,

determining its targets can aid in the directed treatment of these tumors. My work has determined that one of the targets, which very well may be the main target for this compound is IKKβ. Activation of the IKK complex is the main determinant in the induction of NF-κB activity. As discussed, NF-κB induces the expression of many anti-apoptotic and pro-survival genes. Elevated NF-κB is both found in tumors and can be further induced upon chemotherapies and via radiation. The second of which is thought to be a defense mechanism that the tumor turns on in order to evade apoptosis triggered from these treatments. The elucidation that EF24 targets this pathway and exhibits a promising safety profile suggests that it may be useful in treating individuals whose tumors present with elevated NF-κB. As recent advances have not led to as many targeted treatments as one might hope the use of broad spectrum chemotherapies and radiation to treat tumors is still the most practiced form of treatment. However, knowing that NF-κB is induced via these treatments suggest that combining these therapies with EF24 may sensitize tumor cells to these therapies allowing for more promising outcomes.

Indeed the work in this dissertation has shed light onto the transcriptional regulation of a particular pro-survival gene that is upregulated in tumors. The mechanisms leading to its elevation are beginning to be elucidated. Although EF24 does not target the expression of this particular gene, it is able to suppress the activation of an additional pro-survival pathway. Both of these studies together highlight the importance for understanding gene regulation and the ability to control aberrant regulation by small molecule modulation.

# Chapter 5: References

1. Butler, M.S. & Newman, D.J. Mother Nature's gifts to diseases of man: the impact of natural products on anti-infective, anticholestemics and anticancer drug discovery. *Prog Drug Res* **65**, 1, 3-44 (2008).
2. Newman, D.J. & Cragg, G.M. Natural products as sources of new drugs over the last 25 years. *J Nat Prod* **70**, 461-77 (2007).
3. Aggarwal, B.B. & Sung, B. Pharmacological basis for the role of curcumin in chronic diseases: an age-old spice with modern targets. *Trends Pharmacol Sci* **30**, 85-94 (2009).
4. Singh, S. & Aggarwal, B.B. Activation of transcription factor NF-kappa B is suppressed by curcumin (diferuloylmethane) [corrected]. *J Biol Chem* **270**, 24995-5000 (1995).
5. Adams, B.K. et al. Synthesis and biological evaluation of novel curcumin analogs as anti-cancer and anti-angiogenesis agents. *Bioorg Med Chem* **12**, 3871-83 (2004).
6. Adams, B.K. et al. EF24, a novel synthetic curcumin analog, induces apoptosis in cancer cells via a redox-dependent mechanism. *Anticancer Drugs* **16**, 263-75 (2005).
7. Arora, R.B., Kapoor, V., Basu, N. & Jain, A.P. Anti-inflammatory studies on Curcuma longa (turmeric). *Indian J Med Res* **59**, 1289-95 (1971).
8. Ramsewak, R.S., DeWitt, D.L. & Nair, M.G. Cytotoxicity, antioxidant and anti-inflammatory activities of curcumins I-III from Curcuma longa. *Phytomedicine* **7**, 303-8 (2000).
9. Mazumder, A., Raghavan, K., Weinstein, J., Kohn, K.W. & Pommier, Y. Inhibition of human immunodeficiency virus type-1 integrase by curcumin. *Biochem Pharmacol* **49**, 1165-70 (1995).
10. Johnson, J.J. & Mukhtar, H. Curcumin for chemoprevention of colon cancer. *Cancer Lett* **255**, 170-81 (2007).
11. Surh, Y.J. & Chun, K.S. Cancer chemopreventive effects of curcumin. *Adv Exp Med Biol* **595**, 149-72 (2007).
12. Kuttan, R., Bhanumathy, P., Nirmala, K. & George, M.C. Potential anticancer activity of turmeric (Curcuma longa). *Cancer Lett* **29**, 197-202 (1985).
13. Chen, A., Xu, J. & Johnson, A.C. Curcumin inhibits human colon cancer cell growth by suppressing gene expression of epidermal growth factor receptor through reducing the activity of the transcription factor Egr-1. *Oncogene* **25**, 278-87 (2006).
14. Huang, M.T. et al. Inhibitory effects of dietary curcumin on forestomach, duodenal, and colon carcinogenesis in mice. *Cancer Res* **54**, 5841-7 (1994).
15. Singh, S.V. et al. Mechanism of inhibition of benzo[a]pyrene-induced forestomach cancer in mice by dietary curcumin. *Carcinogenesis* **19**, 1357-60 (1998).
16. Dorai, T., Cao, Y.C., Dorai, B., Buttyan, R. & Katz, A.E. Therapeutic potential of curcumin in human prostate cancer. III. Curcumin inhibits proliferation, induces apoptosis, and inhibits angiogenesis of LNCaP prostate cancer cells in vivo. *Prostate* **47**, 293-303 (2001).
17. Chauhan, D.P. Chemotherapeutic potential of curcumin for colorectal cancer. *Curr Pharm Des* **8**, 1695-706 (2002).

18. Anand, P., Kunnumakkara, A.B., Newman, R.A. & Aggarwal, B.B. Bioavailability of curcumin: problems and promises. *Mol Pharm* **4**, 807-18 (2007).
19. Shoba, G. et al. Influence of piperine on the pharmacokinetics of curcumin in animals and human volunteers. *Planta Med* **64**, 353-6 (1998).
20. Wahlstrom, B. & Blennow, G. A study on the fate of curcumin in the rat. *Acta Pharmacol Toxicol (Copenh)* **43**, 86-92 (1978).
21. Garcea, G. et al. Detection of curcumin and its metabolites in hepatic tissue and portal blood of patients following oral administration. *Br J Cancer* **90**, 1011-5 (2004).
22. Pan, M.H., Huang, T.M. & Lin, J.K. Biotransformation of curcumin through reduction and glucuronidation in mice. *Drug Metab Dispos* **27**, 486-94 (1999).
23. Ryu, E.K., Choe, Y.S., Lee, K.H., Choi, Y. & Kim, B.T. Curcumin and dehydrozingerone derivatives: synthesis, radiolabeling, and evaluation for beta-amyloid plaque imaging. *J Med Chem* **49**, 6111-9 (2006).
24. Sen, R. & Baltimore, D. Multiple nuclear factors interact with the immunoglobulin enhancer sequences. *Cell* **46**, 705-16 (1986).
25. Sen, R. & Baltimore, D. Inducibility of kappa immunoglobulin enhancer-binding protein Nf-kappa B by a posttranslational mechanism. *Cell* **47**, 921-8 (1986).
26. Atchison, M.L. & Perry, R.P. The role of the kappa enhancer and its binding factor NF-kappa B in the developmental regulation of kappa gene transcription. *Cell* **48**, 121-8 (1987).
27. Mercurio, F., Didonato, J., Rosette, C. & Karin, M. Molecular cloning and characterization of a novel Rel/NF-kappa B family member displaying structural and functional homology to NF-kappa B p50/p105. *DNA Cell Biol* **11**, 523-37 (1992).
28. Ghosh, S. et al. Cloning of the p50 DNA binding subunit of NF-kappa B: homology to rel and dorsal. *Cell* **62**, 1019-29 (1990).
29. Kieran, M. et al. The DNA binding subunit of NF-kappa B is identical to factor KBF1 and homologous to the rel oncogene product. *Cell* **62**, 1007-18 (1990).
30. Ryseck, R.P. et al. RelB, a new Rel family transcription activator that can interact with p50-NF-kappa B. *Mol Cell Biol* **12**, 674-84 (1992).
31. Ruben, S.M. et al. I-Rel: a novel rel-related protein that inhibits NF-kappa B transcriptional activity. *Genes Dev* **6**, 745-60 (1992).
32. Zhong, H., May, M.J., Jimi, E. & Ghosh, S. The phosphorylation status of nuclear NF-kappa B determines its association with CBP/p300 or HDAC-1. *Mol Cell* **9**, 625-36 (2002).
33. Bull, P., Morley, K.L., Hoekstra, M.F., Hunter, T. & Verma, I.M. The mouse c-rel protein has an N-terminal regulatory domain and a C-terminal transcriptional transactivation domain. *Mol Cell Biol* **10**, 5473-85 (1990).
34. Schmitz, M.L. & Baeuerle, P.A. The p65 subunit is responsible for the strong transcription activating potential of NF-kappa B. *EMBO J* **10**, 3805-17 (1991).
35. Franzoso, G. et al. The candidate oncoprotein Bcl-3 is an antagonist of p50/NF-kappa B-mediated inhibition. *Nature* **359**, 339-42 (1992).

36. Kang, S.M., Tran, A.C., Grilli, M. & Lenardo, M.J. NF-kappa B subunit regulation in nontransformed CD4+ T lymphocytes. *Science* **256**, 1452-6 (1992).
37. Wang, C.Y., Mayo, M.W., Korneluk, R.G., Goeddel, D.V. & Baldwin, A.S., Jr. NF-kappaB antiapoptosis: induction of TRAF1 and TRAF2 and c-IAP1 and c-IAP2 to suppress caspase-8 activation. *Science* **281**, 1680-3 (1998).
38. Duyao, M.P., Buckler, A.J. & Sonenshein, G.E. Interaction of an NF-kappa B-like factor with a site upstream of the c-myc promoter. *Proc Natl Acad Sci U S A* **87**, 4727-31 (1990).
39. Stehlik, C. et al. Nuclear factor (NF)-kappaB-regulated X-chromosome-linked iap gene expression protects endothelial cells from tumor necrosis factor alpha-induced apoptosis. *J Exp Med* **188**, 211-6 (1998).
40. Luque, I. & Gelinas, C. Rel/NF-kappa B and I kappa B factors in oncogenesis. *Semin Cancer Biol* **8**, 103-11 (1997).
41. Gerondakis, S. et al. Rel-deficient T cells exhibit defects in production of interleukin 3 and granulocyte-macrophage colony-stimulating factor. *Proc Natl Acad Sci U S A* **93**, 3405-9 (1996).
42. Lucas, P.C., McAllister-Lucas, L.M. & Nunez, G. NF-kappaB signaling in lymphocytes: a new cast of characters. *J Cell Sci* **117**, 31-9 (2004).
43. Song, J., Lei, F.T., Xiong, X. & Haque, R. Intracellular signals of T cell costimulation. *Cell Mol Immunol* **5**, 239-47 (2008).
44. Welte, T. et al. STAT5 interaction with the T cell receptor complex and stimulation of T cell proliferation. *Science* **283**, 222-5 (1999).
45. Green, D.R. Death and NF-kappaB in T cell activation: life at the edge. *Mol Cell* **11**, 551-2 (2003).
46. Dunn, G.P., Bruce, A.T., Ikeda, H., Old, L.J. & Schreiber, R.D. Cancer immunoediting: from immunosurveillance to tumor escape. *Nat Immunol* **3**, 991-8 (2002).
47. Diehl, L. et al. CD40 activation in vivo overcomes peptide-induced peripheral cytotoxic T-lymphocyte tolerance and augments anti-tumor vaccine efficacy. *Nat Med* **5**, 774-9 (1999).
48. Fowell, D., McKnight, A.J., Powrie, F., Dyke, R. & Mason, D. Subsets of CD4+ T cells and their roles in the induction and prevention of autoimmunity. *Immunol Rev* **123**, 37-64 (1991).
49. Mosmann, T.R. & Coffman, R.L. TH1 and TH2 cells: different patterns of lymphokine secretion lead to different functional properties. *Annu Rev Immunol* **7**, 145-73 (1989).
50. Jankovic, D., Liu, Z. & Gause, W.C. Th1- and Th2-cell commitment during infectious disease: asymmetry in divergent pathways. *Trends Immunol* **22**, 450-7 (2001).
51. Romagnani, S. Lymphokine production by human T cells in disease states. *Annu Rev Immunol* **12**, 227-57 (1994).
52. Lee, P.P. et al. T helper 2-dominant antilymphoma immune response is associated with fatal outcome. *Blood* **90**, 1611-7 (1997).
53. Doherty, P.C., Tripp, R.A. & Sixbey, J.W. Evasion of host immune responses by tumours and viruses. *Ciba Found Symp* **187**, 245-56; discussion 256-60 (1994).

54. Ganss, R. & Hanahan, D. Tumor microenvironment can restrict the effectiveness of activated antitumor lymphocytes. *Cancer Res* **58**, 4673-81 (1998).
55. Cao, S., Zhang, X., Edwards, J.P. & Mosser, D.M. NF-kappaB1 (p50) homodimers differentially regulate pro- and anti-inflammatory cytokines in macrophages. *J Biol Chem* **281**, 26041-50 (2006).
56. Kanaoka, S., Takai, T. & Yoshida, K. Cyclooxygenase-2 and tumor biology. *Adv Clin Chem* **43**, 59-78 (2007).
57. Wang, W., Bergh, A. & Damber, J.E. Cyclooxygenase-2 expression correlates with local chronic inflammation and tumor neovascularization in human prostate cancer. *Clin Cancer Res* **11**, 3250-6 (2005).
58. Murata, H. et al. Cyclooxygenase-2 overexpression enhances lymphatic invasion and metastasis in human gastric carcinoma. *Am J Gastroenterol* **94**, 451-5 (1999).
59. Koshiba, T. et al. Immunohistochemical analysis of cyclooxygenase-2 expression in pancreatic tumors. *Int J Pancreatol* **26**, 69-76 (1999).
60. Form, D.M. & Auerbach, R. PGE2 and angiogenesis. *Proc Soc Exp Biol Med* **172**, 214-8 (1983).
61. Sheng, H., Shao, J., Morrow, J.D., Beauchamp, R.D. & DuBois, R.N. Modulation of apoptosis and Bcl-2 expression by prostaglandin E2 in human colon cancer cells. *Cancer Res* **58**, 362-6 (1998).
62. Liu, X.H., Yao, S., Kirschenbaum, A. & Levine, A.C. NS398, a selective cyclooxygenase-2 inhibitor, induces apoptosis and down-regulates bcl-2 expression in LNCaP cells. *Cancer Res* **58**, 4245-9 (1998).
63. Yang, E. et al. Bad, a heterodimeric partner for Bcl-XL and Bcl-2, displaces Bax and promotes cell death. *Cell* **80**, 285-91 (1995).
64. Karin, M. Nuclear factor-kappaB in cancer development and progression. *Nature* **441**, 431-6 (2006).
65. Wang, C.Y., Cusack, J.C., Jr., Liu, R. & Baldwin, A.S., Jr. Control of inducible chemoresistance: enhanced anti-tumor therapy through increased apoptosis by inhibition of NF-kappaB. *Nat Med* **5**, 412-7 (1999).
66. Kaufmann, S.H. & Vaux, D.L. Alterations in the apoptotic machinery and their potential role in anticancer drug resistance. *Oncogene* **22**, 7414-30 (2003).
67. Vallabhapurapu, S. & Karin, M. Regulation and function of NF-kappaB transcription factors in the immune system. *Annu Rev Immunol* **27**, 693-733 (2009).
68. Li, Q. & Verma, I.M. NF-kappaB regulation in the immune system. *Nat Rev Immunol* **2**, 725-34 (2002).
69. Hatada, E.N. et al. The ankyrin repeat domains of the NF-kappa B precursor p105 and the protooncogene bcl-3 act as specific inhibitors of NF-kappa B DNA binding. *Proc Natl Acad Sci U S A* **89**, 2489-93 (1992).
70. Hacker, H. & Karin, M. Regulation and function of IKK and IKK-related kinases. *Sci STKE* **2006**, re13 (2006).
71. Zandi, E., Rothwarf, D.M., Delhase, M., Hayakawa, M. & Karin, M. The IkappaB kinase complex (IKK) contains two kinase subunits, IKKalpha and IKKbeta,

necessary for IkappaB phosphorylation and NF-kappaB activation. *Cell* **91**, 243-52 (1997).
72. Yamaoka, S. et al. Complementation cloning of NEMO, a component of the IkappaB kinase complex essential for NF-kappaB activation. *Cell* **93**, 1231-40 (1998).
73. Ghosh, S. & Karin, M. Missing pieces in the NF-kappaB puzzle. *Cell* **109 Suppl**, S81-96 (2002).
74. Yamamoto, Y. & Gaynor, R.B. Therapeutic potential of inhibition of the NF-kappaB pathway in the treatment of inflammation and cancer. *J Clin Invest* **107**, 135-42 (2001).
75. Baldwin, A.S. Control of oncogenesis and cancer therapy resistance by the transcription factor NF-kappaB. *J Clin Invest* **107**, 241-6 (2001).
76. Baud, V. & Karin, M. Is NF-kappaB a good target for cancer therapy? Hopes and pitfalls. *Nat Rev Drug Discov* **8**, 33-40 (2009).
77. Richardson, P.G., Hideshima, T., Mitsiades, C. & Anderson, K. Proteasome inhibition in hematologic malignancies. *Ann Med* **36**, 304-14 (2004).
78. Nakanishi, C. & Toi, M. Nuclear factor-kappaB inhibitors as sensitizers to anticancer drugs. *Nat Rev Cancer* **5**, 297-309 (2005).
79. Lee, D.F. & Hung, M.C. Advances in targeting IKK and IKK-related kinases for cancer therapy. *Clin Cancer Res* **14**, 5656-62 (2008).
80. Moore BW, P.V. Specific acidic proteins of the nervous system. *Physiological and Biochemical Aspects of Nervous Integration* 343-59 (1967).
81. Aitken, A., Jones, D., Soneji, Y. & Howell, S. 14-3-3 proteins: biological function and domain structure. *Biochem Soc Trans* **23**, 605-11 (1995).
82. Fu, H., Subramanian, R.R. & Masters, S.C. 14-3-3 proteins: structure, function, and regulation. *Annu Rev Pharmacol Toxicol* **40**, 617-47 (2000).
83. Ichimura, T. et al. Molecular cloning of cDNA coding for brain-specific 14-3-3 protein, a protein kinase-dependent activator of tyrosine and tryptophan hydroxylases. *Proc Natl Acad Sci U S A* **85**, 7084-8 (1988).
84. Prasad, G.L., Valverius, E.M., McDuffie, E. & Cooper, H.L. Complementary DNA cloning of a novel epithelial cell marker protein, HME1, that may be down-regulated in neoplastic mammary cells. *Cell Growth Differ* **3**, 507-13 (1992).
85. Wang, W. & Shakes, D.C. Molecular evolution of the 14-3-3 protein family. *J Mol Evol* **43**, 384-98 (1996).
86. Knetsch, M.L. et al. Isolation of a Dictyostelium discoideum 14-3-3 homologue. *Biochim Biophys Acta* **1357**, 243-8 (1997).
87. van Heusden, G.P., van der Zanden, A.L., Ferl, R.J. & Steensma, H.Y. Four Arabidopsis thaliana 14-3-3 protein isoforms can complement the lethal yeast bmh1 bmh2 double disruption. *FEBS Lett* **391**, 252-6 (1996).
88. Fu, H., Coburn, J. & Collier, R.J. The eukaryotic host factor that activates exoenzyme S of Pseudomonas aeruginosa is a member of the 14-3-3 protein family. *Proc Natl Acad Sci U S A* **90**, 2320-4 (1993).
89. Zhang, L. et al. Residues of 14-3-3 zeta required for activation of exoenzyme S of Pseudomonas aeruginosa. *Biochemistry* **38**, 12159-64 (1999).
90. Isobe, T. et al. Distinct forms of the protein kinase-dependent activator of tyrosine and tryptophan hydroxylases. *J Mol Biol* **217**, 125-32 (1991).

91. Megidish, T., Cooper, J., Zhang, L., Fu, H. & Hakomori, S. A novel sphingosine-dependent protein kinase (SDK1) specifically phosphorylates certain isoforms of 14-3-3 protein. *J Biol Chem* **273**, 21834-45 (1998).
92. Megidish, T. et al. The signal modulator protein 14-3-3 is a target of sphingosine- or N,N-dimethylsphingosine-dependent kinase in 3T3(A31) cells. *Biochem Biophys Res Commun* **216**, 739-47 (1995).
93. Woodcock, J.M., Murphy, J., Stomski, F.C., Berndt, M.C. & Lopez, A.F. The dimeric versus monomeric status of 14-3-3zeta is controlled by phosphorylation of Ser58 at the dimer interface. *J Biol Chem* **278**, 36323-7 (2003).
94. Powell, D.W. et al. Proteomic identification of 14-3-3zeta as a mitogen-activated protein kinase-activated protein kinase 2 substrate: role in dimer formation and ligand binding. *Mol Cell Biol* **23**, 5376-87 (2003).
95. Muslin, A.J., Tanner, J.W., Allen, P.M. & Shaw, A.S. Interaction of 14-3-3 with signaling proteins is mediated by the recognition of phosphoserine. *Cell* **84**, 889-97 (1996).
96. Yaffe, M.B. et al. The structural basis for 14-3-3:phosphopeptide binding specificity. *Cell* **91**, 961-71 (1997).
97. Ganguly, S. et al. Melatonin synthesis: 14-3-3-dependent activation and inhibition of arylalkylamine N-acetyltransferase mediated by phosphoserine-205. *Proc Natl Acad Sci U S A* **102**, 1222-7 (2005).
98. Coblitz, B., Wu, M., Shikano, S. & Li, M. C-terminal binding: an expanded repertoire and function of 14-3-3 proteins. *FEBS Lett* **580**, 1531-5 (2006).
99. Seimiya, H. et al. Involvement of 14-3-3 proteins in nuclear localization of telomerase. *EMBO J* **19**, 2652-61 (2000).
100. Liu, D. et al. Crystal structure of the zeta isoform of the 14-3-3 protein. *Nature* **376**, 191-4 (1995).
101. Xiao, B. et al. Structure of a 14-3-3 protein and implications for coordination of multiple signalling pathways. *Nature* **376**, 188-91 (1995).
102. Petosa, C. et al. 14-3-3zeta binds a phosphorylated Raf peptide and an unphosphorylated peptide via its conserved amphipathic groove. *J Biol Chem* **273**, 16305-10 (1998).
103. Obsil, T., Ghirlando, R., Klein, D.C., Ganguly, S. & Dyda, F. Crystal structure of the 14-3-3zeta:serotonin N-acetyltransferase complex. a role for scaffolding in enzyme regulation. *Cell* **105**, 257-67 (2001).
104. Yang, X. et al. Structural basis for protein-protein interactions in the 14-3-3 protein family. *Proc Natl Acad Sci U S A* **103**, 17237-42 (2006).
105. Ottmann, C. et al. Structure of a 14-3-3 coordinated hexamer of the plant plasma membrane H+ -ATPase by combining X-ray crystallography and electron cryomicroscopy. *Mol Cell* **25**, 427-40 (2007).
106. Ottmann, C. et al. Phosphorylation-independent interaction between 14-3-3 and exoenzyme S: from structure to pathogenesis. *EMBO J* **26**, 902-13 (2007).
107. Porter, G.W., Khuri, F.R. & Fu, H. Dynamic 14-3-3/client protein interactions integrate survival and apoptotic pathways. *Semin Cancer Biol* **16**, 193-202 (2006).

108. Mok, C.L. et al. Bad can act as a key regulator of T cell apoptosis and T cell development. *J Exp Med* **189**, 575-86 (1999).
109. Ottilie, S. et al. Dimerization properties of human BAD. Identification of a BH-3 domain and analysis of its binding to mutant BCL-2 and BCL-XL proteins. *J Biol Chem* **272**, 30866-72 (1997).
110. Zha, J. et al. BH3 domain of BAD is required for heterodimerization with BCL-XL and pro-apoptotic activity. *J Biol Chem* **272**, 24101-4 (1997).
111. Kelekar, A., Chang, B.S., Harlan, J.E., Fesik, S.W. & Thompson, C.B. Bad is a BH3 domain-containing protein that forms an inactivating dimer with Bcl-XL. *Mol Cell Biol* **17**, 7040-6 (1997).
112. Zha, J., Harada, H., Yang, E., Jockel, J. & Korsmeyer, S.J. Serine phosphorylation of death agonist BAD in response to survival factor results in binding to 14-3-3 not BCL-X(L). *Cell* **87**, 619-28 (1996).
113. Brunet, A. et al. Akt promotes cell survival by phosphorylating and inhibiting a Forkhead transcription factor. *Cell* **96**, 857-68 (1999).
114. Brunet, A. et al. 14-3-3 transits to the nucleus and participates in dynamic nucleocytoplasmic transport. *J Cell Biol* **156**, 817-28 (2002).
115. Cahill, C.M. et al. Phosphatidylinositol 3-kinase signaling inhibits DAF-16 DNA binding and function via 14-3-3-dependent and 14-3-3-independent pathways. *J Biol Chem* **276**, 13402-10 (2001).
116. Obsil, T., Ghirlando, R., Anderson, D.E., Hickman, A.B. & Dyda, F. Two 14-3-3 binding motifs are required for stable association of Forkhead transcription factor FOXO4 with 14-3-3 proteins and inhibition of DNA binding. *Biochemistry* **42**, 15264-72 (2003).
117. Basu, S., Totty, N.F., Irwin, M.S., Sudol, M. & Downward, J. Akt phosphorylates the Yes-associated protein, YAP, to induce interaction with 14-3-3 and attenuation of p73-mediated apoptosis. *Mol Cell* **11**, 11-23 (2003).
118. Morrison, D.K., Heidecker, G., Rapp, U.R. & Copeland, T.D. Identification of the major phosphorylation sites of the Raf-1 kinase. *J Biol Chem* **268**, 17309-16 (1993).
119. Thorson, J.A. et al. 14-3-3 proteins are required for maintenance of Raf-1 phosphorylation and kinase activity. *Mol Cell Biol* **18**, 5229-38 (1998).
120. Tzivion, G., Luo, Z. & Avruch, J. A dimeric 14-3-3 protein is an essential cofactor for Raf kinase activity. *Nature* **394**, 88-92 (1998).
121. Takashima, A. GSK-3 is essential in the pathogenesis of Alzheimer's disease. *J Alzheimers Dis* **9**, 309-17 (2006).
122. Agarwal-Mawal, A. et al. 14-3-3 connects glycogen synthase kinase-3 beta to tau within a brain microtubule-associated tau phosphorylation complex. *J Biol Chem* **278**, 12722-8 (2003).
123. Braselmann, S. & McCormick, F. Bcr and Raf form a complex in vivo via 14-3-3 proteins. *EMBO J* **14**, 4839-48 (1995).
124. Vincenz, C. & Dixit, V.M. 14-3-3 proteins associate with A20 in an isoform-specific manner and function both as chaperone and adapter molecules. *J Biol Chem* **271**, 20029-34 (1996).
125. Morrison, D.K. & Cutler, R.E. The complexity of Raf-1 regulation. *Curr Opin Cell Biol* **9**, 174-9 (1997).

126. Fujita, N., Sato, S., Katayama, K. & Tsuruo, T. Akt-dependent phosphorylation of p27Kip1 promotes binding to 14-3-3 and cytoplasmic localization. *J Biol Chem* **277**, 28706-13 (2002).
127. Sekimoto, T., Fukumoto, M. & Yoneda, Y. 14-3-3 suppresses the nuclear localization of threonine 157-phosphorylated p27(Kip1). *EMBO J* **23**, 1934-42 (2004).
128. Heliez, C., Baricault, L., Barboule, N. & Valette, A. Paclitaxel increases p21 synthesis and accumulation of its AKT-phosphorylated form in the cytoplasm of cancer cells. *Oncogene* **22**, 3260-8 (2003).
129. Zhang, L., Chen, J. & Fu, H. Suppression of apoptosis signal-regulating kinase 1-induced cell death by 14-3-3 proteins. *Proc Natl Acad Sci U S A* **96**, 8511-5 (1999).
130. Masters, S.C. & Fu, H. 14-3-3 proteins mediate an essential anti-apoptotic signal. *J Biol Chem* **276**, 45193-200 (2001).
131. Gasco, M. et al. Epigenetic inactivation of 14-3-3 sigma in oral carcinoma: association with p16(INK4a) silencing and human papillomavirus negativity. *Cancer Res* **62**, 2072-6 (2002).
132. Gasco, M. et al. Coincident inactivation of 14-3-3sigma and p16INK4a is an early event in vulval squamous neoplasia. *Oncogene* **21**, 1876-81 (2002).
133. Roesch-Ely, M. et al. Proteomic analysis reveals successive aberrations in protein expression from healthy mucosa to invasive head and neck cancer. *Oncogene* **26**, 54-64 (2007).
134. Moreira, J.M., Gromov, P. & Celis, J.E. Expression of the tumor suppressor protein 14-3-3 sigma is down-regulated in invasive transitional cell carcinomas of the urinary bladder undergoing epithelial-to-mesenchymal transition. *Mol Cell Proteomics* **3**, 410-9 (2004).
135. Osada, H. et al. Frequent and histological type-specific inactivation of 14-3-3sigma in human lung cancers. *Oncogene* **21**, 2418-24 (2002).
136. Suzuki, H. et al. Inactivation of the 14-3-3 sigma gene is associated with 5' CpG island hypermethylation in human cancers. *Cancer Res* **60**, 4353-7 (2000).
137. Vercoutter-Edouart, A.S. et al. Proteomic analysis reveals that 14-3-3sigma is down-regulated in human breast cancer cells. *Cancer Res* **61**, 76-80 (2001).
138. Ferguson, A.T. et al. High frequency of hypermethylation at the 14-3-3 sigma locus leads to gene silencing in breast cancer. *Proc Natl Acad Sci U S A* **97**, 6049-54 (2000).
139. Hermeking, H. et al. 14-3-3 sigma is a p53-regulated inhibitor of G2/M progression. *Mol Cell* **1**, 3-11 (1997).
140. Qi, W., Liu, X., Qiao, D. & Martinez, J.D. Isoform-specific expression of 14-3-3 proteins in human lung cancer tissues. *Int J Cancer* **113**, 359-63 (2005).
141. Hashiguchi, M., Sobue, K. & Paudel, H.K. 14-3-3zeta is an effector of tau protein phosphorylation. *J Biol Chem* **275**, 25247-54 (2000).
142. Omi, K., Hachiya, N.S., Tanaka, M., Tokunaga, K. & Kaneko, K. 14-3-3zeta is indispensable for aggregate formation of polyglutamine-expanded huntingtin protein. *Neurosci Lett* **431**, 45-50 (2008).

143. Umahara, T. et al. 14-3-3 proteins and zeta isoform containing neurofibrillary tangles in patients with Alzheimer's disease. *Acta Neuropathol* **108**, 279-86 (2004).
144. Hsich, G., Kenney, K., Gibbs, C.J., Lee, K.H. & Harrington, M.G. The 14-3-3 brain protein in cerebrospinal fluid as a marker for transmissible spongiform encephalopathies. *N Engl J Med* **335**, 924-30 (1996).
145. Zanusso, G. et al. Phosphorylated 14-3-3zeta protein in the CSF of neuroleptic-treated patients. *Neurology* **64**, 1618-20 (2005).
146. Arora, S., Matta, A., Shukla, N.K., Deo, S.V. & Ralhan, R. Identification of differentially expressed genes in oral squamous cell carcinoma. *Mol Carcinog* **42**, 97-108 (2005).
147. Neal, C.L. et al. 14-3-3zeta overexpression defines high risk for breast cancer recurrence and promotes cancer cell survival. *Cancer Res* **69**, 3425-32 (2009).
148. Chatterjee, D. et al. Reduction of 9-nitrocamptothecin-triggered apoptosis in DU-145 human prostate cancer cells by ectopic expression of 14-3-3zeta. *Int J Oncol* **25**, 503-9 (2004).
149. Jang, J.S., Cho, H.Y., Lee, Y.J., Ha, W.S. & Kim, H.W. The differential proteome profile of stomach cancer: identification of the biomarker candidates. *Oncol Res* **14**, 491-9 (2004).
150. Niemantsverdriet, M., Wagner, K., Visser, M. & Backendorf, C. Cellular functions of 14-3-3 zeta in apoptosis and cell adhesion emphasize its oncogenic character. *Oncogene* **27**, 1315-9 (2008).
151. Takihara, Y., Matsuda, Y. & Hara, J. Role of the beta isoform of 14-3-3 proteins in cellular proliferation and oncogenic transformation. *Carcinogenesis* **21**, 2073-7 (2000).
152. Martin, D., Brown-Luedi, M. & Chiquet-Ehrismann, R. Tenascin-C signaling through induction of 14-3-3 tau. *J Cell Biol* **160**, 171-5 (2003).
153. Li, Z. et al. Down-regulation of 14-3-3zeta suppresses anchorage-independent growth of lung cancer cells through anoikis activation. *Proc Natl Acad Sci U S A* **105**, 162-7 (2008).
154. Montminy, M.R., Sevarino, K.A., Wagner, J.A., Mandel, G. & Goodman, R.H. Identification of a cyclic-AMP-responsive element within the rat somatostatin gene. *Proc Natl Acad Sci U S A* **83**, 6682-6 (1986).
155. Gonzalez, G.A. & Montminy, M.R. Cyclic AMP stimulates somatostatin gene transcription by phosphorylation of CREB at serine 133. *Cell* **59**, 675-80 (1989).
156. Hai, T.W., Liu, F., Coukos, W.J. & Green, M.R. Transcription factor ATF cDNA clones: an extensive family of leucine zipper proteins able to selectively form DNA-binding heterodimers. *Genes Dev* **3**, 2083-90 (1989).
157. Schumacher, M.A., Goodman, R.H. & Brennan, R.G. The structure of a CREB bZIP.somatostatin CRE complex reveals the basis for selective dimerization and divalent cation-enhanced DNA binding. *J Biol Chem* **275**, 35242-7 (2000).
158. Ellenberger, T. Getting a grip on DNA recognition: structures of the basic region leucine zipper, and the basic region helix-loop-helix DNA-binding domains. *Current Opinion in Structural Biology* **4**, 12-21 (1994).

159. Hoeffler, J.P., Meyer, T.E., Waeber, G. & Habener, J.F. Multiple adenosine 3',5'-cyclic [corrected] monophosphate response element DNA-binding proteins generated by gene diversification and alternative exon splicing. *Mol Endocrinol* **4**, 920-30 (1990).
160. Johannessen, M., Delghandi, M.P. & Moens, U. What turns CREB on? *Cell Signal* **16**, 1211-27 (2004).
161. Asahara, H. et al. Chromatin-dependent cooperativity between constitutive and inducible activation domains in CREB. *Mol Cell Biol* **21**, 7892-900 (2001).
162. Shaywitz, A.J. & Greenberg, M.E. CREB: a stimulus-induced transcription factor activated by a diverse array of extracellular signals. *Annu Rev Biochem* **68**, 821-61 (1999).
163. Montminy, M.R. & Bilezikjian, L.M. Binding of a nuclear protein to the cyclic-AMP response element of the somatostatin gene. *Nature* **328**, 175-8 (1987).
164. Gonzalez, G.A. et al. A cluster of phosphorylation sites on the cyclic AMP-regulated nuclear factor CREB predicted by its sequence. *Nature* **337**, 749-52 (1989).
165. Taylor, S.S., Buechler, J.A. & Yonemoto, W. cAMP-dependent protein kinase: framework for a diverse family of regulatory enzymes. *Annu Rev Biochem* **59**, 971-1005 (1990).
166. Hagiwara, M. et al. Coupling of hormonal stimulation and transcription via the cyclic AMP-responsive factor CREB is rate limited by nuclear entry of protein kinase A. *Mol Cell Biol* **13**, 4852-9 (1993).
167. Kitagawa, K. CREB and cAMP response element-mediated gene expression in the ischemic brain. *FEBS J* **274**, 3210-7 (2007).
168. Wilson, B.E., Mochon, E. & Boxer, L.M. Induction of bcl-2 expression by phosphorylated CREB proteins during B-cell activation and rescue from apoptosis. *Mol Cell Biol* **16**, 5546-56 (1996).
169. Jean, D., Harbison, M., McConkey, D.J., Ronai, Z. & Bar-Eli, M. CREB and its associated proteins act as survival factors for human melanoma cells. *J Biol Chem* **273**, 24884-90 (1998).
170. Jean, D. & Bar-Eli, M. Regulation of tumor growth and metastasis of human melanoma by the CREB transcription factor family. *Mol Cell Biochem* **212**, 19-28 (2000).
171. Jean, D. & Bar-Eli, M. Targeting the ATF-1/CREB transcription factors by single chain Fv fragment in human melanoma: potential modality for cancer therapy. *Crit Rev Immunol* **21**, 275-86 (2001).
172. Siu, Y.T. & Jin, D.Y. CREB--a real culprit in oncogenesis. *FEBS J* **274**, 3224-32 (2007).
173. Cheng, J.C. et al. Potential role of CREB as a prognostic marker in acute myeloid leukemia. *Future Oncol* **3**, 475-80 (2007).
174. Shankar, D.B. et al. The role of CREB as a proto-oncogene in hematopoiesis and in acute myeloid leukemia. *Cancer Cell* **7**, 351-62 (2005).
175. Levi, M.S., Borne, R.F. & Williamson, J.S. A review of cancer chemopreventive agents. *Curr Med Chem* **8**, 1349-62 (2001).

176. Cheng, A.L. et al. Phase I clinical trial of curcumin, a chemopreventive agent, in patients with high-risk or pre-malignant lesions. *Anticancer Res* **21**, 2895-900 (2001).
177. Commandeur, J.N. & Vermeulen, N.P. Cytotoxicity and cytoprotective activities of natural compounds. The case of curcumin. *Xenobiotica* **26**, 667-80 (1996).
178. Osawa T, S.Y., Inayoshi M, Kawakashi S. Antioxidative activity of tetrahyrocurcuminids. *Biosci Biotechnol Biochem* **59**, 1609-12 (1995).
179. Satoskar, R.R., Shah, S.J. & Shenoy, S.G. Evaluation of anti-inflammatory property of curcumin (diferuloyl methane) in patients with postoperative inflammation. *Int J Clin Pharmacol Ther Toxicol* **24**, 651-4 (1986).
180. Aggarwal, S. et al. Curcumin (Diferuloylmethane) Downregulates Expression of Cell Proliferation, Antiapoptotic and Metastatic Gene Products Through Suppression of I{kappa}B{alpha} Kinase and AKT Activation. *Mol Pharmacol* (2005).
181. Dhillon N et al. Phase II clinical trial of curcumin in patients with advanced pancreatic cancer. *Journal of Clinical Oncology, 2006 ASCO Annual Meeting Proceedings* **24**, 14151 (2006).
182. Richmond, A. Nf-kappa B, chemokine gene transcription and tumour growth. *Nat Rev Immunol* **2**, 664-74 (2002).
183. Rayet, B. & Gelinas, C. Aberrant rel/nfkb genes and activity in human cancer. *Oncogene* **18**, 6938-47 (1999).
184. Mercurio, F. et al. IKK-1 and IKK-2: cytokine-activated IkappaB kinases essential for NF-kappaB activation. *Science* **278**, 860-6 (1997).
185. Rubinstein, L.V. et al. Comparison of in vitro anticancer-drug-screening data generated with a tetrazolium assay versus a protein assay against a diverse panel of human tumor cell lines. *J Natl Cancer Inst* **82**, 1113-8 (1990).
186. Skehan, P. et al. New colorimetric cytotoxicity assay for anticancer-drug screening. *J Natl Cancer Inst* **82**, 1107-12 (1990).
187. Lin, J.K. Molecular targets of curcumin. *Adv Exp Med Biol* **595**, 227-43 (2007).
188. Singh, S. & Khar, A. Biological effects of curcumin and its role in cancer chemoprevention and therapy. *Anticancer Agents Med Chem* **6**, 259-70 (2006).
189. Rothe, M., Sarma, V., Dixit, V.M. & Goeddel, D.V. TRAF2-mediated activation of NF-kappa B by TNF receptor 2 and CD40. *Science* **269**, 1424-7 (1995).
190. Beg, A.A., Finco, T.S., Nantermet, P.V. & Baldwin, A.S., Jr. Tumor necrosis factor and interleukin-1 lead to phosphorylation and loss of I kappa B alpha: a mechanism for NF-kappa B activation. *Mol Cell Biol* **13**, 3301-10 (1993).
191. Bharti, A.C., Donato, N., Singh, S. & Aggarwal, B.B. Curcumin (diferuloylmethane) down-regulates the constitutive activation of nuclear factor-kappa B and IkappaBalpha kinase in human multiple myeloma cells, leading to suppression of proliferation and induction of apoptosis. *Blood* **101**, 1053-62 (2003).
192. Deeb, D. et al. Curcumin sensitizes prostate cancer cells to tumor necrosis factor-related apoptosis-inducing ligand/Apo2L by inhibiting nuclear factor-

kappaB through suppression of IkappaBalpha phosphorylation. *Mol Cancer Ther* **3**, 803-12 (2004).
193. Karin, M. NF-kappaB and cancer: Mechanisms and targets. *Mol Carcinog* **45**, 355-61 (2006).
194. Mague, J.T., Alworth, W.L. & Payton, F.L. Curcumin and derivatives. *Acta Crystallogr C* **60**, o608-10 (2004).
195. Payton, F., Sandusky, P. & Alworth, W.L. NMR study of the solution structure of curcumin. *J Nat Prod* **70**, 143-6 (2007).
196. Meijer, L. & Raymond, E. Roscovitine and other purines as kinase inhibitors. From starfish oocytes to clinical trials. *Acc Chem Res* **36**, 417-25 (2003).
197. Mukhopadhyay, T., Roth, J.A. & Maxwell, S.A. Altered expression of the p50 subunit of the NF-kappa B transcription factor complex in non-small cell lung carcinoma. *Oncogene* **11**, 999-1003 (1995).
198. Wang, C.Y., Mayo, M.W. & Baldwin, A.S., Jr. TNF- and cancer therapy-induced apoptosis: potentiation by inhibition of NF-kappaB. *Science* **274**, 784-7 (1996).
199. Vasudevan, K.M., Gurumurthy, S. & Rangnekar, V.M. Suppression of PTEN expression by NF-kappa B prevents apoptosis. *Mol Cell Biol* **24**, 1007-21 (2004).
200. Stambolic, V. et al. Negative regulation of PKB/Akt-dependent cell survival by the tumor suppressor PTEN. *Cell* **95**, 29-39 (1998).
201. Selvendiran, K. et al. EF24 induces G2/M arrest and apoptosis in cisplatin-resistant human ovarian cancer cells by increasing PTEN expression. *J Biol Chem* **282**, 28609-18 (2007).
202. Lopez-Girona, A., Furnari, B., Mondesert, O. & Russell, P. Nuclear localization of Cdc25 is regulated by DNA damage and a 14-3-3 protein. *Nature* **397**, 172-5 (1999).
203. Lee, J., Kumagai, A. & Dunphy, W.G. Positive regulation of Wee1 by Chk1 and 14-3-3 proteins. *Mol Biol Cell* **12**, 551-63 (2001).
204. Karolchik, D. et al. The UCSC Genome Browser Database. *Nucleic Acids Res* **31**, 51-4 (2003).
205. Cao, L. et al. Identification of 14-3-3 protein isoforms in human astrocytoma by immunohistochemistry. *Neurosci Lett* **432**, 94-9 (2008).
206. Matta, A., Bahadur, S., Duggal, R., Gupta, S.D. & Ralhan, R. Over-expression of 14-3-3zeta is an early event in oral cancer. *BMC Cancer* **7**, 169 (2007).
207. Fan, T. et al. Up-regulation of 14-3-3zeta in lung cancer and its implication as prognostic and therapeutic target. *Cancer Res* **67**, 7901-6 (2007).
208. Ajjappala, B.S. et al. 14-3-3 gamma is stimulated by IL-3 and promotes cell proliferation. *J Immunol* **182**, 1050-60 (2009).
209. Xie, S. et al. Dominant-negative CREB inhibits tumor growth and metastasis of human melanoma cells. *Oncogene* **15**, 2069-75 (1997).
210. Yang, Y.M., Dolan, L.R. & Ronai, Z. Expression of dominant negative CREB reduces resistance to radiation of human melanoma cells. *Oncogene* **12**, 2223-33 (1996).
211. Hidalgo, M. & Rowinsky, E.K. The rapamycin-sensitive signal transduction pathway as a target for cancer therapy. *Oncogene* **19**, 6680-6 (2000).

212. Corradetti, M.N. & Guan, K.L. Upstream of the mammalian target of rapamycin: do all roads pass through mTOR? *Oncogene* **25**, 6347-60 (2006).
213. Brown, E.J. & Schreiber, S.L. A signaling pathway to translational control. *Cell* **86**, 517-20 (1996).
214. Huang, S. & Houghton, P.J. Mechanisms of resistance to rapamycins. *Drug Resist Updat* **4**, 378-91 (2001).
215. Bruckmann, A., Steensma, H.Y., Teixeira De Mattos, M.J. & Van Heusden, G.P. Regulation of transcription by Saccharomyces cerevisiae 14-3-3 proteins. *Biochem J* **382**, 867-75 (2004).
216. van Heusden, G.P. & Steensma, H.Y. 14-3-3 Proteins are essential for regulation of RTG3-dependent transcription in Saccharomyces cerevisiae. *Yeast* **18**, 1479-91 (2001).
217. Bertram, P.G., Zeng, C., Thorson, J., Shaw, A.S. & Zheng, X.F. The 14-3-3 proteins positively regulate rapamycin-sensitive signaling. *Curr Biol* **8**, 1259-67 (1998).

# Appendix: Identification of genes involved in 14-3-3-dependent rapamycin signaling

## Abstract

The kinase TOR is the target of the immunosuppressive drug rapamycin. If plays an essential role in the progression through G1 phase of the cell cycle. Aberrant TOR signaling is reported in many diseases including cancer. Treatment with rapamycin results in the inability of TOR to act on its targets, ultimately leading to cell cycle arrest. Many tumors acquire resistance to rapamycin, however the mechanism of this resistance is not fully understood. The 14-3-3 proteins have been implicated as one of the key players involved in this resistance. Utilizing a genetics approach, we sought to identify genes that control 14-3-3 dependent rapamycin signaling. Three different approaches were utilized in this study.

## Background and Significance

### *mTOR controls cell growth signaling in normal and cancer cells*

There currently is a high level of interest in signaling through the mammalian target of rapamycin (mTOR, also known as RAFT or FRAP). This reflects both its key role in many cell functions and its involvement in diseases such as cancers [211]. mTOR as well as the yeast homologues Tor1p and Tor2p are members of the phosphatidylinositol kinase (PIK)-related kinase family that control many aspects of cellular physiology, including transcription, translation, cell-size, cytoskeletal organization and autophagy [212]. Activated TOR regulates these cellular functions through phosphorylation of the key translation regulators, ribosomal p70S6 kinase (S6k1), and the translation inhibitor eIF4e binding protein 1 (4EBP1) [212,213]. However, mTOR is dysregulated in an array of human

malignancies and metabolic disorders such as type II diabetes. Thus, targeting mTOR signaling may be an effective anticancer strategy.

***Rapamycin and its analogs have shown promising anticancer properties through inhibition of mTOR***

In an effort to identify mTOR modulators, rapamycin was discovered. It has shown both significant immunosuppressive and anti-tumor properties. Rapamycin inhibits the function of mTOR and suppresses tumor cell growth by arresting cells in G1 phase or inducing apoptosis [214]. Recent clinical trials have demonstrated promising antitumor activity of rapamycin analogues, RAD001 and CC1779 in colorectal and renal cancers. This strongly supports the rational to develop rapamycin-based anticancer agents. Understanding how rapamycin (or its derivatives) induce anticancer activity through other critical signaling pathways is essential for effective therapeutic applications. Genetic analysis has revealed 14-3-3 proteins as critical regulators of rapamycin-mediated signaling.

***14-3-3 proteins contribute to rapamycin resistance***

The 14-3-3 proteins have been implicated as key regulators of diverse intracellular signal transduction processes [82]. They participate in cell cycle control, signal transduction and apoptosis. This is accomplished through three well-established 14-3-3 functions that are in no way mutually exclusive events. 14-3-3 proteins regulate protein-protein interactions, subcellular localization of proteins and enzymatic activity. Direct interaction of 14-3-3 with a number of client proteins has been demonstrated [107]. The majority of 14-3-3 client proteins bind to 14-3-3 through a conserved 14-3-3 binding motif, the main one being, RSXpSXP. Phosphorylation of the serine residue in the motif

results in recruitment and subsequent binding of 14-3-3 through the amphipathic groove of 14-3-3, resulting in alterations in ligand function. Interestingly, mutations within the amphipathic groove that are unable to bind their clients showed sensitization to rapamycin n yeast. This is suggestive of a role of 14-3-3 in cell resistance to rapamycin.

On one hand, identification of proteins that determine 14-3-3-dependent rapamycin resistance is expected to reveal noel molecular targets to enhance mTOR-targeted therapies for the treatments of cancer and other mTOR-mediated diseases. On the other hand, this study may identify new mTOR-mediated signaling pathways that control cell growth. My study is designed to use yeast as a genetic model system to identify such regulator molecules that control rapamycin sensitivity through 14-3-3 proteins.

## Introduction

Many tumors show resistance to rapamycin treatment. Some of this resistance has been attributed to mutations in various components of the mTOR signaling cascade [214]. In addition, the status of ATM, p53, PTEN/Akt and 14-3-3 are also associated with rapamycin sensitivity. Interestingly, 14-3-3 proteins are crucial to tumor stability and are involved in various signaling events leading to sustained cell survival [82]. The mechanism by which 14-3-3 proteins cause rapamycin resistance is unknown. Since the yeast TOR proteins lack consensus sites for 14-3-3 binding, TOR proteins could not directly associate with either of the two yeast homologues of 14-3-3, Bmh1p or Bmh2p. Thus direct interference by Bmh1p and Bmh2p with the FKBP-rapamycin complex binding to Tor1p and Tor2p in the budding yeast may be excluded. This study proposes to identify

functional interaction of 14-3-3 with rapamycin-mediated signaling pathways through a series of genetic approaches in a yeast model system.

The two *Saccharomyces cerevisiae* 14-3-3 homologues, Bmh1p and Bmh2p, share redundant functions for cell viability in most budding yeast strains. Their essential functions can be complemented in trans by at least four of the *Arabidopsis* isoforms, three human isoforms (β,τ and η) and one *Dictyostelium* isoform. Bmh1p and Bmh2p appear to be involved in signaling from the GTPase Ras via protein kinase A, in vesicular transport and in the Ras-activated MAP (mitogen activated protein) kinase cascade. In the Σ1278b genetic background, yeast lacking both BMH1 and BMH2 are viable, but only at permissive temperatures thus conferring a temperature sensitive phenotype [215,216].

Culturing yeast in the presence of rapamycin and isolating suppressors involved in reverting the growth-inhibitory phenotype resulted in the identification of two genes important for rapamycin resistance, Bmh1 and Bmh2 [217]. Deletion of one of the Bmh genes caused hypersensitivity to rapamycin in a manner that was dependent on gene dosage. The binding of 14-3-3 to many of its client proteins has been shown to be dependent on phosphorylation with in a conserved 14-3-3 binding motif (RSXpSXP) [82]. Mutations that prevented 14-3-3 from binding to the phosphoserine motif abolished its ability to confer rapamycin resistance. In contrast, substitution of two residues in 14-3-3 that surround these phosphoserine-binding sites conferred a dominant-resistant phenotype. These preliminary studies identified 14-3-3 as an important component in rapamycin-signaling in yeast. This study begins to determine the role for additional genes that are important to 14-3-3 rapamycin resistance in yeast.

## Materials and Methods

*Yeast strains and culture conditions:* The bmh2 temperature sensitive strain and control strains used in this study have been previously described. Both have mutations in the ura and his locus. Yeast deletion library was obtained from Dr. Paul van Heusden at Leiden University in The Netherlands. All deletion strains have mutations in his, leu and ura. Unless otherwise noted yeast were cultured in either YPD (1% yeast extract, 2% bacto peptone, 2% glucose. pH 6.5) MY media (1x salt solution, 1 x spore element, 1%glucose, 1x vitamin. pH 6.5) or MYZ (same as MY without glucose). MY and MYZ were supplement with appropriate amino acids. All yeast were cultured as noted at the restrictive temperature of 30°C or at the permissive temperature of 22°C. Rapamycin (Alexis Biochemicals) was added to media at concentrations indicated.

*Plasmids and cDNA constructs:* YCplac22 is a single copy plasmid contains the bmh2-ts allele along with a marker for TRP1. YEplac195 is a multi copy plasmid with an insert of either Bmh1 or Bmh2. This vector also has a marker for URA3. The gal inducible cDNA library used in this study expresses the URA gene in addition to the cDNAs. It was obtained from Dr. Martina Nebohacova from Cornell University.

*Transformation:* Yeast were grown in YPD overnight to an OD between 0.2 and 0.8. After multiple washes, $1X10^8$ yeast were resuspended in 30% PEG 3350, 100mM LiAc, and 5 μg single-stranded DNA. Cells were left to incubate for 30 minutes at 30°C followed by a heat shock at 42°C for 20 minutes. Cells were plated on selection media (MY(Z) HIS).

## Results

The first method to identify genes involved in 14-3-3-dependent rapamycin resistance entailed the utilization of the bmh2-ts strain. For these experiments, cells were spread onto culture plates in the presence of rapamycin and exposed to UV light. The rational was to use the UV light to mutagenize the genome. In doing so, it is speculated that various genomic loci will be mutated. If a gene is hit that confers 14-3-3 independent rapamycin resistance, a colony will form on the rapamycin plates. This technique yielded 7 independent clones. At this point these clones have not been further evaluated. Doing so entails mating them do determine if the mutation is dominant or recessive. Recessive mutations will be processed further. A yeast cDNA library will be transformed into the yeast and transformants that cannot grow on the presence of rapamycin will be isolated. The plasmid from the cDNA library extracted and sequenced to determine the gene that was mutated and thus can suppress rapamycin sensitization.

A second approach that was taken in this study to determine the 14-3-3-rapamycin effect. Again the bmht2 strain was used. This time instead of mutating the cells, the yeast cDNA library was transformed into the cells. Yeast cells were then grown at the restrictive temperature of 30°C on plates containing rapamycin. The majority of the yeast could not be sustained on these plates, however, 10 clones that could grow were isolated. The cDNA plasmids from these clones were extracted and sequenced to determine the gene whose overexpression could complement the bmh mutant strain. Although not unexpected, however much to our surprise, all 10 sequences came back resembling either ebmh1 or bmh2. No other genes were identified as being able to revert the phenotype.

This finding suggests two possibilities. The most obvious being that bmh1 and bmh2 truly are master regulators for this pathway and no other genes can compensate for loss of 14-3-3 in this setting. The more likely scenario is that since both bmh1 and bmh2 are expressed at relatively high levels, the cDNA library that we used may have had an overrepresentation of these two genes. This would account for us only pulling these two genes out of our screen. A more preferred approach would be to use a yeast genomic library. Possibly even one that has mutations in both bmh1 and bmh2.

## Discussion

Rapamycin has been quite useful as an immunosuppressive drug to treat organ transplant recipients. Based on its ability to target TOR, it holds promise for treating cancers as well. Indeed, rapamycin analogues have shown promise in clinical trials. Unfortunately, elevations in 14-3-3 proteins can suppress rapamycin induced cell death. It goes with out saying that 14-3-3 protein levels are elevated in multiple tumors. Identification of proteins that determine 14-3-3-dependent rapamycin resistance is expected to reveal novel molecular targets to enhance mTOR-targeted therapies for the treatment of cancer.